ICP-1117

TECHNICAL DIVISION QUARTERLY PROGRESS REPORT JANUARY 1 - MARCH 31, 1977

CYRIL M. SLANSKY B. C. MUSGRAVE
B. R. DICKEY K. L. ROHDE
R. C. SHANK

May 1977

Allied Chemical
IDAHO CHEMICAL PROGRAMS

ENERGY SAFETY ENVIRONMENT

IDAHO NATIONAL ENGINEERING LABORATORY

ENERGY RESEARCH AND DEVELOPMENT ADMINISTRATION

IDAHO OPERATIONS OFFICE UNDER CONTRACT EY-76-C-07-1540

Printed in the United States of America
Available from
National Technical Information Service
U S Department of Commerce
5285 Port Royal Road
Springfield, Virginia 22161
Price Printed Copy $5 50, Microfiche $3 00

DISCLAIMER

ICP-1117

Distributed under Category:
UC-2
General, Misc., Progress . . .
UC-10
Chemical Separations Proc., Pu. . .

TECHNICAL DIVISION QUARTERLY PROGRESS REPORT

January 1 - March 31, 1977

Cyril M. Slansky, Editor

Work performed under the direction of:

B. C. Musgrave, Manager
Technical Division

B. R. Dickey, Manager
Waste Management Branch

K. L. Rohde, Manager
Process Technology Branch

R. C. Shank, Manager
Chemical Research and Analysis Branch

Date Published - June 1977

ALLIED CHEMICAL CORPORATION
IDAHO CHEMICAL PROGRAMS - OPERATIONS OFFICE

Prepared for
ENERGY RESEARCH AND DEVELOPMENT ADMINISTRATION
IDAHO OPERATIONS OFFICE
UNDER CONTRACT EY-76-C-07-1540

ABSTRACT

Progress for the first quarter of 1977 is reported on ERDA-budgeted activities subcontracted to Allied Chemical Corporation at the Idaho National Engineering Laboratory. The work is divided into three categories.

Fuel Cycle Research and Development

Results are presented on the fluidized-bed calcination of high-level radioactive waste from the reprocessing of spent commercial nuclear fuel, on the post treatment of the calcine, and on the removal of actinide elements from the waste prior to calcination. Other projects include the development of storage technology for ^{85}Kr waste; a study of the hydrogen mordenite catalyzed reaction between NO_x and NH_3; the adsorption and storage of ^{129}I on silver exchanged mordenite; physical properties, materials of construction, and unit operations studies on the evaporation of high-level waste; the behavior of volatile radionuclides during the combustion of HTGR graphite-based fuel; and the use of fission product ruthenium in age-dating uranium ore bodies.

Special Materials Production

The long-term management of defense waste from the ICPP covers post-calcination treatment of ICPP calcined waste; the removal of actinide elements from first-cycle raffinate; the retrieval and handling of calcined waste from ICPP storage vaults; and the preparation of the "Defense Waste Document". Process improvements are reported on the Fluorinel headend process for Zircaloy-clad fuels, on the Tory IIA ceramic fuel dissolution step, and on the corrosion behavior of nickel alloys. Other development results cover the process for recovering spent Rover fuel, buried pipeline transfer systems, and support to the Waste Calcining Facility.

Other Projects Supporting Energy Development

In this category are studies on nuclear materials security; application of a liquid-solid fluidized-bed heat exchanger to the recovery of geothermal heat; inplant reactor source term measurements; burnup methods for fast breeder reactor fuels; absolute thermal fission yield measurements; analytical support to light water breeder reactor development; research on analytical methods; and the behavior of environmental species of iodine.

SUMMARY

FUEL CYCLE RESEARCH AND DEVELOPMENT

I. FLUIDIZED-BED CALCINATION AND POST-TREATMENT OF COMMERCIAL WASTES

1. Calcination Studies

Fluidized-bed solidification of simulated Allied General Nuclear Services High-Level Liquid Waste - Intermediate Level Liquid Waste (AGNS HLLW-ILLW), concentrated to 150 gal/MTU, was demonstrated in a 5-day run in the pilot-plant, 12-inch-diameter calciner. The calciner operation was steady; agglomerates were not formed.

Results of long-term tests with denitrated feed in the 3-inch-diameter calciner indicate that complete feed denitration is not desirable because a poor-quality product--soft or sticky--is formed from the completely denitrated feed. Steady-state beds were formed by calcining denitrated feed with indirect heating at 400°C and with in-bed combustion at 550°C. The denitrated feed could not be calcined with indirect heating at any temperature on the steady-state bed (formed at 400°C) because of bed agglomeration. With in-bed combustion, the denitrated feed could be calcined on its steady-state bed only at 550°C and above, combustion quality was poor, and the calcine was soft. In addition, with in-bed combustion, the reductions in ruthenium volatility and off-gas NO_x concentration, anticipated as a result of feed denitration, did not occur.

2. Post-Calcination Treatment of Commercial Wastes

The effect of airflow velocity through a 3-inch-diameter canister of pelleted calcine on the temperature difference between centerline and heated wall was small. DTA measurements show no reaction between the pelleted waste and aluminum alloy up to 900°C. Moisture condensing on pellets during heat treatment causes no physical change in the pellets. Improvements on a bench-scale molten-metal casting unit are being made.

Glass samples were prepared with granular fluidized-bed calcine using two different frits. Glass leach rates in brine solutions at room temperature are similar to rates using either ground water or distilled water.

3. Study of Bidentate Compounds for Separation of Actinides from Commercial LWR Reprocessing Waste

Distribution coefficients were measured for the extraction of Am, Pu, Np and other key elements by dihexyl-N,N-diethylcarbamylmethylene-phosphonate (DHDECMP) from synthetic commercial LWR high-level waste with added nitrate. Extraction measurements also include

E_a^o values for Pu(IV), Np(IV), Np(VI), U(VI), Am(III), and Cm(III) with DHDECMP as a function of nitric acid concentrations and for americium from 3M HNO_3 as a function of DHDECMP concentration in diisopropylbenzene (DIPB).

II. KRYPTON-85 STORAGE DEVELOPMENT

Drafts of "Krypton-85 Storage Development Program Plan" and "Methods of Immobilizing ^{85}Kr Prior to Long-Term Storage" were completed. The scope of work for A-E design of the hydrogen recombiner system for dissolver off-gas (DOG) was completed. Rubidium corrosion (no radiation field) of aluminum cylinder material (observed visually previously) was confirmed by metallography. Pressurized cylinder test specimens in a Rb environment were prepared for a three-month γ-exposure test, and a contract was let for low-rate tensile testing of the specimens after the exposure. The scope-of-work document for A-E conceptual design of a commercial-scale ^{85}Kr storage facility using pressurized cylinders was completed. The compressibility of krypton at high temperatures and pressures was calculated. Preliminary measurements of the leakage of argon from sodalite compare well with earlier literature results. From measurements made of krypton loading on sodalite samples which had been stored at room temperature for $\sim$200 days, no leakage was detected within experimental error. A letter report presenting design options for the pilot-scale system and a draft of the Expenditure Authorization for the pilot-system were completed. Calculated site boundary dosage due to the postulated rupture of a commercial-scale high pressure vessel (20ℓ) containing 30,000 psi of 6% ^{85}Kr in krypton at 25°C was within existing regulations. A conceptual estimate ($500K) and a functional operational requirements document of a GPP facility for housing the pilot-scale system were submitted to ERDA-ID.

III. LWR OFF-GAS TREATMENT

A computer program was written to fit experimental data for the catalyzed reaction between NO_x and NH_3 to a bimolecular surface reaction rate expression by iterative non-linear least-squares analysis. Introductory sections of a topical report dealing with the NO_x - NH_3 reaction catalyzed by hydrogen mordenite were written. The LWR off-gas program was rescheduled for termination at the end of FY 1977; preparation for laboratory experimentation has been discontinued.

IV. IODINE-129 ADSORBENT AND STORAGE DEVELOPMENT

The silver in silver-exchanged mordenite (AgZ) may exist both as the oxide and the metal. The metallic state appears to be more reactive and has a higher iodine-loading capacity than the oxide state. In test streams with a dew point of 23°C, iodine loadings of 137 and 71 mg I_2/g AgZ can be obtained on H_2-pretreated and untreated AgZ, respectively. The mass transfer zone for iodine adsorption is between 7.5 and 10 cm from the inlet with a dew point of 23°C, bed temperature of 100°C, and a face velocity of 15 m/min.

A rough draft of a topical report entitled "Airborne Elemental Iodine Loading Capacities of Metal Zeolites and a Dry Method for Recycling Silver Zeolite", was written. The report includes a process-flow diagram illustrating full-scale application of AgZ regeneration and recycle to iodine recovery from the DOG of LWR fuel reprocessing plants.

V. WASTE MANAGEMENT

Simulated high-level liquid waste (HLLW) solutions having compositions expected during early operation of the Barnwell Nuclear Fuel Plant (BNFP) were evaporated; this waste contains a lower corrosion product concentration and a lower phosphate composition than the previous waste solutions studied; it also contains gadolinium as a nuclear poison. The HLLW-BNFP, concentrated to 336 ℓ/MTU, contained approximately 12.8M nitric acid and smaller amounts of undissolved solids than previous waste solutions at the same acidity.

Physical properties of HLLW-BNFP are presented and include density, boiling point rise, and percent of undissolved solids. Viscosities are reported for several types of HLLW at various degrees of evaporation and temperatures. Slurries were about 1.5 times as viscous as their supernates.

Construction of the small-scale Type 304L stainless steel evaporator was completed. Preliminary runs were made with water and nitric acid at approximately one ft/sec vapor rate in the reboiler tube. Run plans and operating procedures were prepared for testing of Type 304L stainless steel reboiler tube specimens.

Construction of the laboratory, glass-fabricated storage tank, which models selected conditions of a BNFP-type liquid waste storage tank, was completed. The tank will be used to obtain preliminary heat transfer data and to provide design criteria for a small-scale stainless steel storage tank.

Corrosion rates obtained by continuous monitoring of HLLW solutions using Type 304L stainless steel probes compare well with coupon data obtained in the same solution. An average rate of 0.35 mpy was obtained at 60°C for a HLLW solution containing low concentrations of process contaminants and additives.

Corrosion rates are reported for HLLW solutions containing varying amounts of corrosion products. These data indicate that the total corrosion product accumulation in test solutions should be limited to about 0.6 g/ℓ during operation of the small-scale evaporator.

VI. HTGR FUEL RECYCLE WASTE TREATMENT

Work on the removal of HTGR semi-volatiles includes additional volatility experiments in the tube furnace and a literature search for existing data. The chloride compounds of the various fission products are being

tested to see if they can be used in future burner experiments instead of the oxide compounds. The chlorides are readily available. The literature survey and tube furnace experiments allow prediction of volatility and plate-out of the semi-volatiles. These predictions will be verified using a quartz burner.

VII. NATURAL FISSION REACTOR STUDIES

In 1972, the first known example of a neutron-chain reaction in nature was discovered at the Oklo mine site in the Republic of Gabon. In the search for other natural reactors, several rich uranium ore samples from various parts of the world are being analyzed for Ru. These analyses have resulted in the first measurement of the ^{238}U spontaneous fission yields for the stable isotopes of Ru and the development of a new method for dating the age of the formation of the uranium ore bodies.

SPECIAL MATERIALS PRODUCTION

I. LONG-TERM MANAGEMENT OF ICPP HIGH-LEVEL WASTES

1. Post Calcination Treatment of High-Level ICPP Wastes

Thirteen pelleted waste formulations were prepared on the 16-inch-diameter disc pelletizer using boric acid, metakaolin and calcium hydroxide as solid binders; and mixtures of H_3PO_4, and either nitric acid or H_2O, as liquid binders. Eight of these formulations lost less than 1.1 wt% after 100 hours of leaching in 95°C water. Leach rates in brines, acid, and caustic solutions were measured. Pellet impact resistance was measured. Heat-treating times and temperatures to produce leach-resistant pellets were determined.

2. Actinide Removal

Distribution coefficients are reported for the extraction of actinides and key elements between synthetic ICPP zirconium-aluminum first-cycle raffinate and 30% DHDECMP in xylene. An actinide removal workshop at Hanford, Washington was attended. Distribution studies of actinides in their common valence states between synthetic zirconium-aluminum first-cycle raffinate and 30% DHDECMP in diisopropylbenzene have been concluded. A centrifugal molecular still is being tested for use in purifying crude DHDECMP.

3. Calcined Solids Retrievability and Handling

The calcined solids retrieval program was increased in scope to include sampling the contents of selected calcine storage bins. The conditions of the calcine in these bins is important to the design of equipment to retrieve the calcine, to the development of final waste forms for permanent storage, and to the development of a process for removal of actinides from radioactive wastes.

4. ICPP Defense Waste Document

Work continued on preparation of a Defense Waste Document for ICPP high-level waste. Preconceptual designs and cost estimates were completed. Dose calculations were completed and work on the risk analyses continued.

II. ICPP PLANT PROCESS IMPROVEMENT

1. Zirconium Fuel Recovery Process

A preliminary evaluation of filter systems for the cleanup of dissolver product solution showed the Vacco etched-disc filter to be better suited for the Fluorinel Process.

A study of the depletion of soluble cadmium in Fluorinel process solutions has shown that the probability of depletion of soluble cadmium by plate-out, precipitation, and/or co-precipitation is negligible.

Laboratory dissolutions of PWR Core-2 fuels achieved a ninety-eight percent recovery of uranium using 8 M HF - 1 M HNO_3 as the dissolvent.

2. Corrosion of Nickel Alloys

Tests made with factory welded coupons of Inconel 625, Inconel 690, and Incoloy 825 verified previous work and showed that Inconel 625 was the least susceptible to weld decay of these alloys in mixtures of hydrofluoric acid containing low concentrations of nitric acid. Solution heat treatment of Hastelloy C-276 alleviates wel decay; however, the lack of weld decay in the as-welded condition makes Hastelloy C-4 more promising than C-276. Preferential weld decay was not eliminated in either alloy by the heat treatment.

3. Tory IIA Dissolution Process

Tory IIA fuel consists of BeO-UO_2 ceramic which has been crushed, placed in aluminum cans, and shipped to ICPP for reprocessing. Dissolution of the ceramic fuel, stability of resulting solutions with and without the

aluminum dissolver product, and corrosion of materials of construction in dissolvents were investigated. Based on these combined data, a flowsheet has been prepared using boiling 6M H_2SO_4-1M HNO_3 as dissolvent for the ceramic fuel and using the aluminum nitrate, which results from dissolution of the aluminum can, as the salting agent. The preferred alloy for the dissolver vessel is Inconel 625 as determined by corrosion tests.

III. ADVANCED GRAPHITE FUELS REPROCESSING

The sintered-metal filter blowback system for the Rover plant was found to be inadequate; modifications were recommended. The solids-sample funnel and liquid-sample jets were tested and found to be adequate. Operating characteristics of the solids transport system were determined and the operating parameters for the secondary burner were identified. The pilot-plant centrifuge auger was overlaid with Tribaloy 700 to test this hard facing material for erosion. Modifications to the neutron interrogator for improved performance in the processing cell were specified.

IV. WASTE TRANSFER SYSTEMS

A program was established to develop standards or guidelines for the design and construction of safe intraplant transfer systems for radioactive liquid wastes.

Samples of coated pipe for testing in the laboratory and in the field have been prepared. Bare pipe sections of Type 304L, Type 316L, and Type 347 stainless steels also were prepared for field testing.

A program was outlined to determine the relative seismic stability of common secondary pipeline encasements. Encasements under study include 1) stainless steel pipe, 2) fiberglass-reinforced polyester pipe, 3) concrete troughs lined with stainless steel, and 4) walk-in pipeways.

V. ICPP WASTE MANAGEMENT DEVELOPMENT

1. Tank WM-183 Flowsheet Development

Flowsheets are being developed to allow calcination of the waste in ICPP storage tank WM-183 which contains 15 g/ℓ sodium nitrate and 250 ppm chloride. Runs using a 4-inch-diameter calciner indicate that the addition to WM-183 waste of 0.5 to 1.0 moles of powdered iron for each mole of sodium present could prevent fluidized-bed particle agglomeration during calcination of the waste. Other studies show that gas, evolved when iron is added to the waste, contains insignificant amounts of hydrogen, and addition of silver nitrate to the waste may retain chloride in the bed during calcination. Differential thermal analyses indicate blending of WM-183 waste with zirconium waste may prevent agglomeration; such blends would not produce enough solids to cause calciner feed plugging problems.

2. Feed Valve Testing

A full-port ball valve with Kynar ball seats and body seals and Grafoil stem packing is being tested as a possible WCF feed control valve. The valve successfully passed a pressure leak test after first-cycle zirconium waste had been circulated through the 45° open valve for five weeks.

3. Rover Flowsheet

Runs in 4-inch- and 12-inch-diameter calciners indicate that Rover waste can be successfully calcined by using a blend of 1 to 2 volumes of zirconium waste with 1 volume of Rover waste as calciner feed.

OTHER PROJECTS SUPPORTING ENERGY DEVELOPMENT

I. NUCLEAR MATERIALS SECURITY

1. Measurement Equipment for Chemical Plants

An initial version of the experimental plant process surveillance system was installed in the ICPP. The system was set up for a demonstration of theft sensing and on-line collection of accountability data in April. The ultrasonic bubble sensors used in the transit-time flowmeter were redesigned as sealed units. The flowmeter electronics package was remodeled to allow remote readings.

II. GEOTHERMAL ENERGY DEVELOPMENT

Three bed-particle sizes were tested in the 8-inch-diameter liquid fluidized-bed heat exchanger. Apparent maxima were observed in the heat transfer coefficients plotted against shellside velocity. For 0.7 mm diameter particles, the maximum was near 6 ft/min; for 1.0 mm particles, it was 10 ft/min; and for 2.1 mm particles, 14 ft/min. The greatest increase in heat transfer coefficient was observed for the smallest particles, though the maximum was near 1300 Btu/hr-ft^2-^{o}F for all three particle sizes. Shellside velocity varies greatly throughout a horizontal liquid fluidized bed. These experiments demonstrated that the velocity at the midpoint of the vessel best correlates horizontal and vertical heat transfer coefficients.

The vessel constructed to evaluate flow distribution systems was constructed and installed at Raft River. This vessel is a mock-up of a one-ft section of a horizontal preheater. The diameter is three feet. A variety of flow distribution systems will be evaluated. The objective is to provide uniform flow with minimum pressure drop.

III. INPLANT SOURCE TERM MEASUREMENTS

The inplant source term measurements program was continued at the Zion reactor site and concluded at the Ft. Calhoun site. Several reports of the radionuclide data collected have been or are being prepared. All reporting for this program will be by way of EG&G-TREE documents.

IV. BURNUP METHODS FOR FAST BREEDER REACTOR FUELS

Two capsules of ^{241}Am irradiated in EBR-II were dissolved. Development of procedures to separate the bulk of the ^{241}Am from the fission products is in progress. Because of improvements in the response of the mass spectrometer for small peaks, several reruns for La and Ce are in progress. Preliminary ^{242}Pu fast fission yields for isotopes on the light mass peak are given.

V. ABSOLUTE THERMAL FISSION YIELD MEASUREMENTS

Because of measured differences in fission yields for ^{235}U and ^{239}Pu thermal fission, a new thermal fission yield measurement program is under way.

VI. LIGHT WATER BREEDER REACTOR - ANALYTICAL SUPPORT

An agreement was made between Bettis Atomic Power Laboratory and the Radiochemistry Branch at ICPP to analyze forty-two irradiated LWBR fuel rod sections for uranium depletion during the next eighteen months. Twenty of these samples were received. Analysis of these samples is scheduled to begin in early April.

VII. RESEARCH ON ANALYTICAL METHODS

1. AGNS Waste Analysis

Samples of simulated AGNS waste materials submitted for spectrochemical analysis were analyzed in two parts. Filtrate solutions were analyzed directly after appropriate dilutions were made, while the solids were first leached in mineral acids, and the residue was made soluble by fusion with a mixed flux. These solutions were analyzed by atomic absorption and flame emission spectrophotometric methods and by emission spectrography.

2. Computerization of Spectrographic Calculations

Three programs were written for a Hewlett-Packard 9825 calculator to calculate the results of spectrochemical measurements of low element concentrations in water samples. Such calculations are performed faster and more accurately with a programmable calculator than by

hand-computations and graphical methods. Programs 1 and 2 generate standard curves from input data of standard samples, while the third program computes element concentrations directly from intensity ratios.

3. Spark Source Mass Spectrometer

The Spark Source Mass Spectrometer was installed.

VIII. ENVIRONMENTAL IODINE SPECIES BEHAVIOR

Laboratory studies on the production of high purity hypoiodous acid, HOI, and the stability of this species in saturated atmospheres were undertaken. An environmental chamber was installed to test wet deposition of iodine species on grass.

*

CONTENTS

FIGURES AND TABLES (by Section)

FUEL CYCLE RESEARCH AND DEVELOPMENT

Figures

Figures (Continued):

Tables

SPECIAL MATERIALS PRODUCTION

Figures

Tables

Tables (Continued):

OTHER PROJECTS SUPPORTING ENERGY DEVELOPMENT

Figures

Tables

FUEL CYCLE RESEARCH AND DEVELOPMENT

I. FLUIDIZED-BED CALCINATION AND POST-TREATMENT OF COMMERCIAL WASTES

1. Calcination Studies

1.1 Flowsheet Development Studies (J. H. Valentine, R. E. Schindler)

A 5-day flowsheet verification run (Run 60) was made in the 12-inch-square pilot plant calciner to demonstrate solidification of simulated AGNS HLLW-ILLW. About 3500 liters of simulated HLLW-ILLW were solidified using in-bed combustion at 500°C to 485 kg of solids at a normal gross solidification rate of 9 gal/hr-ft^2 (based on the cross section of the fluidized bed). The feed was a simulated blend of the 1974 composition projections for AGNS-sparged, low-acid HLLW and ILLW at a concentration (combined) of 150 gal/MTU. Rare earths were substituted for uranium, and iron was added to complex sodium. The feed was similar to the feed used in Run 58 except that the acidity was increased to 2-4M (most of the Run 58 feed was slightly basic). The fuel nozzle was the unshrouded nozzle used in the first half of Run 58.

The calciner operation was smooth. The particle size (MMPD) increased during the run from 0.40 mm at 90% bed turnover to 0.47 mm at the end of the run 70 hours later. The run was too short to determine whether or not there is a particle-size-control problem. The product-to-fines ratio was 2.5 to 2.8 which is about the same as observed in Run 58. The final bed was considerably harder--attrition index of 40 to 50--than in Run 58 where the attrition index was about 30. The clinkers formed during Run 58 were not observed. This observation confirms the earlier tentative conclusion that the Run 58 clinkers resulted from excessive shroud temperatures during operation of the shrouded nozzle in the last half of Run 58.

1.2 Feed Denitration Studies (M. S. Walker, R. E. Schindler)

A series of tests was made in the 3-inch-diameter calciner to evaluate the feasibility and desirability of calcining a denitrated waste. Feed denitration would be desirable if it either (1) reduced ruthenium volatility, or (2) reduced the off-gas NO_x concentration without adverse side effects. The denitration method tested was in-bed denitration; formic acid was mixed with the feed shortly before it was sprayed into the calciner so that denitration would occur in the nozzle or in the calciner bed during calcination. The formic acid concentration in the tests ranged from stoichiometric to 20% excess.

As shown in Table 1, the anticipated reduction in ruthenium volatility and off-gas NO_x concentration did not occur during the steady-state run with in-bed combustion at 550°C. Apparently, the denitration reaction occurring in the bed produces as much NO_x as the calcination of feed with nitrates. The combustion quality was poor with the denitrated feed. When a steady-state bed was formed while calcining the

TABLE 1

Effects of Feed Denitration on Calciner Operation, In-Bed Combustion at 550°C

	Feed with Nitrates	Denitrated Feed
Ruthenium volatility, %	0.002-0.01	0.007-0.01
Off-gas NO_x, ppm	13,000	13,000
Combustion quality	Good	Poor
Product:fines ratio	6-7	2
Bed attrition index	55	22

denitrated feed at 550°C, the combustion quality deteriorated as the bed approached steady state. Unburned kerosene condensed in the off-gas system and above-bed burning occurred during one period. The denitrated feed also produced a softer product. The product-to-fines ratio decreased with denitration from 6 to 7 without denitration, to 2 with denitration, and the bed attrition index decreased from 55 to 22.

Attempts to calcine the denitrated feed with indirect heating in the 3-inch-diameter calciner were unsuccessful because of bed agglomeration. A steady-state bed was formed while calcining denitrated feed at 400°C with indirect heating. When steady-state was reached, the bed temperatures began fluctuating and agglomerates built up around the feed nozzle. Subsequent efforts to calcine denitrated feed on the steady-state bed were unsuccessful because of bed agglomeration at temperatures of 300, 400, 500, and 550°C.

The test results described above indicate that complete feed denitration by mixing formic acid at the feed nozzle is not a desirable option. However, this may not be true of feed denitration in general. Some of the adverse effects may have been a result of the in-bed denitration process. For example, the denitration reaction may have produced foaming that contributed to the softer product and increased fines. However, the poor combustion is probably characteristic of all denitration processes; nitrates catalyze the combustion process.

Plans for Next Quarter

The new, 4-inch, enclosed calciner will be operated. Flowsheet-verification testing and ruthenium volatility evaluation will be shifted to the new 4-inch calciner. Flowsheet-verification and ruthenium-volatility tests will be made with feed compositions based on the following AGNS feed-composition projections: (1) 1974 low-acid, (2) 1976 steady-state, and (3) 1976 early-operation. The effect of uranium concentration on calciner operation will be evaluated.

2. Post-Calcination Treatment of Commercial Wastes

(K. M. Lamb and H. S. Cole)

Work continued to determine operating parameters for the metal-matrix incorporation of pelleted commercial waste. A 3-inch-diameter by 30-inch-long canister filled with simulated waste pellets was used to study canister centerline heating rates. Temperature differences between pellets at the wall and at the center of the canister using several internal air velocities were determined. Air is passed through the canister while heating the pellets before casting to remove NO_x and water vapor and to control temperature gradients. Airflow rates (SCF/ft^2 of empty canister/sec) in the canister were varied from zero to 0.3 SCF/ft^2/sec at a constant heat input rate. Zero air flow corresponded to the fastest heating rate (see Figure 1) which indicates that conduction heating is a better mechanism than forced convection heating for a 3-inch-diameter canister. The effects of conduction and forced convection heat transfer for larger (6- to 10-inch-diameter) canisters will have to be evaluated in each case to determine required airflow rates to properly control temperature gradients and to achieve maximum heating rates.

Temperature gradients in the canister (as shown in Figure 2) were lowest at zero airflow. The first part of the 0.3 SCF/ft^2/sec curve did not follow the pattern of the other airflow rate curves. This was probably due to moisture remaining in the pellets as temperatures were first measured with the 0.3 SCF/ft^2/sec airflow. The differences at 0.1 SCF/ft^2/sec and at zero airflow were measured using pellets which had previously been heated. The increased temperature difference between wall and center point at increased airflow rates indicates that the air is cooling the pellets, which is consistent with Figure 1. Cooling of the pellets is required when radioactive materials are used, because radiolytic decay heat must be removed or distributed to prevent overheating during treatment.

Differential thermal analyses were run using (1) A-380 aluminum alloy and pelleted simulated commercial calcine, and (2) A-380 alloy and scale coating from a mild steel casting canister. Neither analysis showed exothermic reactions between the pellets or scale and the aluminum alloy up to 900°C.

A 4-inch-diameter by 36-inch-long glass canister was filled with pelleted waste and maintained at 110°C for several hours to determine if pellets agglomerate during drying. A large amount of moisture was observed to condense upon cooler pellets at the top of the canister and the exit tube of the canister. The moisture did not cause agglomeration; all pellets remained intact and free-flowing.

Equipment development on the bench-scale metal-matrix casting unit continued. New metal-gasketed flanged connections to attach canisters to the casting system were fabricated. Clamp-on freeze valves were fabricated to improve valve life by avoiding direct welding to the molten aluminum transfer tube. With this system, canisters can be filled with green pellets while in the casting furnace.

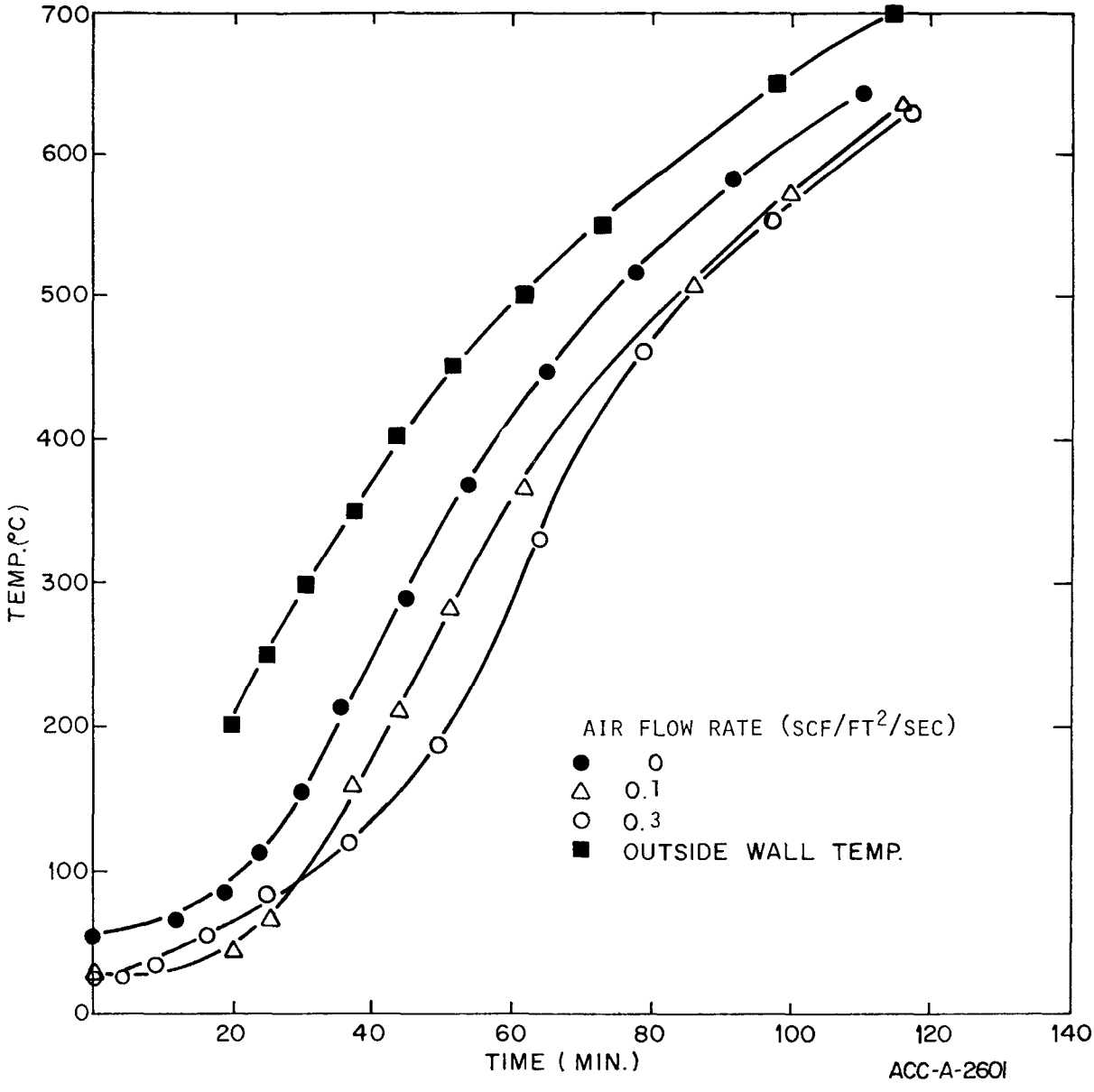

Figure 1. Centerline temperatures of pellets during heating at a uniform rate for three different air flow velocities through the canister.

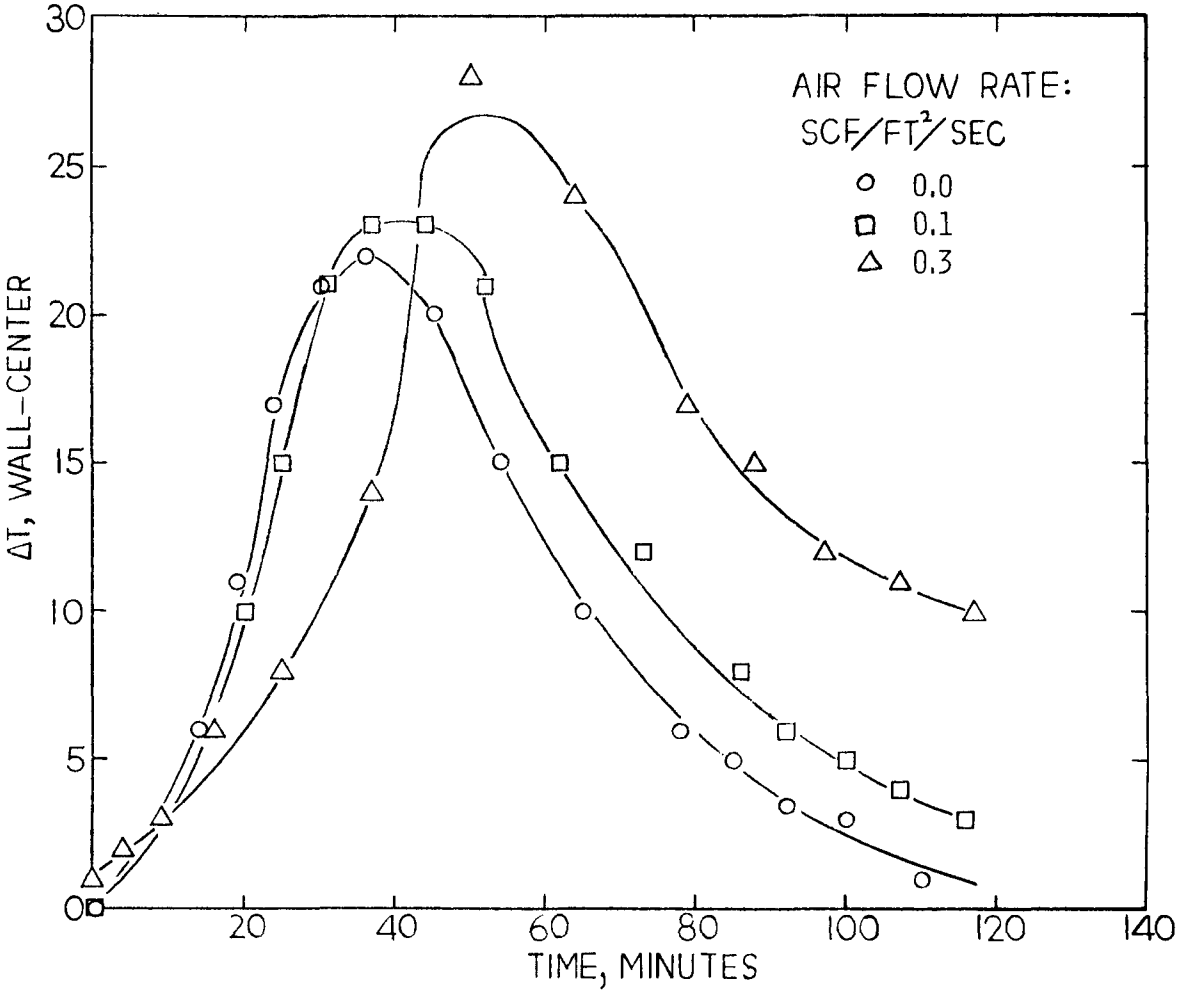

Figure 2. Effect of heating time at constant heating rate on temperature difference between wall and centerline for three internal air flow rates.

Laboratory experiments were performed to determine the ease with which granular (median particle size 0.35 mm) fluidized-bed calcine will dissolve in frit to form a waste glass. Uniform samples were made by holding the glass melt at 1050°C for approximately two hours. The glasses were prepared using simulated fluidized-bed HLW-ILW commercial waste and either BNWL frit 73-1[a] or an experimental high silica frit. Frit compositions are shown in Table 2. Calcine contents are given in Table 3 along with results of room temperature leach tests (19 hr) using simulated salt strata brines, acetic acid (pH 3.5) solution, and an NH_4OH (pH 9.5)solution. Soxhlet leach rates using distilled water at 95°C are also given. Brine solution "A" was high (306.3 g/ℓ dissolved solids, pH = 6.5) in Na^+, K^+, Mg^{++}, and Cl^- ions; solution "B" (297.2 g/ℓ dissolved solids, pH = 6.5) was high in Na^+ and Cl^- ions; solution "C" was a simulated ground water containing 3.7 g/ℓ, (pH = 7.5) dissolved solids. The glass prepared using the high silica frit has lower leach rates than that using the 73-1 frit during acid leaching and comparable leach rates under the other leach conditions tested. Leach rates for the calcine are also shown for comparison.

Plans for Next Quarter

Additional solid binders to produce leach-resistant pellets with current commercial waste compositions will be tested on the 16-inch pelletizer. Bench-scale casting equipment will be tested and conceptual design for a metal-casting pilot plant will proceed.

3. Study of Bidentate Compounds for Separation of Actinides from Commercial LWR Reprocessing Waste

(L. D. McIsaac, J. D. Baker, R. E. LaPointe, N. C. Schroeder)

Introduction

Bidentate organophosphorus compounds have been under study for about three years as possible extractants of actinides from ICPP high-level wastes. The expertise gained with these extractants is presently being applied to the problem of actinide removal from high-level liquid waste generated by reprocessing commercial LWR fuel. As is the case with ICPP waste, attention will focus principally on the use of the bidentate compound, DHDECMP. This work is under subcontract to Oak Ridge National Laboratory, UCC Nuclear Division.

Synthetic LWR Waste

Distribution coefficients for actinides and key elements between synthetic commercial LWR high-level waste and 30% dihexyl-N,N-diethylcarbamylmethylenephosphonate (DHDECMP) in diisopropylbenzene (DIPB) are being measured. Initial experiments have been with synthetic waste brought to 0.1 molar in nitrite by the addition of $NaNO_2$.

[a] J. L. McElroy, "Quarterly Progress Report Research and Development Activities Waste Fixation Program, Jan.-March 1976", BNWL-2070.

TABLE 2

Frit Compositions

Component	Frit 73-1 wt%	High Silica Frit wt%
SiO_2	37.0	54.2
B_2O_3	15.1	12.5
Na_2O	5.5	11.6
K_2O	5.5	1
ZnO	28.9	6.7
CaO	2.0	3.8
MgO	2.0	--
SrO	2.0	--
BaO	2.0	--
Li_2O	--	3.8
Al_2O_3	--	5.0
F_2	--	1.4

TABLE 3

Leach Resistance of HLW-ILW Waste Glass to Various Solutions

Composition		Wt% Lost 19 hr at room temperature					
		Brine Solution					
Wt% Calcine	Glass Frit	A	B	C	Acid	Caustic	95°C H_2O per 100 hr
--	73-1	1.7	0.67	1.4	60.1	1.4	2.1
35	73-1	0.1	0.1	0.1	34.4	0.2	0.3
100	--	16.9	14.3	15.1	19.9	14.4	14.5
--	High Silica	0.7	0.5	1.1	1.2	0.6	0.8
35	High Silica	0.2	0.2	0.2	2.7	0.2	0.6
25	High Silica	0.3	0.2	0.1	0.3	0.1	0.9

Radioactive tracers were used for all but the acid analysis. Vacuum distilled DHDECMP, which was found to be ~86% pure as determined by gas chromatography, was diluted to 30 vol% with DIPB. The extractant was treated sequentially with half volumes of 0.5M Na_2CO_3 and water before use. Tracers as the nitrates were equilibrated with the synthetic waste for at least one hour before extraction measurements were made. Organic and aqueous samples were agitated for five minutes at 23°C with a mechanical wrist shaker. Equal volume extraction measurements were followed by two one-fifth volume 3M HNO_3-0.05M $H_2C_2O_4$ scrubs and three equal volume strips using 0.05M HNO_3-0.05M $NH_2OH \cdot HNO_3$.

Alpha tracers were counted in a liquid scintillation counter. Gamma-ray emitting tracers were analyzed either with a Ge(Li) or NaI(Tl) spectrometer. Results of these extraction studies are tabulated in Table 4. In many cases, the tracer activities available did not allow us to make complete sets of measurements. Measurements for elements missing from this table (i.e., U, Cm, Cr, etc.) will be completed soon.

TABLE 4

Distribution Coefficients (E_a^o) for Actinides and Other Key Elements Between 30% DHDECMP in DIPB and Synthetic Commercial LWR High-Level Waste[a]

Element	Extraction ($V_o/V_a = 1$)[e]	Scrub 1 ($V_o/V_a = 5$)	2[b,c]	Strip 1 ($V_o/V_a = 1$)	2	3[b,d]
Am (III)	4.3	4.1	5.7	0.70	0.13	0.18
Pu (IV)	304	122	25	0.70	0.068	0.16
Np(V,VI)	2.2	2.0	2.6	0.06	0.84	-
Gd	2.1	2.4	2.6	0.33	0.061	-
Eu	2.9	3.2	3.3	0.46	0.086	0.048
Sm	3.4	-	-	-	-	-
Pm	4.2	-	-	-	-	-
Nd	4.3	-	-	-	-	-
Pr	5.3	-	-	-	-	-
Ce	5.8	5.2	7.1	1.02	0.18	<0.1
La	6.5	6.1	7.8	1.01	0.16	0.085
Ba	0.013	0.012	-	-	-	-
Cs	0.00050	-	-	-		-
Te	0.020	0.0084	-	-	-	-
Sb	0.036	-	-	-	-	-
Sn	0.0021	-	-	-	-	-

TABLE 4 (Cont):

Cd	0.0067	-	-	-	-	-
Ag	0.028	0.026	-	-	-	-
Pd	0.53	0.47	0.41	1.10	1.20	2.8
Rh	0.018	-	-	-	-	-
Ru	0.27	0.96	-	15	15	-
Tc	2.3	1.40	-	8.3	5.1	-
Mo	0.39	0.10	0.04	-		-
Nb	0.51	0.017	0.75	-	-	
Zr	1.8	0.022	0.0028	0.076	<0.1	-
Sr	0.017	0.019	-	-	-	-
Rb	0.00064	-	-	-	-	-
Fe	0.0015	-	-	-	-	-
H^+	0.23	-	-	-	-	-

[a]Waste solution made 0.1M $NaNO_2$

[b]All values, except where noted, have an estimated uncertainty of ± 10%

[c]Scrub is 3M HNO_3-.05M $H_2C_2O_4$

[d]Strip is 0.05M HNO_3-0.05M $HN_2OH \cdot HNO_3$

[e]Vo/Va is the volumetric ratio of organic/aqueous

Bidentate extraction of synthetic LWR waste treated with a reducing agent such as hydrazine will be studied next. Extraction data for neptunium, plutonium, ruthenium, rhodium and paladium will be of particular interest. It will not be necessary to measure distribution coefficients for elements not affected by hydrazine (i.e., Cs, Rb, Ba, Sr, Zr, etc.).

A conceptual flowsheet will be formulated for actinide removal from commercial LWR high-level waste after distribution studies are completed. Minimixer-settler experiments will be made using synthetic waste to verify flowsheet parameters.

Extraction Mechanisms

In addition to the distribution studies with synthetic waste, other actinide extraction measurements basic to this program were made. The distribution coefficients for Cm(III), Am(III), Pu(IV), Np(VI), and U(VI) were determined for 30% DHDECMP in DIPB and various nitric acid concentrations. Results are shown in Figure 3. The extractant and its

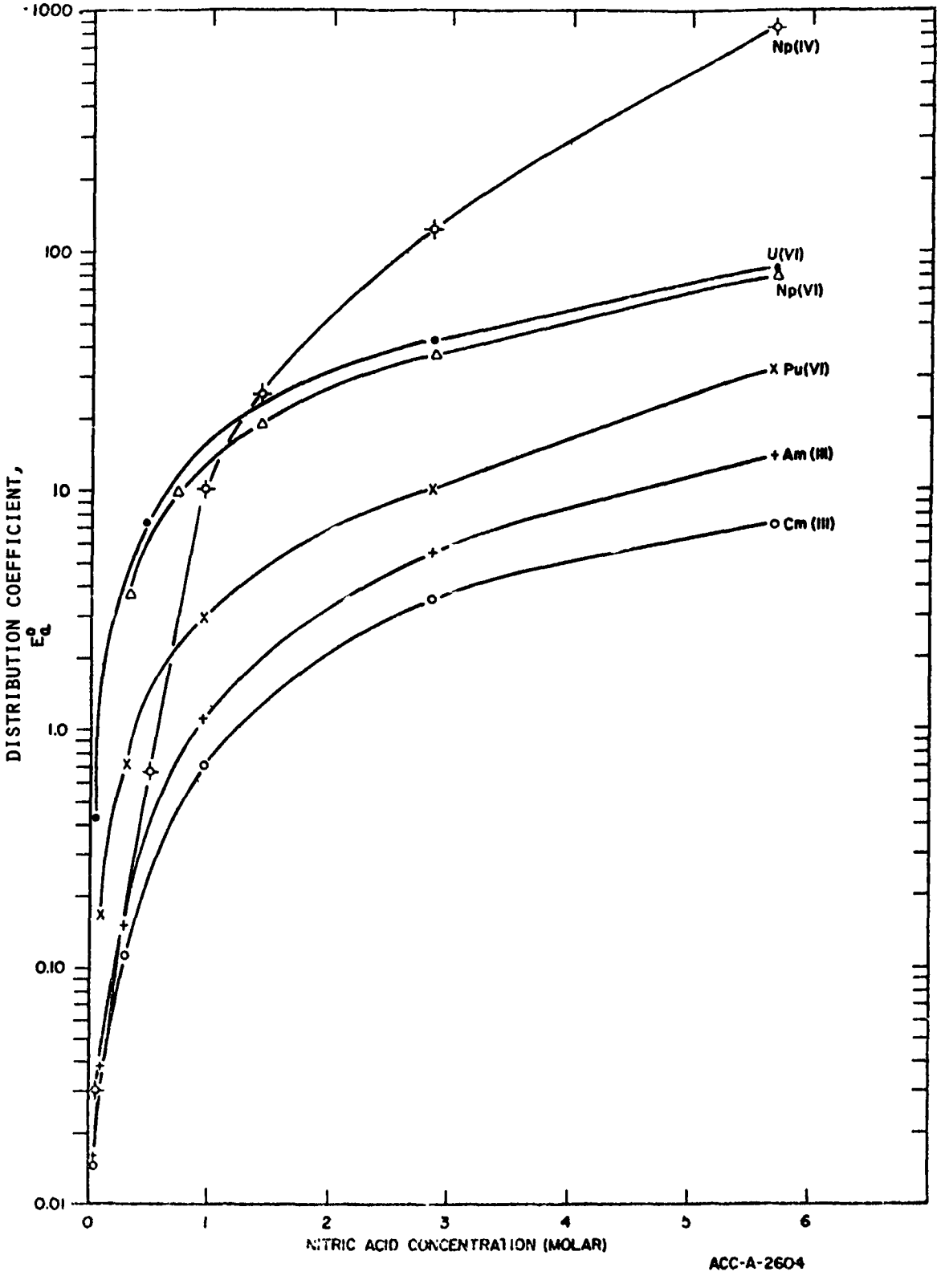

Figure 3. Actinide distribution coefficients between nitric acid and 30% DHDECMP in DIPB.

treatment were described above. After the desired oxidation states were assured, extractions were made using equal volumes of aqueous and organic phases. Samples were equilibrated for five minutes at 23°C.

Pu(VI) oxidation state was set using 0.025M $NaBrO_3$-0.001M $Ce(NH_4)_2(NO_3)_8$. Np(IV) and Np(VI) states were set using 0.025M $Fe(NH_2SO_3)_2$ and 0.026M $NaBrO_3$-0.001M $Ce(NH_4)_2(NO_3)_6$, respectively. Americium and curium are normally in the (III) valence and therefore required no redox treatment. Several hours at 60°C were required to complete the oxidation of Pu(VI) in the highest acidity used. One hour at 60°C was required to complete other oxidations of plutonium and neptunium. One hour at 23°C was used to assure the reduction of neptunium to Np(IV). Similar extraction studies with Pu(III) and (IV) are planned in the near future.

Americium distribution coefficients were measured as a function of nitric acid concentration and DHDECMP concentration. A logarithmic plot of americium extraction data from 3M HNO_3 is shown in Figure 4. The observed slope of 2.9 is an indication of third-order dependence on DHDECMP concentration. Americium extraction by DHDECMP can most likely be represented as:

$$Am^{3+} + 3NO_3^- + 3\ \text{DHDECMP} \rightleftharpoons Am(NO_3)_3 \cdot 3\ \text{DHDECMP}$$

Third-power dependency was also observed by Siddall[a] in extraction of cerium from nitric acid with dihexyl-N,N-dibutylcarbamylmethylenephosphonate (DHDBCMP). Siddall's acid dependency studies indicated that at least two molecules of nitric acid are associated with each cerium-bidentate complex. Acid dependency results with americium are shown in Figure 5. The slope, which is significantly less than 2, suggests that more than one reaction is involved.

Plans for Next Quarter

Extraction studies will continue with synthetic LWR waste which has been treated with nitrite. Plutonium extraction parameters for the (III) and (IV) oxidation states will be measured as a function of nitric acid concentration. Preparation of "extraction grade" DHDECMP will be studied using our new centrifugal molecular still.

---

[a] T. H. Siddall, III, J. Inorg. Nucl. Chem. 26, 1991 (1964).

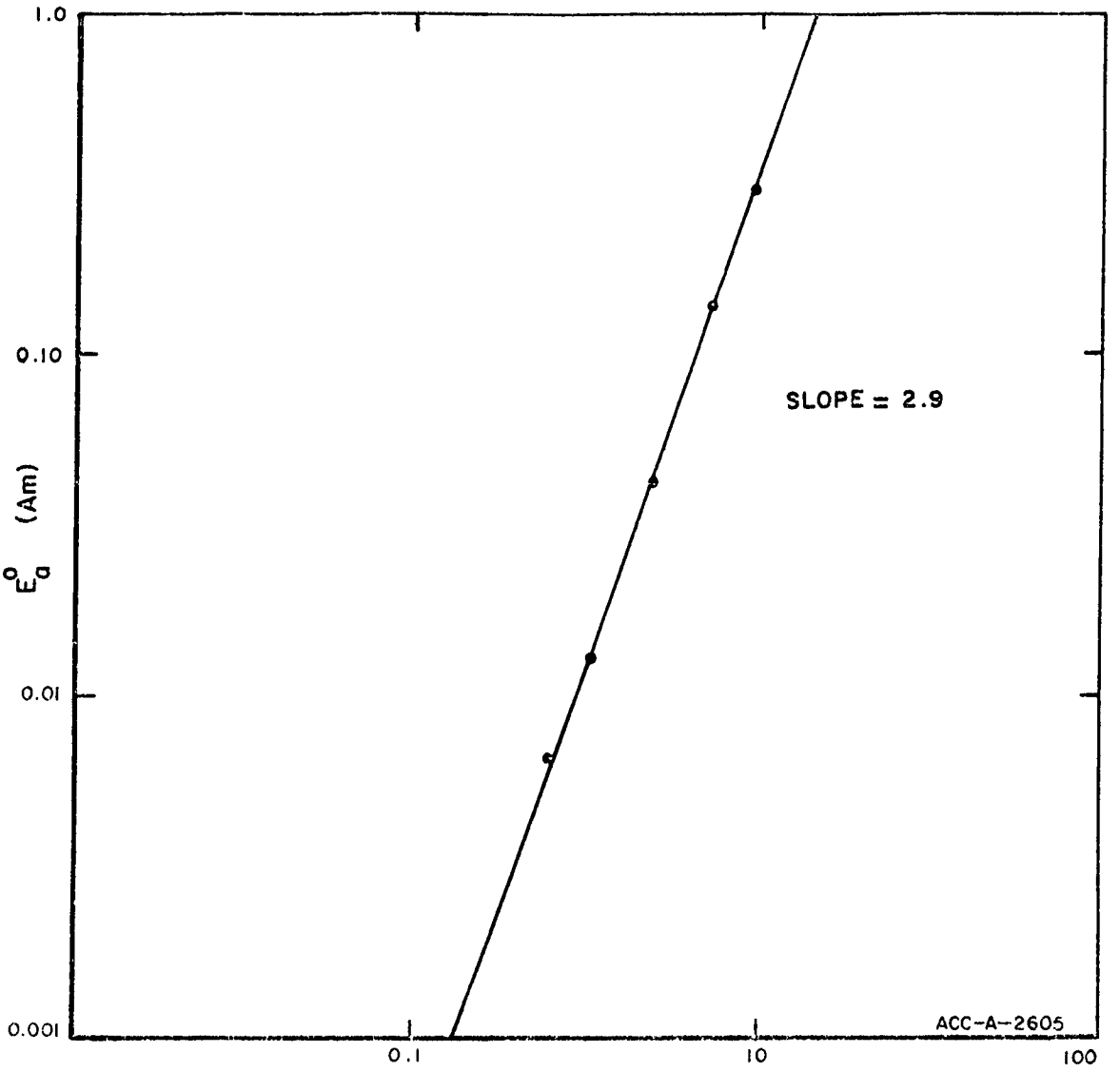

Figure 4. Americium distribution coefficients between 3M HNO_3 and DHDECMP in DIPB.

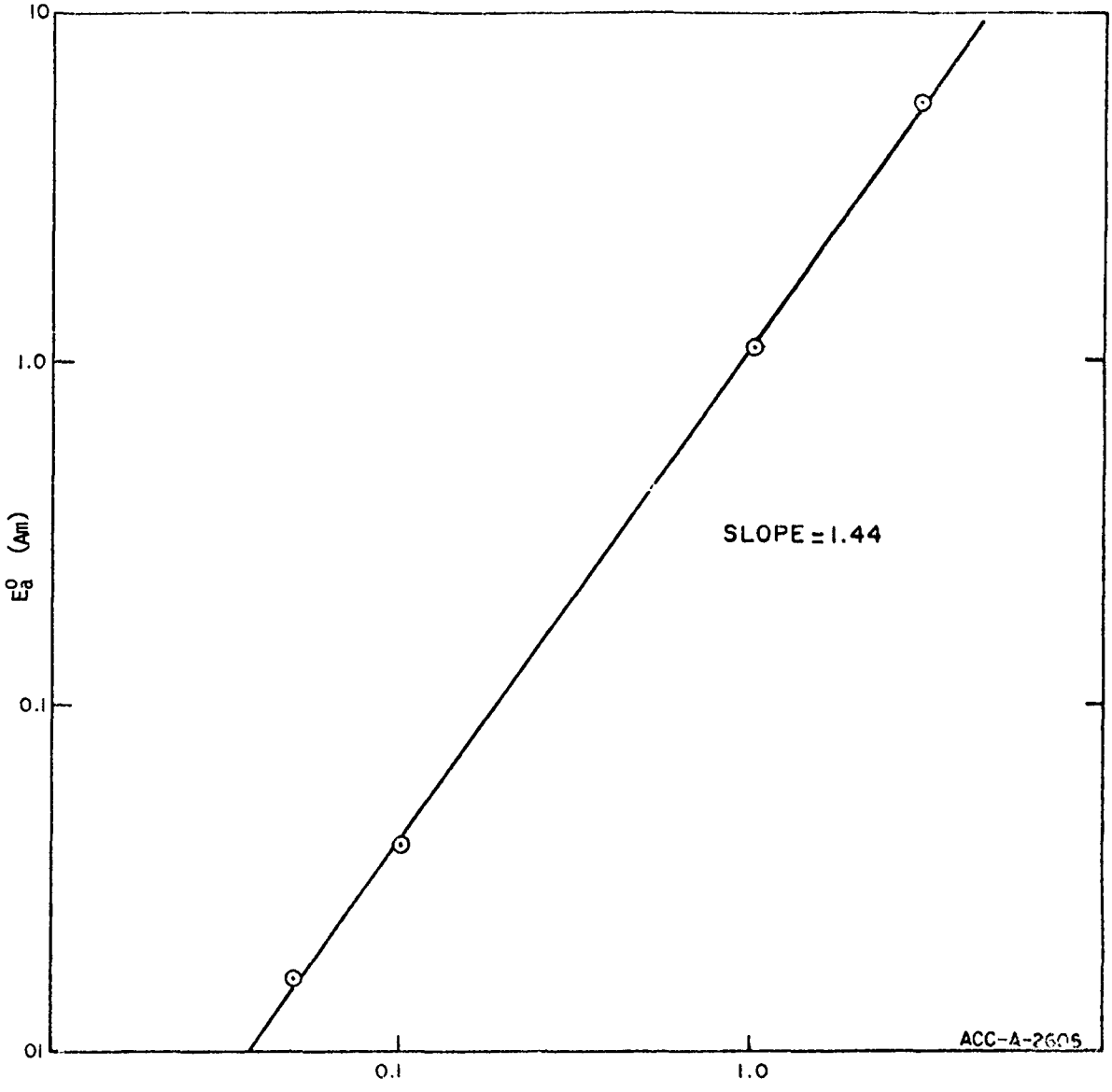

Figure 5. Americium distribution coefficients between 30% DHDECMP in DIPB and nitric acid.

II. KRYPTON-85 STORAGE DEVELOPMENT

(R. Benedict, A. B. Christensen, L. T. Cole, M. Hoza, D. A. Knecht)

1. Storage Alternatives

Drafts of "Krypton-85 Storage Development Program Plan" and "Methods of Immobilizing ^{85}Kr Prior to Long-Term Storage" were prepared. Methods of immobilization examined were: (a) high temperature, high pressure sorption by zeolite, metal, glass, and other materials, (b) ion impaction/sputtering, and (c) low temperature metal vapor deposition. All three methods appear promising in concept, but require increasing technical development (in the order listed). Work is in progress at Battelle Northwest Laboratories to develop ion impaction/sputtering technology, in addition to the work on high pressure encapsulation at the INEL.

The scope of work for the architect-engineer services required for a conceptual design of the hydrogen recombiner for ICPP dissolver off-gas was completed and is being reviewed prior to submission to ERDA-ID. Preliminary ERDA-ID approval was obtained for proposed architect-engineer work on the conceptual design of the hydrogen recombiner being carried out as part of an existing contract. Significant time and money would be saved using such a procedure. A sampling system was designed to determine off-gas compositions from the aluminum and zirconium dissolvers in the upcoming coprocessing fuel dissolution campaign. The analysis of the off-gas (for O_2, F^-, I_2, noble metals) will be used in detailed design for the hydrogen recombiner.

2. Pressurized Cylinder Storage

Rubidium Corrosion - A new glovebox for Rb loading of sample specimens for corrosion studies was installed. Metallography of C-ring specimens, which had been exposed to Rb at 127°C, was completed. Corrosion observed visually (reported in previous quarterly) with the 6061 T6 aluminum specimens was confirmed. The 4130 steel specimen, which had observable surface corrosion near the region of contact with the stainless steel bolt and nut, was shown by the metallography analyses to have no penetrating corrosion.

Preparations for exposing hollow, notched, and C-ring tensile specimens to γ-radiation in the presence of rubidium and argon were made. Hollow specimens, each containing 2g Rb, were pressurized to 1200 psi Ar and were stressed to 0.45 yield strength. Notched and C-ring specimens were stressed to 0.9 yield strength. All samples are ready to begin γ-exposure tests. A contract was signed with Colorado School of Mines to perform low-rate tensile testing (18 mo) of test specimens from γ-exposures.

Erratum - Previous quarterly reports presented preliminary corrosion results of C-ring specimens in Rb-Ar environments without γ-exposures, not with γ-exposures as had been reported.

Conceptual Design of Storage Facility - A scope of work document for architect-engineer design of a commercial-scale ^{85}Kr storage facility using pressurized cylinders was written and is being reviewed prior to submission to ERDA.

3. Zeolite Encapsulation Storage

Laboratory-Scale - Based on the ability to predict experimental specific volume data, the Redlich-Kwong equation of state[a] has been selected to describe krypton behavior at high temperatures and pressures. Using the Redlich-Kwong equation of state, thermodynamic properties of krypton at high pressures and temperatures were calculated. The resulting behavior of the compressibility is shown in Figure 6.

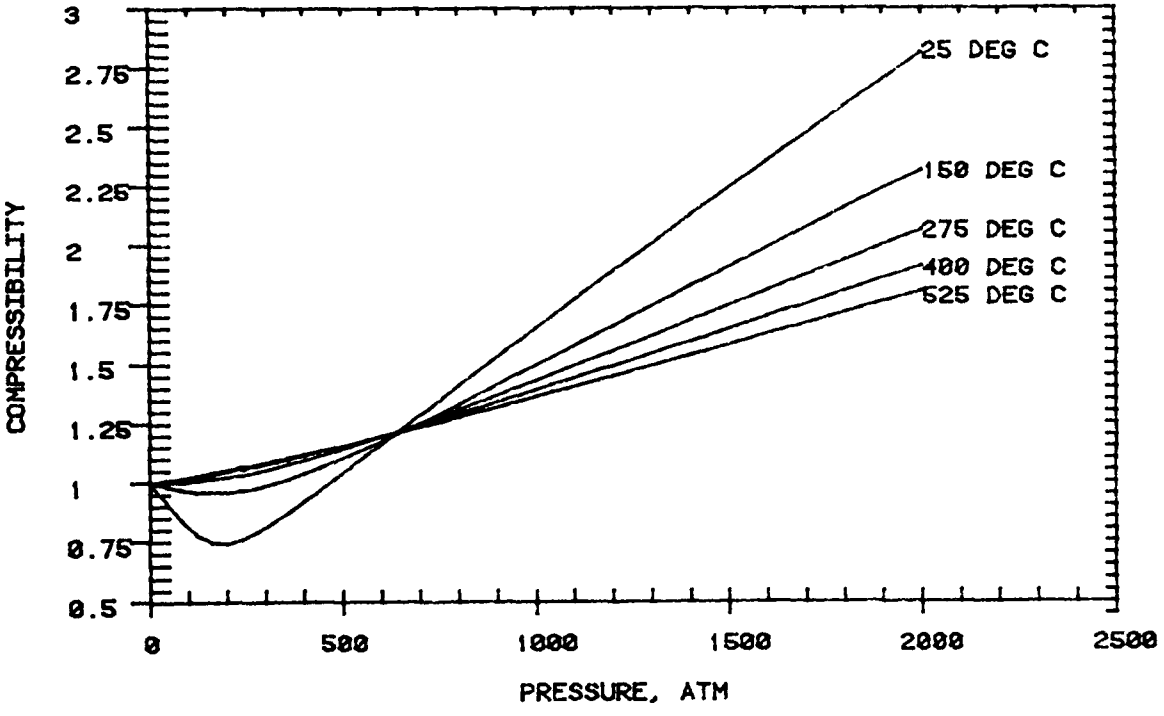

Figure 6. Compressibility of Kr as a function of T, P

Encapsulation experiments were run at 540°C, 23,000 psi, and 2.5 hr; 32 $cm^3\ g^{-1}$ krypton was loaded on leached sodalite. The corresponding values at 500 and 462°C are 26 and 23 $cm^3\ g^{-1}$, respectively. The mass spectrometric leakage measurement system is about 80% complete. Preliminary measurements of rates of pressure increase due to argon leakage from leached sodalite were made at three temperatures. Figure 7 compares

[a] J. M. Prausnitz and P. L. Chueh, Computer Calculation for High Pressure Vapor-Liquid Equilibria, Prentice-Hall, Englewood Cliffs, NJ, 1968.

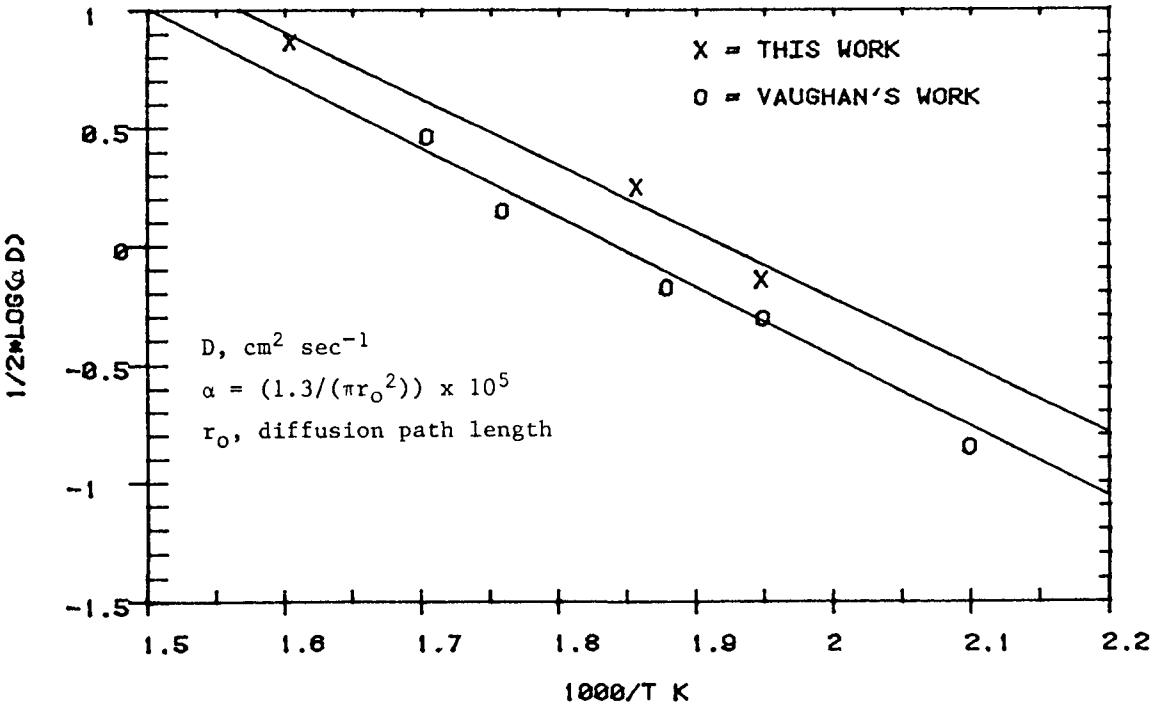

Figure 7. Temperature Dependence of Diffusion of Argon in Leached Sodalite

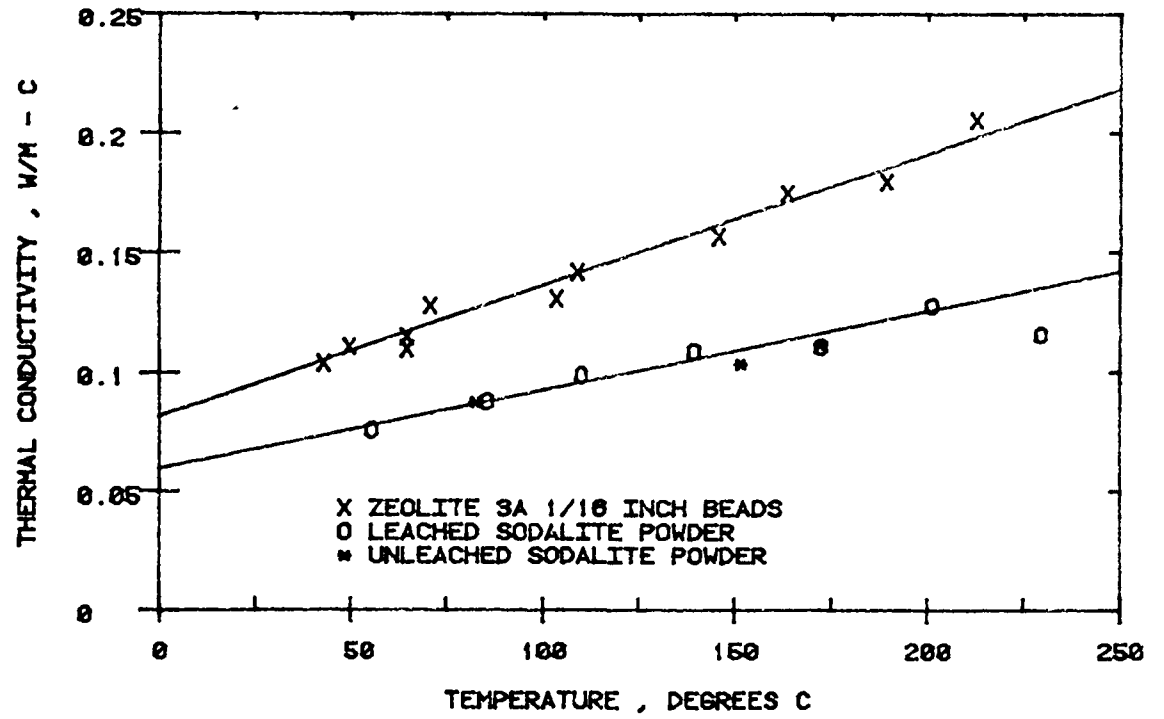

Figure 8. Thermal Conductivity of Unactivated Zeolite Samples

our values with those obtained by Vaughan.[a] For activated diffusion, the slope of the lines in Figure 8 is proportional to the activation energy (E) of diffusion. For leached sodalite, E is 27 and 25.9 kcal for our results and Vaughan's, respectively. The reason that the two plots are displaced may be due to different values of α (i.e., r_o, the diffusion path length) for the two different samples of sodalite.

Mass spectrometric measurements were made of krypton loading in sodalite samples which had been stored at room temperature for ~200 days. Within measured experimental precision, no leakage of the encapsulated krypton has been detected.

The thermal conductivity of sodalite powder was measured as a function of temperature and compared with earlier measurements using zeolite 3A beads (Figure 8). Unleached sodalite contains intercalated sodium hydroxide. The difference in values between sodalite and zeolite 3A may be due to differences in sample form (powder vs. beads) rather than zeolite type. Additional measurements are planned for sodalite beads.

Pilot-Scale - A trip report of the visit with high pressure laboratories and vendors (which presents design options for the pilot-scale system) was released. Representatives of one of the vendors, Pressure Products, visited us and discussed pilot-scale design and radiation resistance of materials used in various compressors and valve packing. Current users of high pressure equipment were contacted to determine quality and reliability of various components which will be required for the pilot-scale system. INEL experts in high pressure containment were consulted concerning pilot-scale barricade design and capability. Worst-case calculations were made of the dosage that would result at the site boundary should a commercial-scale encapsulation vessel (20ℓ, 30,000 psi, and 25°C) rupture; the resulting values of 242 mrem skin and 3.2 mrem whole body doses are within existing regulations. On-site doses can be much more severe and require more detailed study. Design criteria based on the trip report and subsequent discussions are being compiled. A draft of the Expenditure Authorization for the pilot-scale system was completed and is being reviewed. Design of a GPP-funded high pressure test facility to house the pilot-scale system was made; the facility would have about 1000 sq ft of foundation, with two stories, one above and one below grade level. The high pressure system, control area, laboratory and storage space will be housed in the building; a blow-out wall will be included for the high pressure system. A conceptual estimate ($500K) was made and the functional operational requirements document was completed and submitted to ERDA-ID.

Plans for Next Quarter

A-E work on the conceptual design of the hydrogen recombiner will be started. Zirconium dissolver off-gas composition will be analyzed for O_2, F^-, I_2, and noble metals. Radiation testing (γ) of cylinder sample specimens in rubidium and argon and low-rate tensile baseline tests of

---

[a] D. E. W. Vaughan, Encapsulation of Rare Gases, Ph.D Thesis, Imperial College, London (1967).

sample specimens will begin. An architect-engineer will be selected for conceptual design work of a commercial scale ^{85}Kr storage facility using pressurized cylinders. Encapsulation and leakage experiments will be continued to provide data for a detailed model. Assembly of the mass spectrometric leak detection system will be completed. A report will be written on heat transfer considerations in ^{85}Kr storage. Capital equipment funds for the pilot-scale encapsulation system will be committed and design criteria will be submitted for bids.

III. LWR OFF-GAS TREATMENT[a]

(R. A. Brown, D. H. Munger, T. R. Thomas)

Preparation for laboratory study of the NO_X-NH_3 reaction catalyzed by hydrogen mordenite was continued. All required equipment has been ordered. Each of the reactions of NH_3 with NO, NO_2, O_2, and N_2O is assumed to be described by the bimolecular surface reaction rate expression:

$$r = \frac{-d(A)}{dt} = \frac{K(A)(NH_3)}{(1 + \alpha A + \beta NH_3)^2}$$

where r is the rate at which NO, NO_2, O_2, or N_2O disappears, α and β are the equilibrium adsorption constants of A and NH_3, K is the rate constant, and t is the contact time in the plug-flow reactor. A computer program was written which uses iterative non-linear least-squares analysis to estimate all constants. A 5-cm-diameter by 60-cm-long stainless steel reactor with thermocouple and pressure transducer ports was fabricated. A new chemiluminescence monitor for NO_X analysis, which was made available from another project, was checked out. Construction of the test apparatus was scheduled to begin in April. However, due to termination of this program at the end of FY 1977, further preparation for a laboratory study is being discontinued.

A topical report is being written to summarize the thermodynamics, gas-phase kinetics, and bimolecular surface reaction kinetics of the NO_X-NH_3 reaction. The report will also include a survey of other publications on the catalyzed NO_X-NH_3 reaction, published and unpublished experimental data previously obtained by the authors, and a description of the experimental system and procedure.

Plans for Next Quarter

A topical report on the NO_X-NH_3 reaction catalyzed by hydrogen mordenite will be prepared.

---

[a]Part of the program on LWR Fuel Reprocessing and Recycle administered by Savannah River Operations and Savannah River Laboratory.

IV. ^{129}I ADSORBENT AND STORAGE DEVELOPMENT[a]

(J. T. Nichols, L. P. Murphy, B. A. Staples, T. R. Thomas)

The effects of pretest purge and hydrogen pretreatment on the iodine loading of silver-exchanged mordenite Zeolon 900 (AgZ) were examined. Five-cm-deep beds, containing 10-20 mesh AgZ, were loaded with I_2(g) in a dry airstream at a superficial face velocity of 15 m/min and a bed temperature of 100°C until breakthrough was detected (DF > 500). The results are given in Table 5.

TABLE 5

Effect of Dry Air Pretest Purge on I_2 (g) Loading on AgZ

Pretest Purge (hr)[a]	H_2 Pretreatment[b]	No. of Replicate Tests	Loading[c] (mg I_2/g AgZ)
1	no	1	60 ± 9[d]
1	yes	1	67
16-64	no	4	24 ± 9
16-120	yes	3	62 ± 9

[a]Purged by dry air at 100°C

[b]Exposed to pure H_2 stream at 500°C for 20 hr

[c]Based on a dry density of 0.79 g/cm^3 for AgZ

[d]The 95% confidence interval based on a pooled variance

The data indicate that increased exposure of the AgZ to dry air at 100°C decreases the iodine loading about 60%. However, this effect is eliminated by pretreating the AgZ with H_2.

Tests were repeated using the conditions which gave the low results in Table 5 (i.e., 24 mg I_2/g AgZ) except that the bed temperature was raised to 150°C. The results of three tests were 57 ± 9 mg I_2/g AgZ. The 95% confidence interval is based on pooling the variance of this set of tests with those in Table 5. The results indicate that the effect of pretest purge can also be removed by raising the test temperature to 150°C in the absence of H_2 pretreatment.

Based on the data, we have hypothesized that an equilibrium similar to:

$$Ag_2O(s) \rightleftarrows 2\ Ag(s) + 1/2\ O_2(g)$$

[a]Part of the program LWR Fuel Reprocessing and Recycle administered by Savannah River Operations and Savannah River Laboratory.

exists in the silver-exchanged substrate. The oxygen involved is part of the alumino-silicate structure. Hydrogen pretreatment would protonate the oxygen anion, reduce the Ag to the metallic state and block the return of the Ag to the oxide. This mechanism would predict the absence of a pretest purge effect; the high loading in the H_2-pretreated material would indicate that the metallic state is more active for iodine recovery. The same mechanism can be used to explain the temperature effect in the untreated AgZ. In the ideal state, the equilibrium has a zero free energy at 180°C, with the oxide being favored at lower temperatures and the metal at higher temperatures. When the AgZ is prepared, part of the procedure is to bring it to constant weight at 150°C. This would establish an equilibrium mixture of Ag_2O/Ag. Running the iodine-loading test at 100°C would upset the equilibrium, causing more oxide formation during testing. Running the iodine-loading test at 150°C would not upset the equilibrium, and no pretest-purge effect would be noted as was the case. The low loading at 100°C would indicate that the silver oxide is less reactive for iodine recovery than the metal.

Using a face velocity of 15 m/min, a bed temperature of 100°C, and a dew point of 23°C, the effect of contact time and H_2 pretreatment on the iodine-loading of AgZ was examined. The results, along with the distribution of the iodine from the top to the bottom of the bed, are shown in Table 6.

TABLE 6

Effect of Contact Time and H_2 Pretreatment on the I_2 Loading of AgZ

Bed Depth (cm)	mg I_2/g Ag in each 2.5 cm segment						Avg Loading (mg I_2/g AgZ)
	1	2	3	4	5	6	
5	57	10					33 ± 7[b]
5[a]	60	12					36 ± 7
15	71	70	68	67	47	9	56 ± 7
15[a]	138	136	123	94	34	5	88 ± 7

[a] H_2 pretreated

[b] Duplicate tests were run in all cases. The 95% confidence interval is based on a pooled variance.

All the above tests were pretest purged 16 hr with the carrier gas before testing. In the short beds, no effect due to H_2 pretreatment is noted, whereas the effect is quite large in the deeper beds. The same mechanism used to explain the results in Table 5 can be applied here if one considers the kinetics of the Ag_2O/Ag equilibrium to be slower in the presence of water vapor. The deeper beds provided the reaction time needed for conversion to the oxide. Of more importance, data from the 15-cm beds indicate a mass-transfer zone of 7.5 to 10 cm under these conditions. The iodine loadings obtained above the mass-transfer zone

are the loadings expected in deep beds. Thus, the data in the first 5 cm of the bed depth indicate loadings of 71 and 137 mg I_2/g AgZ for untreated and H_2-pretreated AgZ, respectively, could be obtained in deep beds. Again, the oxide is shown to be less reactive for iodine recovery than the metal.

A rough draft of a topical report entitled "Airborne Elemental Iodine Loading Capacities of Metal Zeolites and a Dry Method for Recycling Silver Zeolite", has been written. The topical report covers all the laboratory work done between January 1975 and February 1977. It includes a process-flow diagram illustrating full-scale application of AgZ regeneration and recycle to iodine recovery from the dissolver off-gas (DOG) of LWR fuel reprocessing plants. Sufficient engineering details are given to permit a preliminary cost analysis.

A conceptual design of a pilot plant to simulate DOG test streams and demonstrate the regeneration and recycle concept of AgZ for iodine recovery has been drafted. However, the Iodine Adsorbent and Storage Development program will be stopped at the end of FY 1977. Therefore, no further work on the conceptual design or fabrication of a pilot plant is planned.

Plans for Next Quarter

The effect of dew point, NO_2, and NO concentration on the iodine loading of 15-cm-deep beds of AgZ will be studied. Particular attention will be paid to the length of the mass-transfer zone and the iodine loadings in the saturation zone.

A 15-cm bed of AgZ will be loaded, regenerated, and recycled under conditions expected in the DOG to determine its loading capacity vs the number of times recycled. The stripped iodine will be chemisorbed on load-exchanged zeolite (PbX) downstream, and loading capacities at breakthrough will be determined.

The physical properties of the iodine on the PbX for storage will be determined. The iodine vapor pressure of the PbX vs temperature will be measured, and solubility of the adsorbed iodine in hexane and water evaluated.

The topical report will be published.

V. WASTE MANAGEMENT[a]

(B. E. Paige)

Liquid waste from the reprocessing of spent nuclear reactor fuels must be concentrated prior to and/or during interim storage to increase storage capacity and thereby reduce the cost of chemical reprocessing. The light water reactor liquid waste contains high concentrations of

[a]Part of the program LWR Fuel Reprocessing and Recycle administered by Savannah River Operations and Savannah River Laboratory.

fission products; thus, it requires greater heat transfer capability than has previously been required in the management of radioactive liquid waste. The primary purpose of the waste evaporation and storage program is to study factors which affect the rate of heat transfer as well as the service life of the equipment. This includes: (1) investigation of solids formation, fouling tendencies, and off-gas behavior during evaporation and storage, and (2) evaluation of materials of construction.

Simulated high-level liquid waste (HLLW) solutions are being used for current investigations in order to avoid the difficulties and expenses of experimenting extensively with actual radioactive LWR waste. Considerable attention is being given to the composition and preparation of the simulated wastes in order to produce solutions which resemble the actual wastes as closely as possible. Three types of simulated HLLW solutions which have been used for laboratory evaporations and waste storage studies were described previously.[a] In current work, HLLW solutions with a composition similar to that of the Barnwell Nuclear Fuel Plant waste, designated HLLW-BNFP, have also been prepared and investigated. Data obtained are compared to data from the three previous waste compositions. Simulated wastes are being evaluated to determine the effects of fission product substitutions and concentrations of process contaminants upon solids formation and materials behavior. This information will make future tests in the small-scale evaporators and storage tanks more meaningful. Results from these studies should finally be verified with actual LWR waste, for limited process conditions, using the experimental techniques developed in these studies with simulated waste.

1. Evaporation

Laboratory tests and evaporations of simulated HLLW have been performed to obtain data (boiling point rise, density, viscosity, and percent solids) for use in the design and operation of commercial HLLW evaporators and storage tanks and to provide criteria for construction of small-scale units for program studies. Precipitates have been characterized at various levels of evaporation. Current laboratory work primarily has been performed using a waste composition expected at the BNFP; this HLLW is considered more typical for currently planned LWR reprocessing plants than the three general HLLW compositions previously studied. The HLLW-BNFP waste contains lower corrosion product concentrations to reflect the use of a titanium waste evaporator and dissolver, and the phosphate concentration has been lowered to reflect more effective solvent cleanup systems. The HLLW-BNFP contains gadolinium as a nuclear poison. The HLLW-BNFP solution will be used for future small-scale evaporator studies and for laboratory waste storage tank studies.

---

[a] LWR Fuel Reprocessing and Recycle Progress Report for April 1 - June 30, 1976, ICP-1011 (November 1976).

1.1 Simulation of HLLW from BNFP (P. A. Anderson)

Early laboratory tests were performed on three types of waste solutions which were selected as representative of HLLW expected from future reprocessing plants. The three original solutions are designated HLLW-0 (containing minimal process additives), HLLW-Fe (containing high iron concentrations from dissolved basket liners), and HLLW-UP (containing high uranium and phosphate concentrations from extractant degradation).[1] The compositions of solutions currently being studied and designated HLLW-BNFP are shown in Table 7. The composition of wastes expected during early operation of the BNFP is based on longer-term cooling of stored fuel. The steady-state composition represents processing of short-term-cooled fuel. Simulated waste solutions were prepared from a series of stock solutions by a procedure previously reported.[1] For the present studies, waste having the composition of the early operation was used. Manganese, cobalt, and nickel were substituted as less expensive simulants for the fission products technetium, rhodium, and palladium, respectively. Ruthenium

TABLE 7

Composition of HLLW-BNFP Test Solutions

	Early Operation*	Steady State** Operation
Evaporated Volume	336 ℓ/MTU***	1375 ℓ/MTU
Total Fission Product Conc.	65 g/ℓ	22.4 g/ℓ
Uranium at 1% Process Loss	29.8 g/ℓ	7.3 g/ℓ
Soluble Poison (Gd)	66.7 g/ℓ	24.9 g/ℓ
Phosphate	0.50 g/ℓ	0.12 g/ℓ
Free HNO_3	4-7 M	4-7 M
Total NO_3^-	10 M	8 M
Corrosion Products****	0.22 g/ℓ	0.083 g/ℓ

*Based upon an estimated cooling period of 6.25 yr
**Based upon a cooling period of 1.8 yr
***Liters per metric ton of uranium
****Fe = 74%, Cr = 18%, Ni = 8%

was omitted from laboratory studies because of its high cost; no known simulant is considered satisfactory with respect to volatility and formation of solids. Previous studies have shown that these substitutions and omissions do not affect solids formation or physical properties of the slurries.[2]

[1] LWR Fuel Reprocessing and Recycle Progress Report for April 1-June 30, 1976, ICP-1101.

[2] LWR Fuel Reprocessing and Recycle Progress Report for October 1-December 31, 1976, ICP-1110 (January 1977).

1.2 Laboratory Evaporation of HLLW-BNFP (P. A. Anderson)

HLLW-BNFP solutions for laboratory evaporations were adjusted to 4918 ℓ/MTU in 2.5M HNO_3 to approximate the expected concentration of first cycle extraction raffinate at the BNFP prior to evaporation.

1.21 Acidity and Undissolved Solids Formation During Evaporations

HLLW-BNFP solutions were batch evaporated essentially without reflux from 4918 ℓ/MTU at 2.5M HNO_3 to 336 ℓ/MTU. As shown in Figure 9, the nitric acid concentration increased during evaporation to a concentration of approximately 12.8M which is considerably higher than predicted by LWR flowsheets and is also higher than waste compositions used in most solidification programs. Figure 10 illustrates that the quantity of undissolved solids in HLLW-0 decreases in higher concentrations of nitric acid regardless of the degree of evaporation. This shows that higher acid concentrations in the stored waste offer a possible process advantage of smaller quantities of undissolved solids.

Figure 11 illustrates the effect of acid concentration upon the undissolved solids content of two evaporated HLLW solutions. The HLLW-BNFP initially contained 2.5M HNO_3, while HLLW-0 contained 8.3M HNO_3. At the beginning of the evaporation, the undissolved solids content was lower in HLLW-0 solution which had the higher acid concentration. At about 700 ℓ/MTU, the acid concentrations become approximately the same. As the evaporation continued, the undissolved solids contents of both solutions increased rapidly.

A comparison of HLLW-BNFP evaporations to those made previously with HLLW-0, HLLW-Fe, and HLLW-UP[a] showed that smaller amounts of undissolved solids were present in the HLLW-BNFP solutions when the acidity was the same, regardless of the degree of evaporation. The reduced quantity of undissolved solids HLLW-BNFP may be attributed either to the reduced phosphate content or to the increased content of soluble gadolinium and uranium.

The undissolved solids from the HLLW-BNFP are easily suspended at all degrees of evaporation. Fewer solids plated on the laboratory evaporator heat transfer surfaces with HLLW-BNFP than with solutions previously studied, whereas higher acid concentrations tend to increase plating in other HLLW solutions.

1.22 Physical Properties of Evaporated HLLW-BNFP

Evaporated HLLW-BNFP at 336 ℓ/MTU contains approximately 30% total dissolved and undissolved solids compared to approximately 20% for HLLW-0 at the same degree of evaporation. The density of HLLW-BNFP slurry as it is evaporated is presented in Figure 12. The density of HLLW-BNFP is higher than for HLLW-0 because of higher dissolved solids concentrations. The boiling point rise is presented in Figure 13 for use in design and operation of waste evaporators. The boiling point rise, with respect to dissolved solids content, is approximately the same for HLLW-BNFP as for

[a] LWR Fuel Reprocessing and Recycle Progress Report for July 1 - September 30, 1976, ICP-1108 (December 1976).

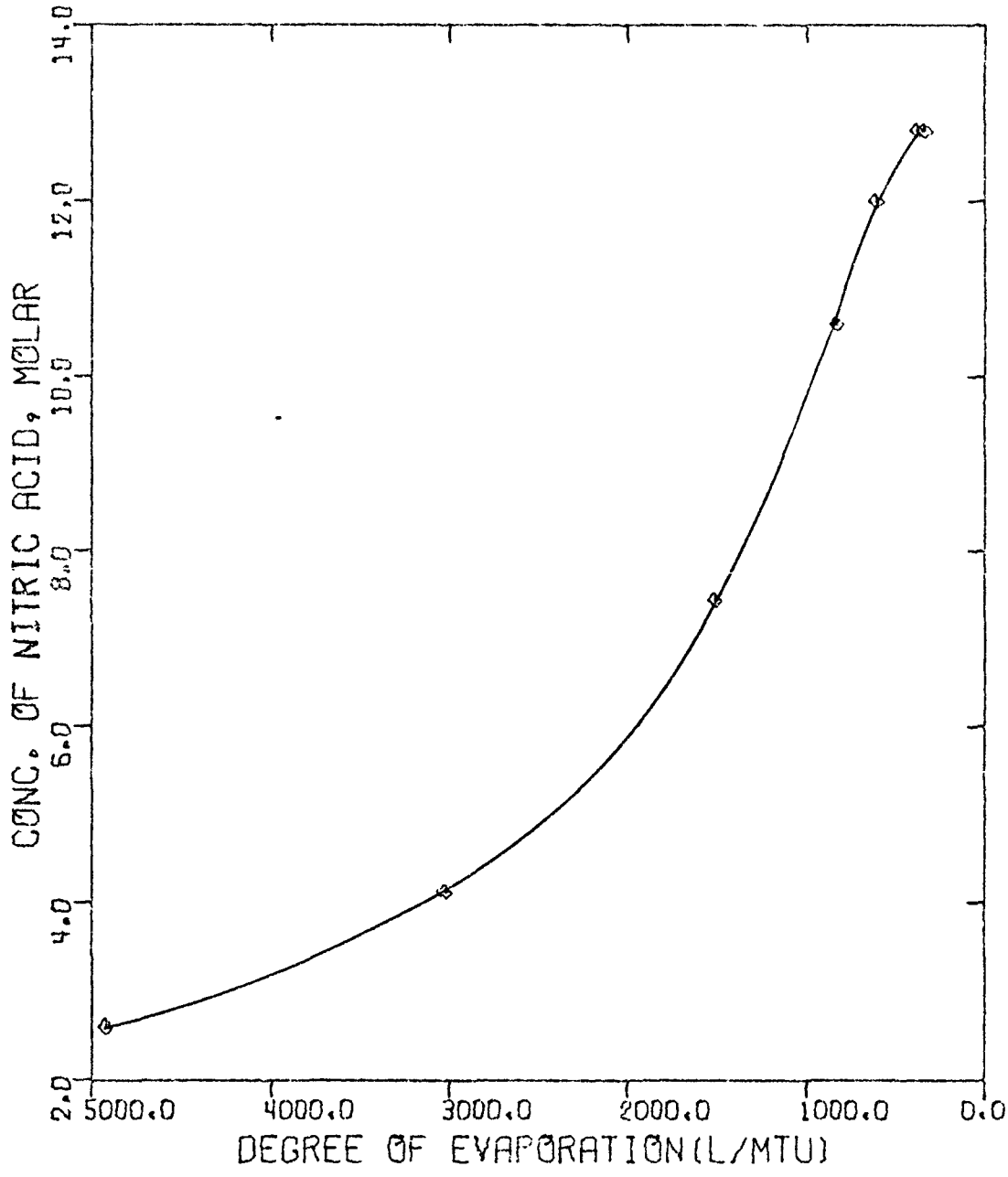

Figure 9. Acid Concentration of Evaporated HLLW-BNFP vs Liters per MTU

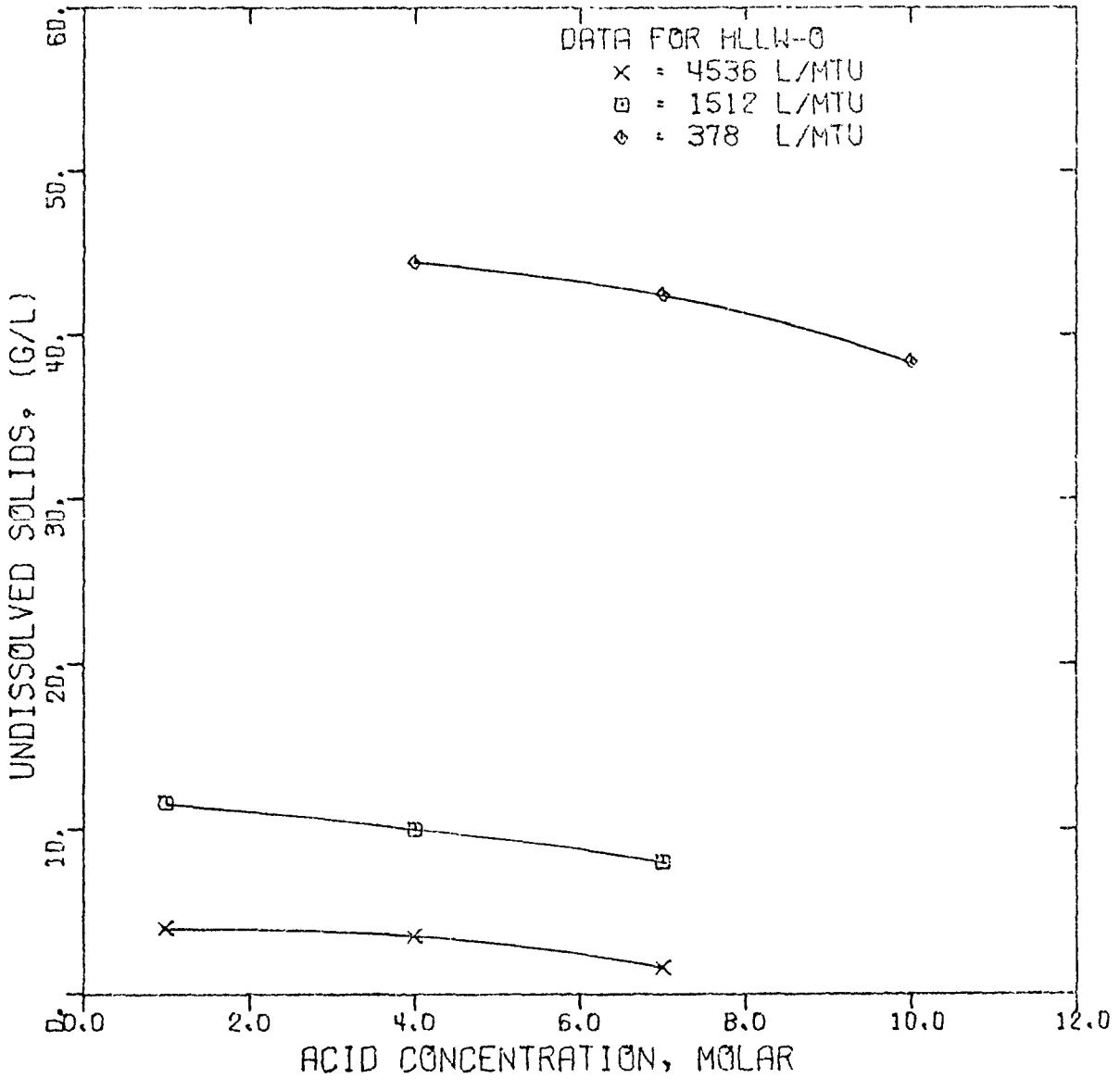

Figure 10. Effect of Nitric Acid Concentration in High-Level Liquid Waste

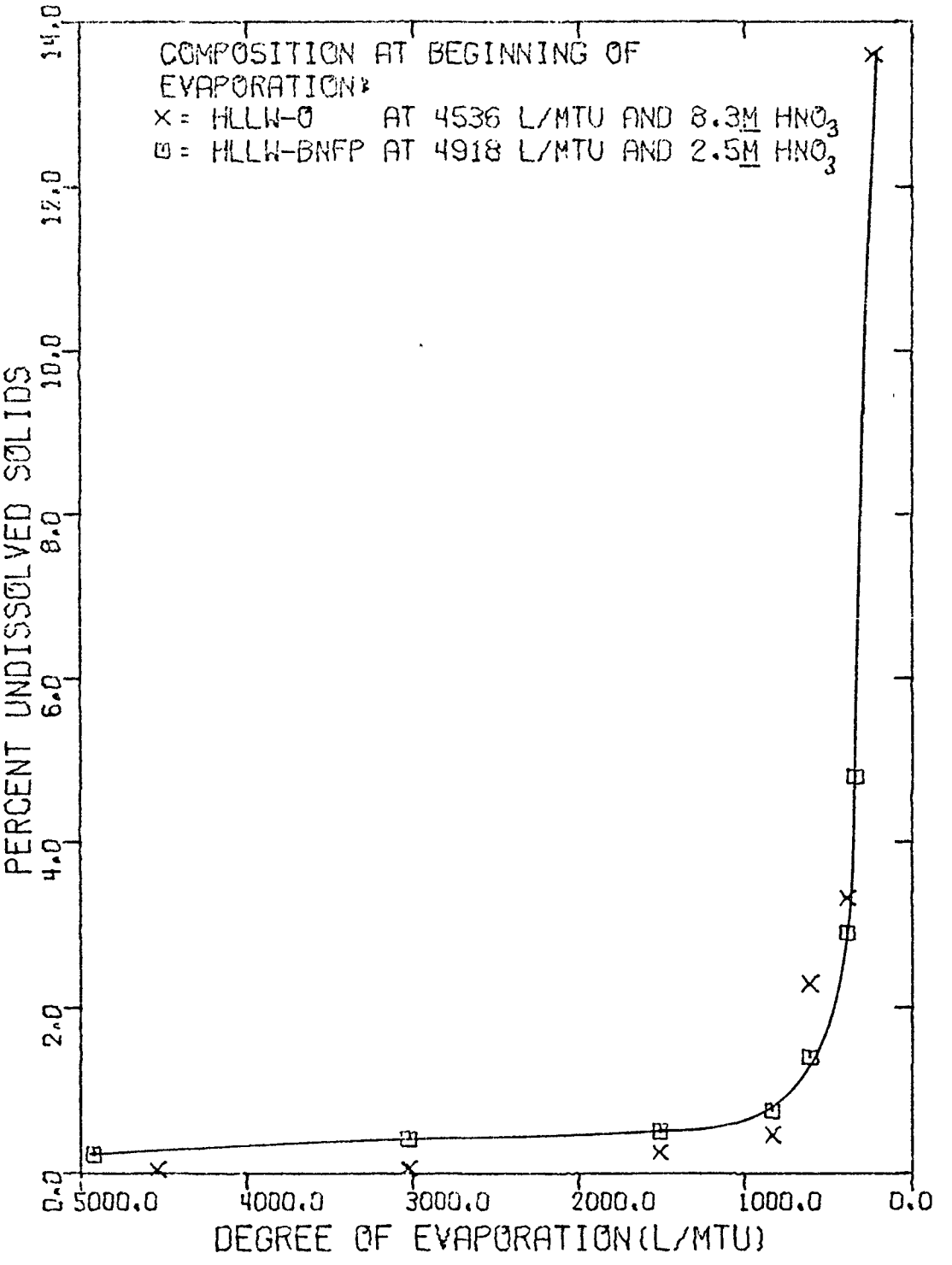

Figure 11. Relative Undissolved Solids in Evaporated High-Level Liquid Waste

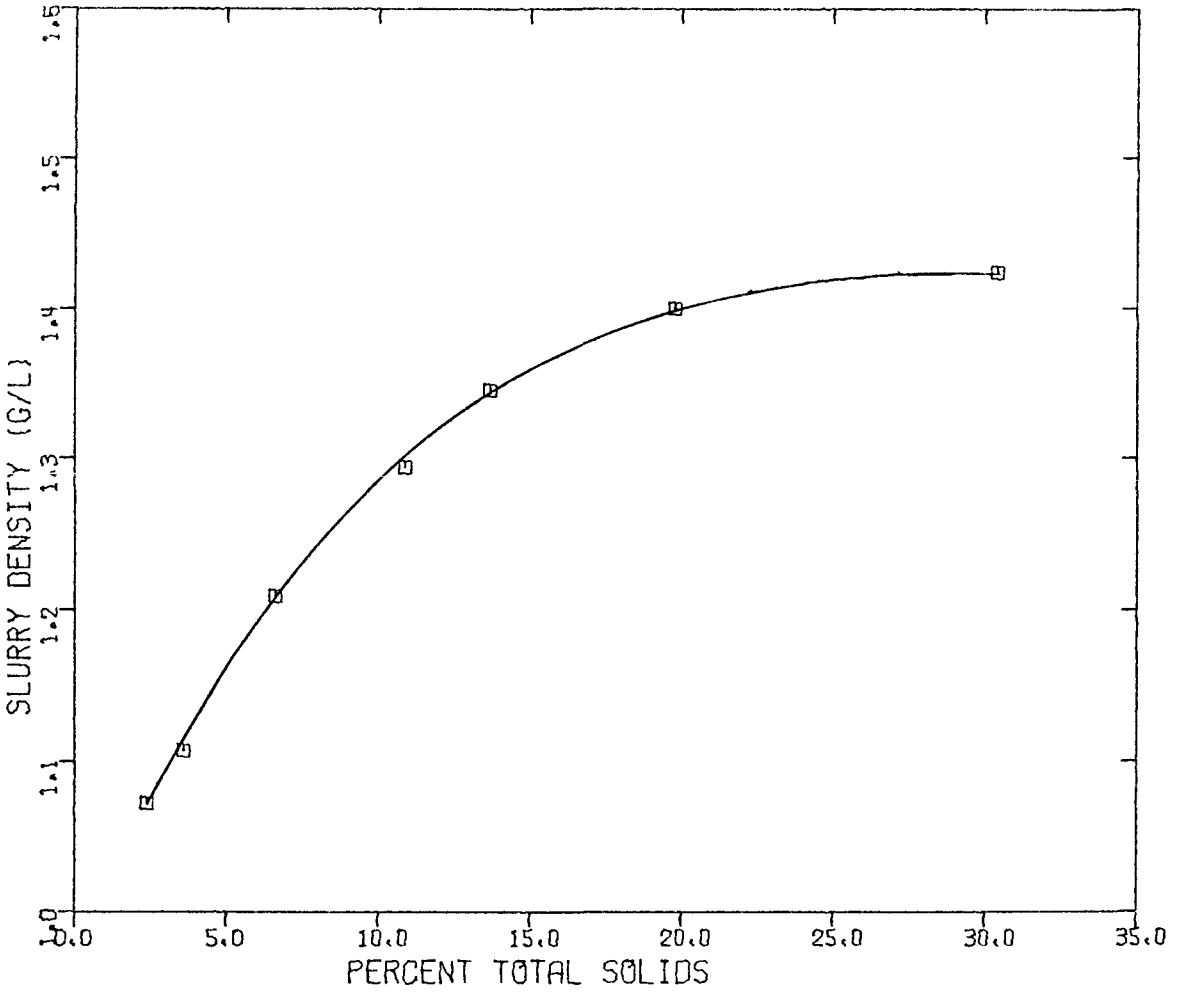

Figure 12. Slurry Density of HLLW-BNFP Relative to Total Solids (Dissolved plus Undissolved)

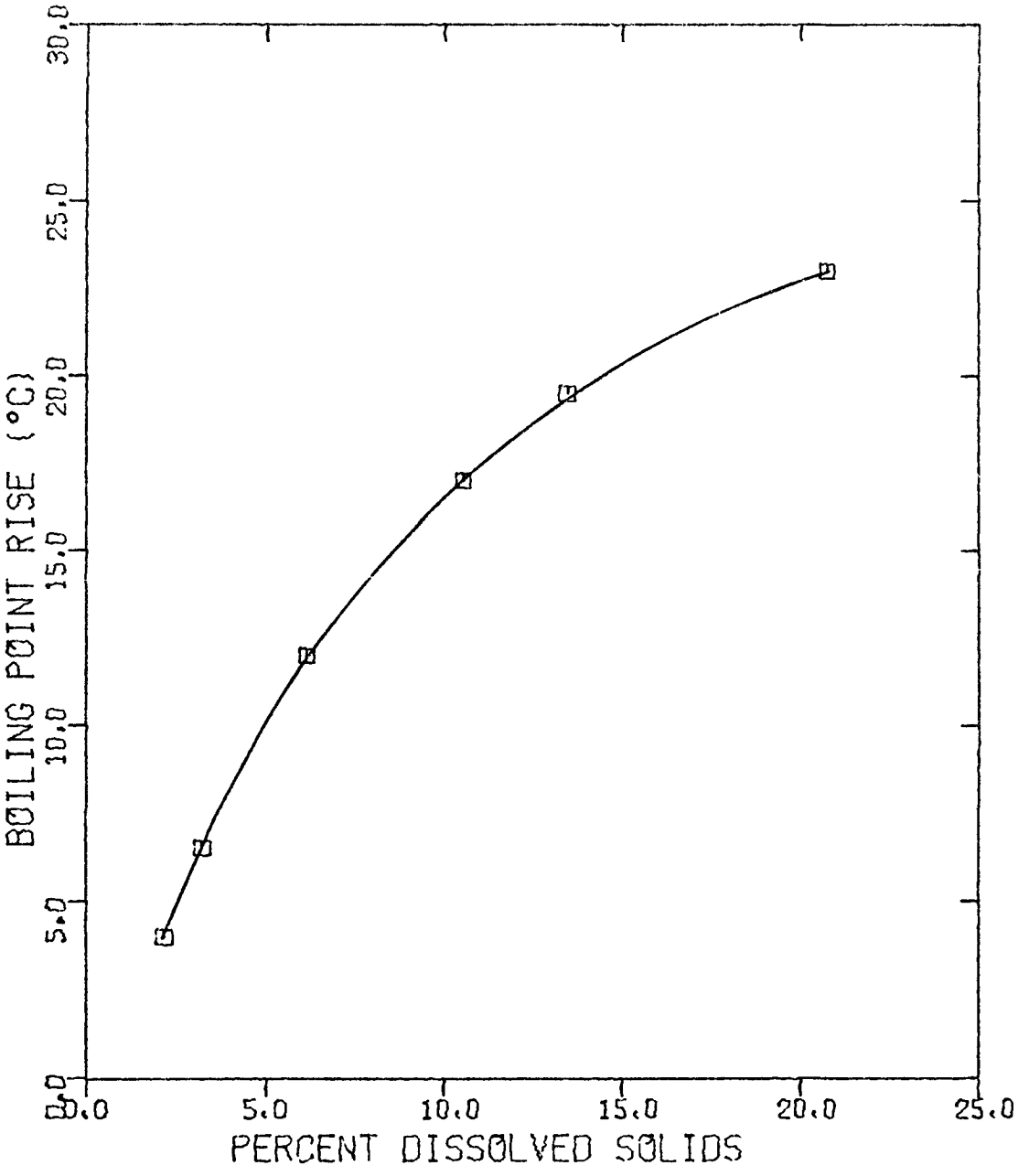

Figure 13. Boiling Point Rise During Evaporation of HLLW-BNFP (Based on 95.0 $\pm$ 0.5°C, The Boiling Point of water at approx. 630 mm local pressure.

HLLW-0. However, the temperatures encountered with HLLW-BNFP waste in a thermosiphon evaporator will be about 10°C higher at the 336 ℓ/MTU level due to the higher levels of dissolved solids. A boiling point increase of approximately 25°C (the maximum expected for evaporation to 336 ℓ/MTU) should not greatly affect evaporator design.

1.23 Characterization of Solids

Freshly prepared simulated solutions of HLLW-BNFP at 4918 ℓ/MTU contain essentially no visible solids, but increasing cloudiness appears within 10 minutes at room temperature. The rate of formation of visible solids also increases with temperature. Freshly prepared (<5 minutes) HLLW-BNFP at 4918 ℓ/MTU contained <0.1 g/ℓ undissolved solids at room temperature. The same solution held at 70°C contained 2.2 g/ℓ after 68 hours and 2.4 g/ℓ after an additional 22 hours. Freshly prepared solution which was heated to boiling over a two-hour period, also contained 2.4 g/ℓ undissolved solids. This indicates that the undissolved solids content should not increase in the BNFP-type first-cycle raffinate, which is boiled in the dissolver, even if the solution is stored for several days before it is evaporated.

When stored at 60°C, the undissolved solids in HLLW-BNFP concentrated to 336 ℓ/MTU are easily suspended with gentle agitation. Most of the solids settle again within 5 to 10 minutes when agitation ceases, which is considerably faster than in HLLW-0. HLLW-BNFP slurries at 336 ℓ/MTU form copious amounts of crystalline solids when stored at room temperature; therefore, solutions should not be cooled below 60°C during storage.

The elements contained in the undissolved solids in HLLW-BNFP are identical to those in HLLW-0. X-ray diffraction data show the presence of a distinct crystalline compound with its most intense lines at d=5.70, 4.20, 3.62, and 3.11 angstroms. It appears to be a hydrated form of $ZrMo_2O_8$. Slurries at 336 ℓ/MTU also contain small amounts of the nitrates of cesium, barium, and strontium which salt out in high concentrations of nitric acid.

1.3 Small-Scale Evaporator (G. R. Villemez)

The construction of the small-scale thermosiphon evaporator was completed. The unit will be operated to evaporate simulated HLLW from LWR fuel reprocessing waste to evaluate the effects of fouling, corrosion, contamination, and fission product entrainment in the off-gases.

The small-scale evaporator unit was checked out with water at two vapor rates in the reboiler tube. The overall heat transfer coefficient was 105 Btu/hr/ft^2/°F with a vapor rate of 1.0 ft/sec and 290 Btu/hr/ft^2/°F at a vapor rate of 2.9 ft/sec.

1.31 Evaporation of Nitric Acid

The evaporator was operated in a continuous mode for 30 hours using a 2.5M nitric acid feed. The product was 8.6M nitric acid and the vapor condensate was 1.28M nitric acid. During this preliminary run, the overall

heat transfer coefficient was 377 Btu/hr/ft^2/^{o}F with a vapor rate of 1.25 ft/sec in the reboiler tube. A complete run will be made with nitric acid to establish the baseline for each reboiler tube test material.

1.32 Operating Criteria for HLLW

The operation of the small-scale thermosiphon evaporator will be directed toward the study of variables related to the evaporation of HLLW-BNFP solutions (See Section 1.1). The same dependent variables will be used for Type 304L stainless steel and titanium reboiler tube materials. Each reboiler material will be inspected after 158 hours of operating time for the effects of exposure to the HLLW-BNFP solutions. Each run includes three operating conditions during the total of 158 hours operating evaporation time as follows:

(1) Evaporate 20 liters of HLLW-BNFP solution at 2.5M nitric acid from 4918 ℓ/MTU to 1375 ℓ/MTU in 48 hr.

(2) Evaporate 20 liters of reconstituted HLLW solutions from Run 1 from 4918 ℓ/MTU to 336 ℓ/MTU in 62 hr.

(3) Recirculate vapor condensate together with a HLLW-BNFP solution from Run 2 at 336 ℓ/MTU for 48 hr. The solution will be 12.5M nitric acid at 336 ℓ/MTU according to laboratory evaporation data.

The independent variables to be studied include the waste feed compositions. Initially, HLLW-BNFP in 2.5M nitric acid, which represents raffinate from the extraction cycle, will be used. Changes in composition which may be investigated in the future include the concentration level (ℓ/MTU), corrosion product level, acid concentration, and the phosphote content. The maximum temperature difference will be 14^{o}C based upon the boiling point of the HLLW solution and the safety limit of 130^{o}C for Purex waste evaporations. The reboiler tube materials used in these tests will be Type 304L stainess steel and titanium metal. The dependent variables will be fouling, scaling, heat transfer, corrosion rate of reboiler material, and contamination of solution with corrosion products. In addition, the effects of corrosion and fission products entrainment in the off-gas system will be investigated. Later tests will investigate other materials.

2. WASTE STORAGE

Storage studies will determine the behavior of stored HLLW and provide design and operational data for efficient and economical storage of commercial LWR liquid waste until it is solidified. In the initial studies, three types of evaporated HLLW are being tested over an extended period for solution stability, undissolved solids formation, and corrosion of Type 304L stainless steel. Viscosities of evaporated HLLW slurries and supernates have been measured and are reported for use in heat transfer calculations for liquid waste storage tanks.

A laboratory storage tank is being designed and constructed for preliminary studies to determine the effect of solution mixing, solids suspension, scaling, and other phenomena on heat transfer to the cooling coils. The glass equipment is patterned after the BNFP waste tanks for interim liquid waste storage.[a] Preliminary data and operational experience obtained with this laboratory unit will be applied to the design of a small-scale stainless steel storage tank. This will provide criteria for the operation of existing waste tanks, and design of future waste tanks, and can serve as a prototype for any future studies with actual LWR waste.

2.1 Storage of Evaporated HLLW (P. A. Anderson)

Long-term storage studies, with three types of HLLW slurries at constant temperature and without agitation, are continuing. HLLW-BNFP has also been stored at 60°C and will be evaluated for stability with respect to undissolved solids. The physical changes to date are small in the slurries which have been stored up to 8 months.

2.2 Viscosity of HLLW (C. B. Millet)

Viscosity values, which are required for calculation of heat transfer and flow characteristics, have been obtained for HLLW solutions. The viscosities have been measured for both slurries and supernates at various temperatures and degrees of evaporation. Both HLLW-0 and HLLW-BNFP solutions were investigated.

The viscosity of the HLLW-BNFP at 25°C is 0.97 centipoise (cp) at 4918 ℓ/MTU and increases to 1.86 cp as the waste is evaporated to 336 ℓ/MTU. The viscosity begins to increase rapidly as the solution is evaporated to less than 1512 ℓ/MTU as shown in Figure 14.

Temperature has a very pronounced effect on the viscosity of a liquid. For nonassociated liquids, the logarithm of the viscosity is an almost linear function of the reciprocal of the absolute temperature. Figure 15 shows almost a linear relationship of the log of viscosity to reciprocal of the absolute temperature for water; the values for water plotted were obtained from the Lange Handbook of Chemistry.[b] The viscosity of HLLW-0 and HLLW-BNFP solutions was measured at several temperatures; the relationship plotted in Figure 15 is also nearly linear. This plot may be used to approximate viscosities of HLLW solutions at other temperatures. The viscosity of HLLW-Fe slurry at 378 ℓ/MTU was measured at 60 and 70°C and found to be 1.66 cp and 1.42 cp., respectively. The viscosity of HLLW-UP slurry under the same conditions was 2.86 and 2.64 cp, respectively.

---

[a] LWR Fuel Reprocessing and Recycle Progress Report for October 1 - December 31, 1976, ICP-1110 (January 1977).

[b] N. A. Lange, Handbook of Chemistry, New York: McGraw-Hill, (1961).

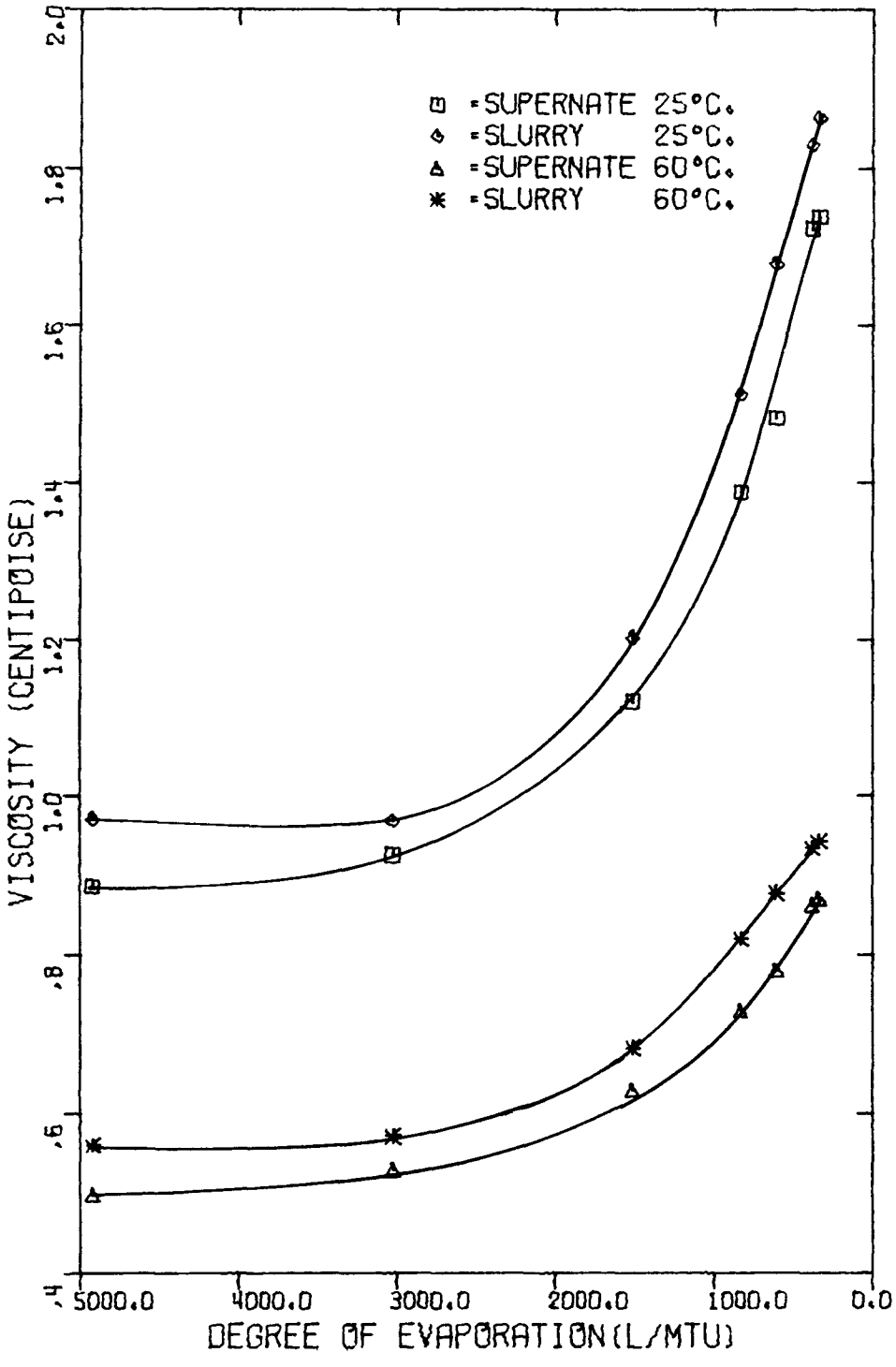

Figure 14. Viscosity of Evaporated HLLW-BNFP

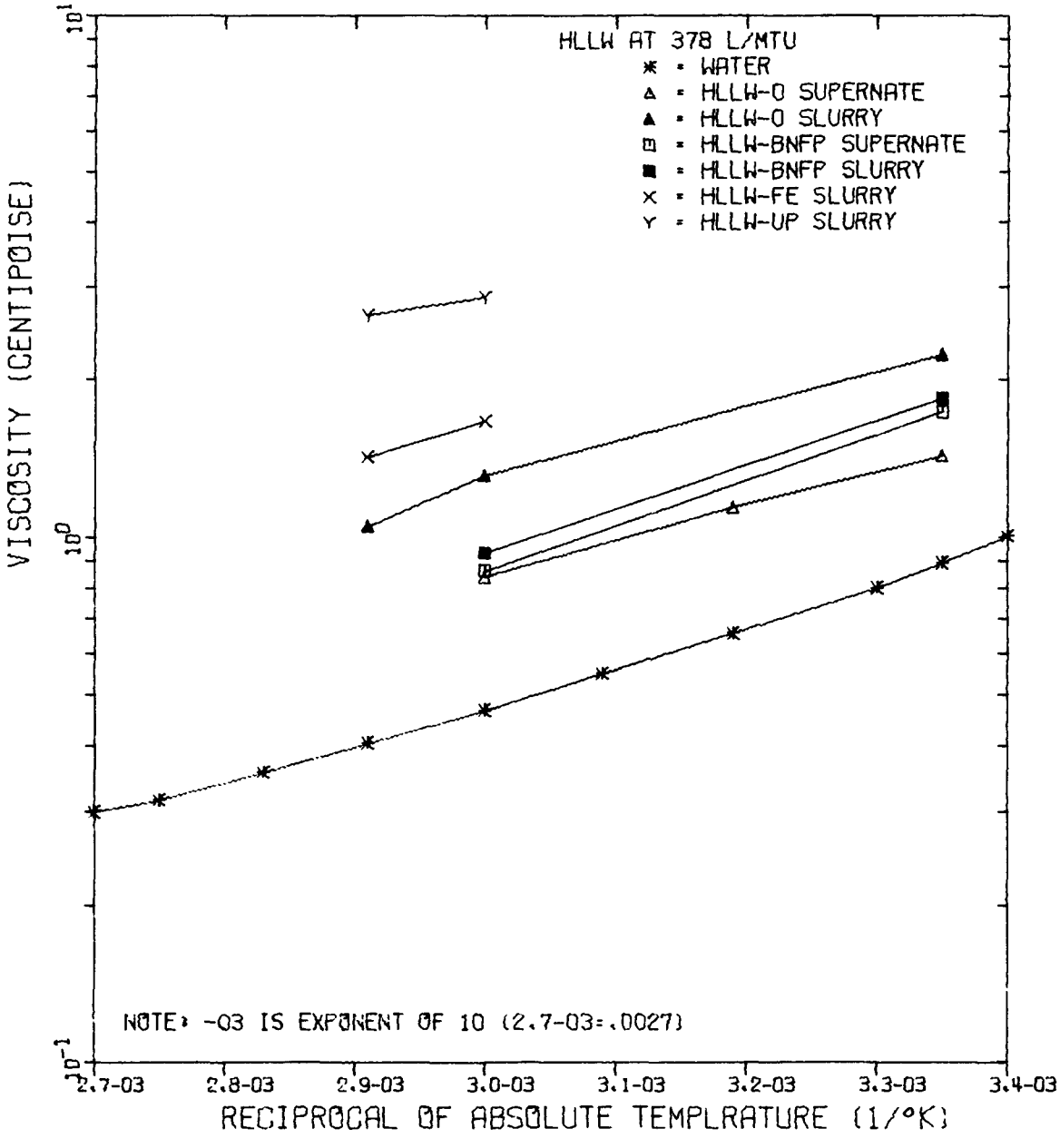

Figure 15. Effect of Temperature on Viscosity of High-Level Liquid Waste

The viscosity of supernates of centrifuged HLLW solutions at 378 ℓ/MTU were measured to determine the effect of suspended solids. The viscosity of the supernate was 1.43 cp at 25°C and 0.84 cp at 60°C. As shown in Figure 15, the slurry solutions containing the precipitated solids exhibited a viscosity 1.55 times that of the supernate both at 25 and 60°C. Figure 15 also shows that for each HLLW-0 and HLLW-BNFP solution, the slope of the supernate line is the same as that of the slurry.

2.3 Bench-Scale Storage Tank (P. A. Anderson, C. B. Millet)

Assembly of the laboratory storage tank is complete. The experimental unit consists of a 12-inch-diameter glass tank with a 3.6 gallon capacity. It is designed to model selected conditions in a large HLLW storage tank and will establish operational and design criteria for future experimental storage equipment. The primary emphasis of the present equipment design is to obtain preliminary heat transfer data and to establish criteria for the small-scale stainless steel storage tank. The glass tank is enclosed in a constant temperature Plexiglas cubicle to minimize heat loss from the tank and to allow visibility during mixing and to observe behavior of the undissolved solids. Mixing of the solution and suspension of the solids will be accomplished with two glass ballast tank agitators and two glass air-lift circulators. The tank geometry is not intended to model the exact mixing conditions in a large HLLW storage tank, but it will serve to verify the adaptability of the mixers to small-scale experimental storage equipment. The tank is vented through a total reflux condenser to minimize evaporation losses via air from the ballast tank agitators or air-lift circulators.

Based on previous laboratory evaporation studies, initial tests will be made at 60°C using HLLW-BNFP evaporated to 336 ℓ/MTU and containing approximately 12.8M nitric acid. The solution will be monitored for changes in the heat transfer coefficient with respect to changes in acidity, density, viscosity, settling, undissolved solids content, and caking or plating of solids on the heat transfer surfaces.

3. MATERIALS AND CORROSION

Materials and corrosion studies are being conducted both in the laboratory and in small-scale equipment to (1) establish the effect of waste composition and components on materials of construction, and (2) to investigate new materials for evaporators and for waste tanks and their auxiliary components. In addition, methods for monitoring corrosion of liquid waste tanks during interim storage of liquid waste are being investigated.

3.1 Laboratory Corrosion Tests (G. R. Villemez, C. B. Millet)

Modified Huey tests are being used to determine corrosion rates for the materials of construction for evaporators, storage tanks, and auxiliary equipment. In current work, unwelded coupons are submerged in boiling solution to determine the corrosion rates. Loss of weight is usually determined for three 24-hour periods and one 96-hour period to complete one week of total exposure. In cases where initial rates were considerably higher, the coupon was exposed for an additional week.

Laboratory corrosion tests are being continued to determine the effects of various fission product substitutions so that simulated HLLW will resemble actual LWR waste as closely as possible in the small-scale evaporator.

3.11 Variation in Corrosion Product Level

The effect of the corrosion products in different HLLW simulated waste solutions has been determined. Tests with Type 304L stainless steel coupons have been performed in HLLW-0 evaporated to 378 ℓ/MTU containing 7M nitric acid. The corrosion product level was varied from zero to 9.15 g/ℓ as shown in Figure 16. The corrosion rate increased from 77 to 130 μm/yr as the corrosion product level increased from 0.62 g/ℓ to 1.83 g/ℓ, respectively; at a corrosion product level of 9.14 g/ℓ, the corrosion rate was accelerated to 1100 μm/yr. The normal corrosion product level of the HLLW-BNFP is 0.22 g/ℓ.

Acceleration of the corrosion rate occurs at a corrosion product level of about 0.6 g/ℓ. Based on these data, the small-scale evaporator operation will be designed to keep the corrosion product concentration in HLLW below this point of accelerated corrosion whenever possible.

The normal corrosion product level of the HLLW-BNFP will be set at 0.001 g/ℓ in the initial feed to the evaporator. This level was determined by calculating the total wetted area of all dissolution and separation vessels having significant residence times and adding 50% of this area for piping and miscellaneous small equipment.

The corrosion product level of the HLLW-BNFP solution used for liquid waste studies is 0.22 g/ℓ for early operation with longer-cooled fuel. This level was determined by calculating the total wetted area of the storage tank and computing the corrosion product level in the liquid waste after five years storage.

3.12 Process Variables

Type 304L stainless steel coupons with surfaces as-received in the hot rolled and annealed condition were exposed for 168 hr in boiling solutions of HLLW-BNFP. Corrosion rates were about 100 μm/yr, which was less than half the rate observed in HLLW-0 solution at the same conditions.

The corrosive effect of two potential descaling solutions was also investigated. A 5% solution of Turco Alkaline Rust Remover[a], which was found to corrode Type 304L stainless steel at only 31 μm/yr for a 24-hr test, looks promising. A 2M oxalic acid solution had a corrosion rate of 2640 μm/yr for a 24-hr period and, therefore, will probably receive no further consideration as a descaling agent.

---

[a]Turco Products, Inc., Division of Purex Corporation, Carson, Calif.

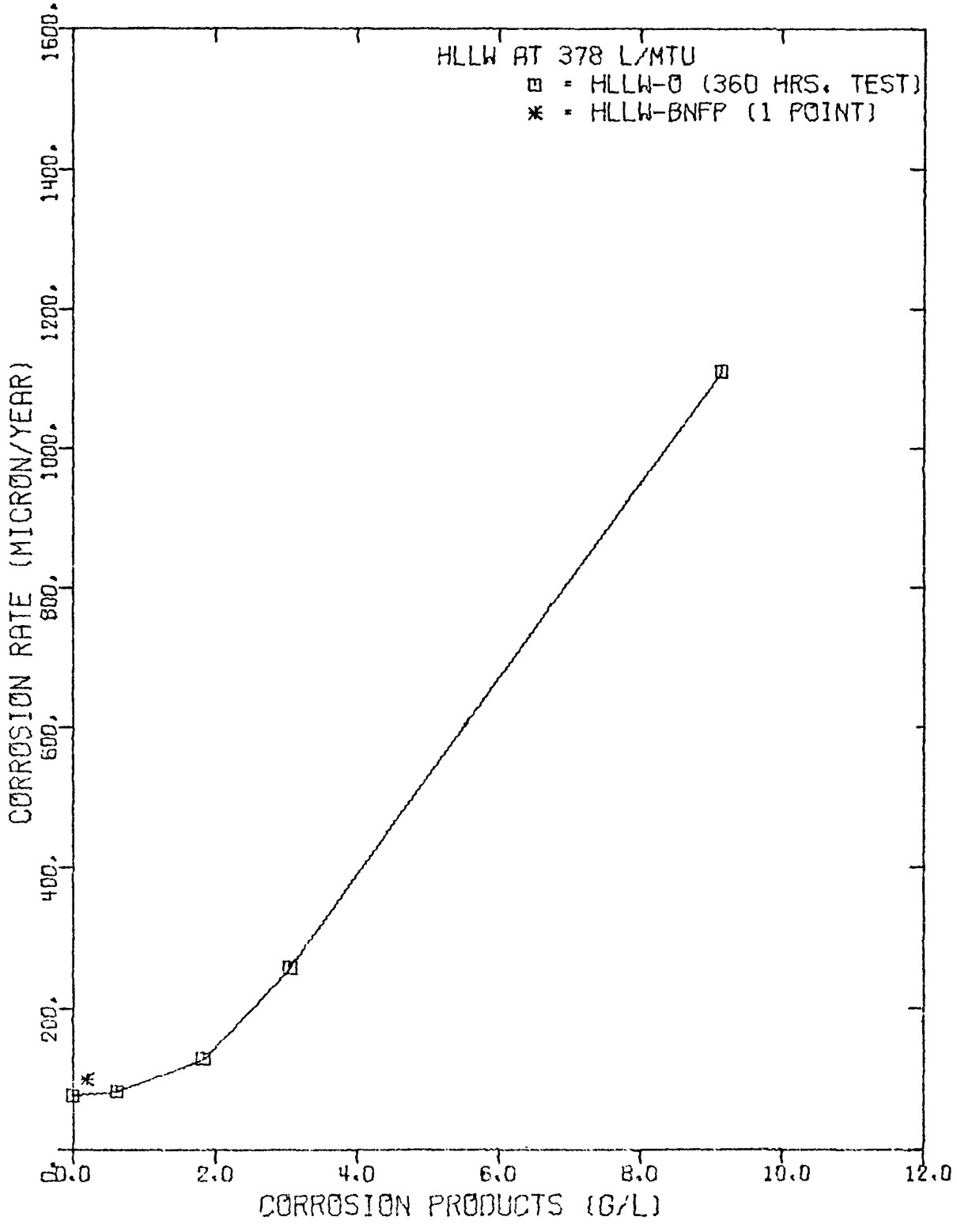

Figure 16. Effect of Corrosion Products Concentration in High-Level Liquid Waste

3.2 Monitoring of Storage Tanks

Laboratory tests to evaluate the effectiveness of electronic corrosion monitoring probes are proceeding. The use of electronic corrosion monitoring equipment offers the advantage of remote monitoring without the contamination and personnel exposure problems associated with retrieving metal coupons. Individual Type 304L stainless steel probes are immersed at 60°C in HLLW-0, HLLW-Fe, and HLLW-UP solutions which are stirred at one-hour intervals to suspend the solids. Corrosion readings were made with a corrosometer and probes. Probes in the HLLW-0 and HLLW-Fe solutions showed continuous corrosion throughout the test period. Rates for the HLLW-UP solution fluctuated, possibly because of plate-out of the solids on the electrode. The corrosion rates obtained by the electronic probes over a four-month period were confirmed by the weight loss of the coupons immersed in the same solutions as is shown in Table 8.

TABLE 8

Corrosion Rates in Stored HLLW Solutions

Type of Solution at 378 ℓMTU	From Electronic Probe[a], μm/yr	From Coupons μm/yr[b]
HLLW-0	8	9
HLLW-Fe	21	19
HLLW-UP	13	5

[a]Average corrosion rates over time periods of 49 to 73 days at 60°C

[b]Average corrosion rates over time period of 22 days at 60°C

Remote corrosion monitoring of actual HLLW solutions will require probes constructed of radiation resistant materials. Present probes contain small amounts of Teflon and plastic, chiefly as electrical insulators. These materials could deteriorate when exposed to actual HLLW. The estimated dose rate is 2.6×10^6 rad/hr for a probe extending 3.6 inches into a large storage tank containing HLLW at 378 ℓ/MTU with a burnup of 35,000 MWd/MTU and a cooling period of one year. Communications with corrosion probe manufacturers indicate that probe construction can be modified to use electrical insulating materials which will tolerate such exposure.

Two types of electronic corrosion monitoring equipment are generally available. One monitors the amounts of corrosion experienced over an entire exposure period, while the other provides an instantaneous reading of corrosion rate. The latter has not been used for the present studies because long-term corrosion monitoring in large storage tanks does not require instantaneous rate information. However, such instrumentation could be considered for monitoring corrosion in process equipment which is in contact with solutions of varying composition.

VI. HTGR FUEL REPROCESSING AND WASTE MANAGEMENT

(L. W. McClure)

During reprocessing of high temperature gas-cooled reactor (HTGR) fuel blocks, the fuel is crushed and the graphite matrix is burned which exposes the fuel particles. The fuel particles are then crushed and burned in a secondary, fluidized-bed burner. During the burning, fission-product oxides will be volatilized. Laboratory tests are being conducted to study the nature of the vaporized fission products and their condensing characteristic. Studies are also underway to design a device to remove the volatilized fission products from the off-gas stream. The work is being done under subcontract to Oak Ridge National Laboratory.

1. Tube Furnace Experiments

(K. L. Wagner)

The volatility of the fission products expected to be present in the HTGR secondary burner are being determined in tube furnace experiments. Vapor pressure information on many of the elemental and oxide forms of the expected fission products in an oxygen rich atmosphere is available;[a] however, information on the carbides and chlorides and the effects of the burning graphite environment on their stability and volatility had not previously been reported.

The chemical nature of the fission products in the irradiated fuel particles when they enter the secondary burner is not presently known. The elemental, oxide, and carbide forms of the fission products predicted to be present at more than 0.1 g per fuel element,[b] were selected for study and comparison in the tube furnace volatility tests. Most of the tracers which will be used are available only as chlorides; therefore, determination of the volatility of the chlorides of the selected fission products was included in this study for comparison with volatilities of the elemental, oxide, and carbide forms. This information is presented in Table 9.

The experiments were conducted in a simple tube furnace apparatus (Fig. 17) located in a hood. Approximately a 1-5 ratio of sample to graphite was used. A quartz sample boat, containing the mixture of sample and graphite was placed in a 2.5-cm-diameter quartz furnace tube. The sample was heated in stages to 900°C under 5 scfm of dry air which entered at one end of the furnace tube. The other end of the tube was connected to a modified "Millipore" fritted glass filter support which holds a 5-cm-diameter glass fiber filter circle. The air stream was scrubbed before release into the hood.

---

[a] Ray G. Bradford, Donald D. Jackson, "Volatilities of the Fission Product and Uranium Oxides", UCRL-12314 (January 20, 1965).

[b] A Fort St.Vrain Reactor (FSVR) fuel element weighs 116 kg of which 10.35 kg are fissile plus fertile heavy metals.

TABLE 9

SUMMARY OF TUBE FURNACE VOLATILITY TESTS

Species	Grams/FSVR Element (6 year burnup, 1 year cooling, fissile plus fertile)	Observation
Barium	56.7 g	Not volatile at 900°C-form $BaCO_3$
BaO_2		Not volatile at 900°C-form $BaCO_3$
BaC_2		Not volatile at 900°C-form $BaCO_3$
Cadmiun	0.699 g	Volatile at 700°C-form CdO
CdO		Volatile at 900°C
$CdCl_2$2-1/2 H_2O		Volatile at 700°C
Cerium	99.2 g	Not volatile at 900°C
CeO_2		Not volatile at 900°C
CeC_2		Appears volatile at 900°C-analyses pending
Cs_2O	76.9 g	Volatile at 300°C
CsCe		Volatile at 900°C
Eu_2O_3	3.84 g	Not volatile at 900°C
Molybdenum	105.0 g	Volatile at 900°C-forms MoO_3
MoO_3		Volatile at 500°C
$MoCl_5$		Volatile at 200°C
Rb_2O_4	18.6 g	Volatile at 500°C
RbCl		Volatile at 900°C
Ruthenium on carbon	47.5 g	Volatile at 900°C
RuO_2		Volatile at 900°C
$RuCl_3xH_2O$		Volatile at 500°C
Strontium	39.2 g	Not volatile at 900°C-forms SrO and SrO_2
SrO		Not volatile at 900°C
$SrCl_2.6H_2O$		Volatile at 900°C
SrC_2		Appears volatile at 900°C-analyses pending
Tellurium	18.2 g	Volatile of 500°C-forms TeO_2
TeO_2		Volatile at 700°C
$TeCl_4$		Volatile at 300°C

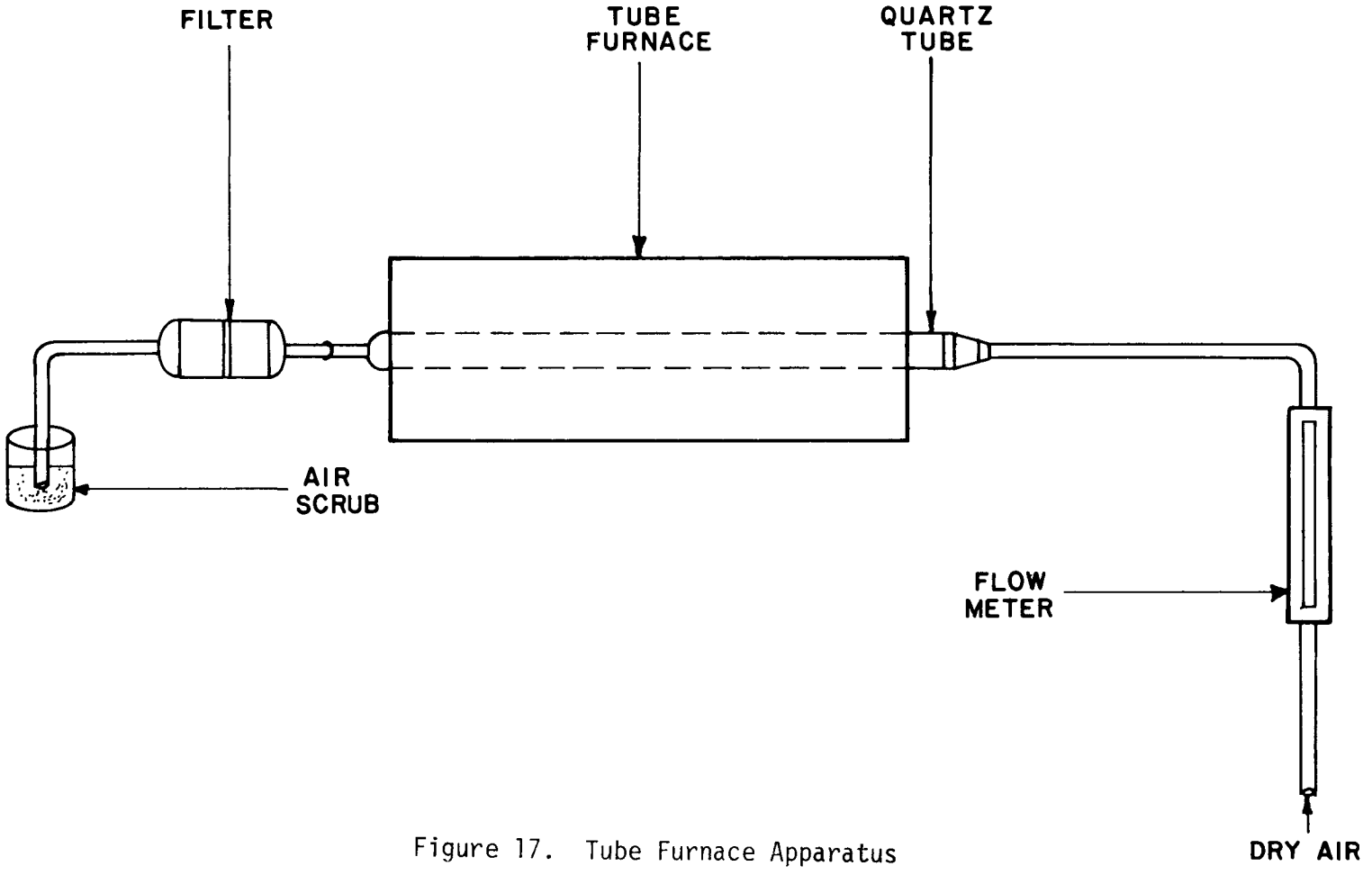

Figure 17. Tube Furnace Apparatus

Observations of volatility and condensation were made at 300, 500, 700, and 900°C. Analyses of the sample boat residue, washings from the quartz furnace tube, filter deposits and the scrub solution were made to determine a mass balance.

2. Semi-Volatile Fission Product Literature Search

(G. O. Haroldsen)

Chemical equilibrium and volatility data from the literature relevant to HTGR semi-volatile fission products has been collected and examined. Extensive use was made of the data from Bradford and Jackson and from Williams[a]. Additionally, a significant amount of information was obtained from handbooks, books,.and reports pertaining to the chemistry of molybdenum, technetium, tellurium, and ruthenium. These data plus data derived from our own current tube-furnace tests give considerable insight into anticipated chemical forms and vapor pressures.

Figure 18 displays the vapor pressures of five of the semi-volatiles anticipated in HTGR fuel reprocessing. Table 10 lists the amounts of the eight most abundant species to be found in spent Fort St. Vrain Reactor fuel. The estimated yield is for the fertile particle fraction of the fuel. These values were selected because FSVR fuel may be the first HTGR fuel to be reprocessed. The quantities of the individual species, as well as the total of all the species,indicate the magnitude of the semi-volatiles. Molybdenum, which will probably be converted to the trioxide in the crushed particle burning step, is the constituent in greatest abundance. This fission product contributes very little towards the radioactive level of the fission products, but is very significant in physical quantity.

The conclusions of the evaluation of the data from the literature are:

(1) In fluidized-bed burning, the vaporization of the semi-volatiles can be expected to be quite rapid and to occur early in the burning cycle. (If the kinetics of chemical conversion from one oxide to another is slow, the vaporization period could be prolonged. Pu could be an example.)

(2) During vaporization, the partial pressure of several of the semi-volatiles will probably be approximately 100 mm Hg. The combined partial pressure, assuming overlapping boil-off characteristics, would likely be greater than 100 mm Hg. The relatively high vapor pressures will accentuate deposition and plate-out as the off-gases are carried through the processing equipment and cooled.

[a]W. Reid Williams, "Removal of Volatile Fission Products by Condensation, and Evaluation of Methods for Predicting Performance", ORNL/ENG/INF-76/3 (November 1976).

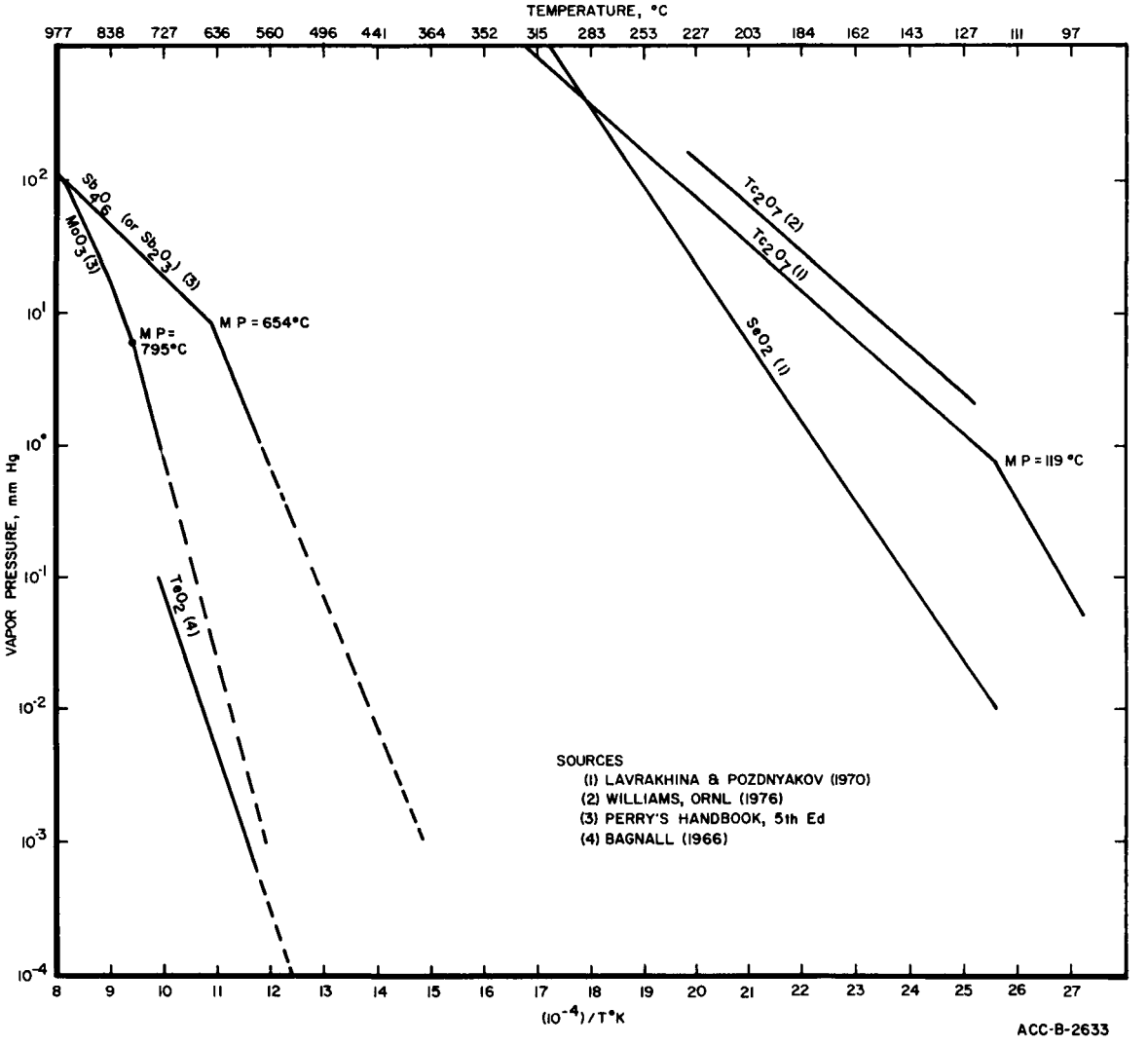

Figure 18. Vapor Pressure of Some of the Semi-Volatile Oxides

TABLE 10

SEMI-VOLATILE FISSION PRODUCT YIELD FROM FSVR FUEL[a]

Element	Yield Per FSVR Fuel Element (g)	% Yield in Fertile Particles	Yield in Fertile Particles, FSVR (g)	Probable Oxide Form (Gaseous Phase)	Yield of F.P. Oxide/FSVR Fuel Element (g)
Se	2.69	54.2	1.46	SeO_2	2.05
Rb	18.6	58.7	10.9	RbO	12.9
Mo	105.0	33.6	35.3	$(MoO_3)_3$	53.4
Te	22.6	33.9	7.66	Tc_2O_7	12.0
Ru	47.6	26.1	12.4	RuO_4	20.3
Sb	.373	65.7	.245	Sb_2O_3	.29
Te	18.2	51.7	9.41	TeO_2	11.8
Cs	78.6	37.3	29.3	CsO	32.8
TOTALS	293.7		106.6		145.5

(a) Six year irradiation, 6 months cooling.

(b) Estimated from inspection of Chemical equilibrium data. Does not consider possible interactions of the semi-volatiles themselves.

Plans for Next Quarter

The tube furnace experiments will be continued to complete the data on the remaining chloride and carbide fission-product forms.

A bench-scale, quartz fluidized-bed burner will be operated to verify the tube furnace tests on a larger scale. Vaporization and deposition of various forms of fission products will be observed.

An off-gas cleanup device will be designed, fabricated and tested. This cleanup device will provide a controlled deposition point for the fission products and will be designed to allow removal of the deposited fission products from the system.

VII. NATURAL FISSION REACTOR STUDIES (OWI Funding via LASL)

(W. J. Maeck, R. L. Eggleston, F. A. Duce, J. E. Delmore, R. A. Nielsen, W. A. Emel)

A unique approach to the study of the long-term behavior of waste containing fission products and the actinide elements in geologic environments is through the analysis of the remains of natural fission reactors. In 1972, the natural fission reactor at the Oklo pit in the Republic of Gabon was discovered. Initial studies conducted by both the French CEA and United States ERDA laboratories and reported at the IAEA Conference on the Oklo Phenomenon[a] showed that most of the fission products had remained in place for a period of ∿2000 million years. Of particular importance was the high degree of retention of plutonium and the higher actinides in the vicinity of the natural reactor.

The major effort during the report period was the analysis of ∿25 rich uranium ore samples for Ru in an attempt to determine if other natural reactors once existed. Ruthenium is an ideal monitor for fossil reactor remains, because the natural occurrence of Ru in the earth's crust is very small, i.e., approximately one part in 10^9. Thus, the isotopic composition of natural occurring Ru is significantly altered if contaminated with fission product Ru, whose isotopic composition is significantly different from that of natural.

In all cases, the measured Ru isotopic composition for these 25 samples could not be attributed solely to natural Ru or that expected from pure ^{235}U thermal fission. After correction for natural Ru, the resulting isotopic composition varied from sample to sample, and in all cases was still significantly different from that produced by ^{235}U thermal fission. We now believe that the observed isotopic composition is the result of Ru produced by a mixture of ^{238}U spontaneous fission and induced ^{235}U thermal fission.

---

[a] "The Oklo Phenomenon", Proceedings of an IAEA Symposium, Libreville, Gabon, (June 1975).

Unlike the fission product Ru isotopic abundances for ^{235}U thermal fission, which decreases with increasing mass number, the Ru isotopic abundances for these samples increased with increasing mass; the abundance of ^{101}Ru being larger than ^{99}Ru, and ^{102}Ru being larger than ^{101}Ru. The abundance of ^{104}Ru was less than that of ^{102}Ru. Although no ^{238}U spontaneous fission yield data exist for the stable fission products of Ru, we believe that the ^{238}U spontaneous fission yields for the stable Ru isotopes can be estimated from these data. For the present, we have assumed that the Ru isotopic data which shows the greatest divergence from that expected from ^{235}U thermal fission most closely approximates the fission product distribution for ^{238}U spontaneous fission. All other values are the result of a mixture of induced ^{235}U thermal fission and ^{238}U spontaneous fission. Assuming further that the mass 99 fission yield is equal (6.15%) for ^{235}U thermal fission and ^{238}U spontaneous fission, we have calculated the ^{238}U spontaneous fission yields for ^{101}Ru, ^{102}Ru, and ^{104}Ru. These values are given in Figure 19 along with the ^{235}U thermal fission yields over the mass range of 99 to 106. Also included are literature values[a] for ^{238}U spontaneous fission for masses 103, 105, and 106. The significant fine structure in the ^{238}U spontaneous fission mass-yield curve can be correlated with reflected measured yields[a] on the heavy mass peak, assuming a value of 2 for nubar. We believe these new ^{238}U spontaneous yields are within ±10% of the true value.

To further pursue the measurement of the ^{238}U spontaneous fission yields for the stable isotopes of Ru, the Los Alamos Scientific Laboratory (LASL) has provided an ore sample in which the fissiogenic Ru is believed to be only representative of ^{238}U spontaneous fission. This sample is currently being analyzed.

Knowledge of the ^{238}U spontaneous fission yields for Ru is important to the development of a new method for dating the age of formation of uranium ore bodies. The proposed method is based on the relationship,

$$T = \frac{N_{Ru}}{(\lambda^{SF})(N_u)(FY_{Ru})} ,$$

where T is the time in years since the formation of the ore body, N_{Ru} is the number of atoms of fission product Ru produced from the spontaneous fission of ^{238}U per unit of sample, λ^{SF} is the spontaneous fission decay constant for ^{238}U ($8.46 \times 10^{-17} yr^{-1}$), N_u is the number of U atoms per unit of sample, and FY_{Ru} is the fractional ^{238}U spontaneous fission yield for the isotopes of Ru measured (FY_{Ru} = 0.26 for ^{99}Ru + ^{101}Ru + ^{102}Ru + ^{104}Ru). To calculate the true age, the decay of ^{238}U since the time of formation of the ore body must also be considered.

[a] D. L. Swindle, R. J. Wright, P. K. Kuroda, J. Inorg. Nucl. Chem. 33, pp 876-879 (1971).

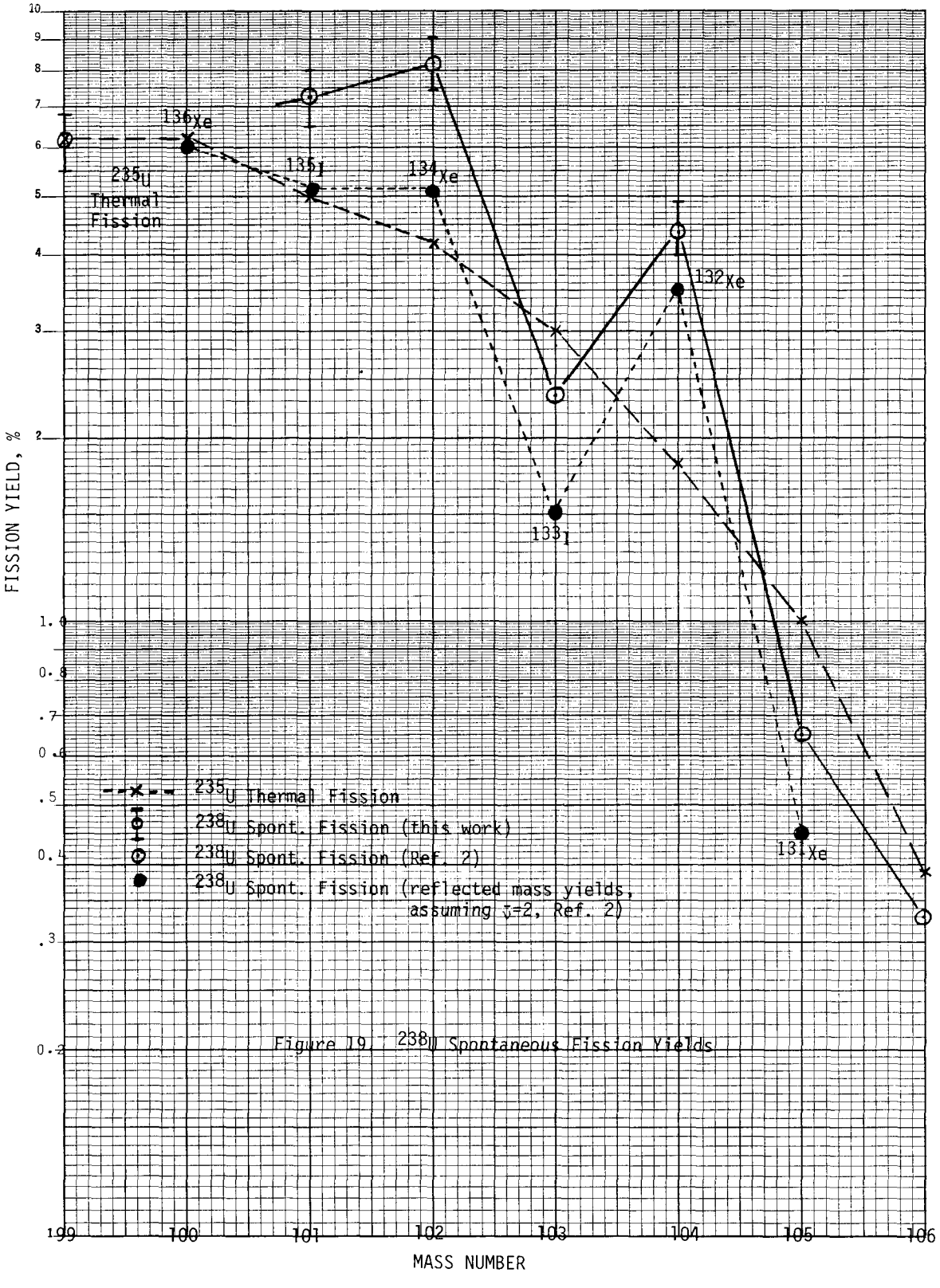

Figure 19. ^{238}U Spontaneous Fission Yields

In a normal uranium ore sample, Ru can originate from three sources: natural Ru, ^{238}U spontaneous fission, and ^{235}U induced thermal fission. After correction for the natural Ru component, the resulting isotopic mixture can be separated into the ^{238}U spontaneous fission component and the ^{235}U induced fission component based upon a knowledge of the fission yields for the respective sources of fission. Hence, the need to know the ^{238}U spontaneous fission yields.

Using the ^{238}U spontaneous fission yield values for Ru generated from the ore samples analyzed to date, several age dating calculations have been made, especially for samples collected by LASL during a recent visit to the major Canadian ore producing regions. The initial results are most encouraging. Triplicate analyses of one ore sample for U and Ru gave the age of the deposit as $1.21 \pm 0.06 \times 10^9$ yrs. This is within the estimated age range for samples from this particular area. The amount of ^{238}U spontaneous fission produced Ru in this sample was $\sim 3 \times 10^{13}$ atoms ($\sim$5 ng) per gram of sample. The uranium content was $\sim$40%. The analysis of other samples gave ages in general agreement with the expected ages.

This age dating technique is especially attractive because, 1) the natural abundance of Ru in the earth's crust is very low ($\sim 1 \times 10^{-9}$), 2) the formation of the stable measured product is almost instantaneous with no intermediate highly soluble elements with long half-lives in the decay chain, and 3) to the best of our knowledge, no significant migration of Ru occurs from the uranium mineral in which it was formed.

Investigation of this technique in a cooperative effort with LASL will continue.

*

SPECIAL MATERIALS PRODUCTION

I. LONG-TERM MANAGEMENT OF ICPP HIGH-LEVEL WASTES

1. Post Calcination Treatment of High-Level ICPP Wastes

Pellet Formation and Pellet Properties Studies (K. M. Lamb, H. S. Cole)

A pelleted waste form is being considered as an advanced product for on-site storage of ICPP high-level wastes. Pelletizing the calcine reduces dispersibility, improves retrieval and imparts high leach resistance. If necessary for repository storage, pellets could be converted to a monolithic form by incorporation in concrete or conversion to a glass or metal matrix.

Thirteen pellet formulations, using boric acid, calcium hydroxide and metakaolin as solid binders plus 85% phosphoric and 70% nitric acid as liquid binders, were prepared on the 16-inch-diameter disc pelletizer. The characteristics of these pellets are listed in Table 1. Pellets P-3 and P-8A were the most free-flowing from the pelletizer and had the best physical properties. Pellet compositions P-I and P-3 had the fewest off-sized pellets. These pellets were spherical with an irregular surface caused by protruding calcine particles. Pellet composition P-3 was chosen for more detailed property evaluations.

Leach rates and impact resistance of the various pellet compositions are shown in Table 1. These properties were measured after drying at 200°C, and after heat treating for one hour at 750°C. The pellets were spheres of about 7 mm diameter and 1.8 g/cc density. This low density is attributed to the density (~1.3 g/cc) of the calcine bed granules, which do not densify on pelletizing. Leach rates were determined by Soxhlet extraction at 95°C for 100 hours in distilled water. The impact resistance of the pellets was determined by dropping them from a height of 9.75 meters (32 ft) onto a steel surface. Broken pellets most often remained in large pieces; 25 to 50% of the fragments were greater than 1.2 mm diameter. Less than 10% of the fragments were below 0.42 mm diameter.

Pellet leach rates also were measured in three simulated salt-bed brine solutions, in NH_4OH (pH 9.5), and in acetic acid (pH 3.5). Leaching solutions were stirred at room temperature for 19 hours. Soxhlet leach data are reported for comparison in Table 2. Pellets in brine solutions "A" and "B" invariably gained weight possibly because they absorb dissolved solids from the nearly saturated brine solutions. Solution "A" was high (306.3 g/ℓ dissolved solids, pH = 6.5) in Na^+, K^+, Mg^{++}, and Cl^- ions; solution "B" (297.2 g/ℓ dissolved solids, pH = 6.5) was high in Na^+ and Cl^- ions. Pellets had slight weight losses in brine solution "C" (a simulated ground water containing 3.7 g/ℓ dissolved solids pH = 7.5) and in the caustic solution. Losses of ~1 wt% were observed in the acid solution. Based on data presented in Tables 1 and 2, pellets P-3 and P-8A appear to have the best overall properties.

TABLE 1

Properties of Various Pelleted ICPP Waste Compositions

Sample No.	Pellet Compositions, wt%				Liquid Binder	Physical Characteristics	Pellet Size (in.)	Treatment Temperature	95°C Leach Rate, (wt% loss 100 hr)	Impact Test, wt% broken
	Calcine	Meta-Kaolin	H_3BO_3	$Ca(OH)_2$						
P-1	90	--		10	2:1 H_3PO_4-H_2O	Uniform spheres	1/4-3/8	200	--	--
								750	0.42	10.6
P-2	80	20	--	--	2:1 H_3PO_4-H_2O	Irregular shapes	1/8-3/8	200	--	1.3
								750	0.38	3.4
P-3	85	5	10	--	3:1 H_3PO_4-HNO_3	Uniform spheres with some roughness	1/4-1/2	200	--	0
								750	0.60	3.0
P-4	80	--	--	20	3:1 H_3PO_4-HNO_3	Irregular and dusty	1/8-12	200	28.7	22.7
								750	0.42	5.5
P-5*	80	10	--	10	3:1 H_3PO_4-HNO_3	Irregular and rough	<1/8	---	--	--
P-6*	85	5	5	5	3:1 H_3PO_4-HNO_3	Irregular, dusty, agglomerated	<1/8-1/4	---	--	--
P-6A*	85	5	5	5	2:1:1 H_3PO_4-HNO_3-H_2O	Irregular, dusty, agglomerated	<1/8	---	--	--
P-7*	90	--	10	--	3:1 H_3PO_4-HNO_3	Spheres with flat spots	1/8-3/8	---	--	--
P-7A	90	--	10	--	2:1 H_3PO_4-H_2O	Some irregular shapes	1/8-1/4	200	29.6	2
								750	1.10	33.5
P-8	90	5	5	--	2:1 H_3PO_4-H_2O	Spherical, some oversize	~1/8	200	11.1	4.7
								750	0.84	10.5
P-8A	90	5	5	--	2:1:1 H_3PO_4-HNO_3-H_2O	Spherical	1/4-3/8	200	11.8	1.2
								750	0.92	1.7
	90	5	5	--	3:1 H_3PO_4-HNO_3	Spherical and rough	~1/4	200	13.4	2.6
								750	0.96	1.9
P-9*	85	10	5	--	3:1 H_3PO_4-HNO_3	Irregular	<1/8-3/8	---	--	--

Not tested because of undesirable physical properties.

TABLE 2

Leach Rates for Several Pelleted Waste Compositions

Sample No.	wt% Change after 19 hr: In Brine Solution A	In Brine Solution B	In Brine Solution C	Acid Leach	Caustic Leach	Soxhlet Leach, wt% lost in 100 h @95°C
P-3[a]	+4.54	+4.50	-0.03	-0.84	-0.09	0.6
P-3[b]	+3.30	+3.72	-0.03	-0.94	-0.08	1.0
P-7	+2.87	+3.93	-0.01	-1.22	-0.09	1.1
P-8	+2.41	+1.70	+0.01	0.86	0.09	0.8
P-8A	+4.48	+4.01	-0.05	-0.85	-0.28	0.9
P-8B	+2.87	+2.59	-0.002	-1.11	-0.08	1.0

[a] = heat treated for 1 hr at 750°C
[b] = heat treated for 1 hr at 850°C

TABLE 3

Effect of Heat Treatment Temperature on Leach Rate for Pellet Composition P-3

Time, hr.	Treatment °C	Leach Rates, wt% Loss (-) or Gain (+) in 19 hr. In Brine Solution A	In Brine Solution B	In Brine Solution C	Acid Leach	Caustic Leach	Dist. H_2O @ 95°C
1	700	-	-	-	--	--	-0.74
2	700	-	-	-	-0.44	-0.26	-0.37
1	750	+4.54	+4.50	-0.03	-0.84	-0.09	-0.37
2	750	+4.58	+5.03	-0.02	-0.54	-0.16	-0.25
1	800	-	-	-	-0.96	-0.22	-0.35
2	800	+3.70	+3.85	+0.03	-0.59	-0.14	-0.22
1	850	+3.30	+3.72	-0.03	-0.94	-0.08	-0.28
2	850	+3.14	+3.33	-0.02	-0.67	-0.05	-0.23
1	900	-	-	-	-1.06	-0.09	-0.15
2	900	+3.48	+3.14	+0.05	-0.72	-0.03	-0.19

The effect of heat-treatment temperatures, as determined by both Soxhlet and brine leaches, is shown in Table 3 for pellet composition P-3. Heating the pellets for two hours at 750 to 800°C produces leach rates equivalent to heating for one hour at 850 to 900°C (see Figure 1).

Plans for Next Quarter

Pellet formulations will be compression tested and evaluated for long-term weight loss on heating at 450°C to determine nitrate loss and change in leach resistance (if any) at prolonged intermediate temperature storage. Glass formulations with ICPP calcine will be prepared and tested.

Pneumatic transport and flow properties of pelleted waste will be investigated to determine the limit in pellet size.

Design of a microwave heated pellet dryer will begin.

2. Actinide Removal Studies

(L. D. McIsaac, J. D. Baker)

Distribution coefficients for actinides and key elements between synthetic ICPP zirconium-aluminum first-cycle raffinate and the extractant, dihexyl-N,N-diethylcarbamylmethylenephosphonate (DHDECMP) were measured. These data are presented in Table 4. The acid value was obtained by titration. Tracers were used for all other measurements except for aluminum and fluorine. All tracers were added as the nitrates and allowed to equilibrate for at least one hour before extraction. The neptunium value was determined with an 0.01M Cr+6 oxidant present to raise the inextractable Np(V) to Np(VI).

The DHDECMP extractant was purified before use by vacuum distillation and was ~85% pure as determined by gas chromatography. After dilution to 30% with xylene, the extractant was scrubbed sequentially with half-volume portions of 0.5M Na_2CO_3 and water.

No practical tracers are available for aluminum and fluorine, and common analytical procedures have inadequate accuracy; therefore, the distribution coefficients for these elements were determined by activation analysis. The short half-lives of the neutron activation products (^{26}Al $t_{1/2}$=2.2m, ^{20}F $t_{1/2}$=11s) necessitated setting up the Ge(Li) radiation detection system next to the CFRMF[a] reactor at the test reactor area. Extractions were performed and aliquots of aqueous and organic were activated and analyzed for gamma-rays present in the decay of the aluminum and fluorine activities.

[a] Coupled Fast Reactivity Measurement Facility

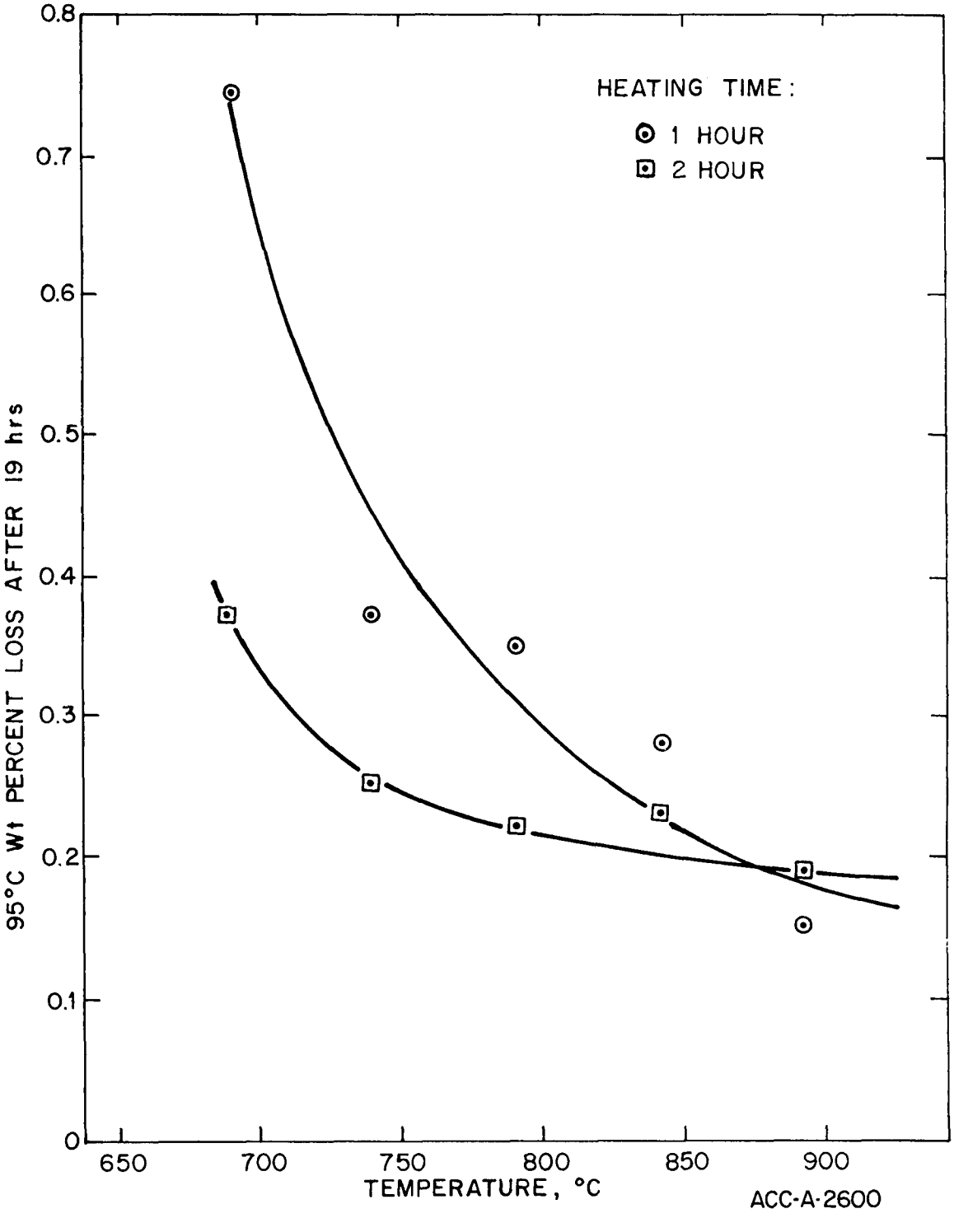

Figure 1. Effect of Heat treatment Time and Temperature on Leach Rates of Pellets

TABLE 4

Extraction, Scrubbing and Stripping Distribution Coefficients (E_a^o) using 30% DHDECMP in Xylene and Synthetic Zr-Al First Cycle Raffinate

Element	Extraction	Scrub[a]	Strip 1	2	3[b]
	$V_o/V_a = 1$	$V_o/V_a = 5$		$V_o/V_a = 1$	
Pu(IV)	7.6	43	0.04	<0.01	-
Np(VI)[c]	44	29	4.8	<0.10	-
Am(III)	5.0	3.7	0.34	0.006	-
U	91	27	9.2	0.076	0.014
Hg	2.6	8.5	~30	~20	-
Eu	21	2.7	0.22	0.002	-
Nd	3.1	3.4	0.34	<0.1	-
Ce	3.6	3.8	0.52	0.015	-
La	3.5	4.2	0.48	0.016	-
Ba	0.0075	0.0053	-	-	-
Cs	0.00026	<0.004	-	-	-
Te	0.013	-	-	-	-
Sb	<0.005	-	-	-	-
Sn	<0.0005	-	-	-	-
In	<0.004	-	-	-	-
Ag	0.032	0.044	-	-	-
Pd	1.65	0.23	0.45	~3	-
Rh	0.12	0.056	-	-	-
Ru	0.58	0.34	6.7	5.7	5.4
Tc	1.10	0.25	1.8	2.3	-
Mo	0.27	0.14	-	-	-
Nb	0.13	0.074	0.032	-	-
Zr	0.015	0.066	0.044	-	-
Y	0.30	0.66	0.039	<0.02	-
Sr	0.0094	<0.006	-	-	-
Rb	0.00018	-	-	-	-
Cu	<0.002	<0.02	-	-	-
Co	<0.001	-	-	-	-

TABLE 4 (Cont):

Element	Extraction	Scrub[a]	Strip 1	2	3[b]
	V_o/V_a = 1	V_o/V_a=5	V_o/V_a = 1		
Fe	<0.002	<0.005	-	-	-
Cr(III)	0.0087	-	-	-	-
Al	0.0025	-	-	-	-
F	0.043	-	-	-	-
H^+	0.34	-	-	-	-

Except where noted, all values have an estimated accuracy of ± 10%.

[a] 6M HNO_3-Vo/Va is the volume ratio of organic/aqueous

[b] 0.05M HNO_3-0.05M $H_2C_2O_4$

[c] Aqueous made 0.01M Cr(VI) before extraction

An actinide removal workshop at Hanford, Washington was attended by L. D. McIsaac. Mr. W. Schulz, of Atlantic Richfield Hanford Co., and his staff demonstrated a procedure using A26[a] resin in the OH^- form and ethylene glycol for purification of crude DHDECMP. Gas chromatographic methods for analyzing impurities present in DHDECMP were discussed.

Distribution coefficients have been measured for the extraction of Cm(III), Am(III), Np(IV), Np(VI), Pu(IV), and U(VI) from various nitric acid solutions with 30% DHDECMP in diisopropylbenzene. The analysis of these results will be reported in the next quarterly report.

The centrifugal molecular still purchased from CVC Products, Inc., Rochester, N.Y. has arrived. Leaking valves have been repaired and the unit is being tested for use in the purification of DHDECMP.

Plans for Next Quarter

We expect to use the new molecular still for purifying DHDECMP. This will involve the slow process of determining distillation parameters for components present in the crude extractant. Preparations will begin for a hot minimixer-settler run using DHDECMP as extractant.

[a] A26 is a macroreticular anion resin marketed by Rohm and Haas, Philadelphia, PA.

3. Calcined Solids Retrievability and Handling

(B. D. Rose, J. S. Schofield)

Work began on methods to sample the radioactive calcine in Bin Set N.2. Further development of prototypical retrieval equipment has been postponed until representative calcine samples can be obtained.

Examination of the stored calcine is needed to assure that subsequent equipment design is adequate to retrieve the calcine. A survey was made of sampling equipment which could remove a 1-2-inch-diameter sample from the entire bin depth and cause minimum material disturbance. Either a small drill rig or drop weight penetration unit will be required. Modifications have been identified which are required to adapt equipment to service with radioactive material.

It is not expected that extensive layers of nonretrievable calcine exist in storage. Previous work has shown sintering does not occur at recorded storage temperatures. A sample of simulated zirconium calcine was tested to determine if combined temperature and pressure could cause the material to become agglomerated. After 1500 hours at 450°C and 12.5 psi, the sample was examined; no signs of agglomeration were present.

A concept of an agglomerate breaker device was prepared for use in conjunction with the previously designed pneumatic transport system in the event some material cannot be retrieved as planned.

Plans for Next Quarter

Testing of pneumatic retrieval nozzles will continue. Design of a nozzle capable of retrieving 750 lb/hr of calcine in a plant facility will be prepared. Design and procurement will be initiated for the calcine sampling equipment.

4. ICPP Defense Waste Document

(W. B. Kerr, R. N. Drake, H. R. Maxey, N. A. Chipman, R. L. Nebeker)

As reported previously, a Defense Waste Document is being prepared to evaluate alternatives for the long-term management of ICPP high-level waste. The DWD will describe methods for treating and storing ICPP high-level wastes and will evaluate processing and storage risks associated with each method. Preconceptual designs and preliminary costs will be presented.

The scope of the document has changed significantly from that which was originally proposed. Because the proposed processes are in an early state of development, probability numbers were not originally intended to be used in the risk analysis. A general risk analysis was planned which would be updated as more better probabilities become available.

During this period, the preconceptual designs were completed for the following processes:

1. Calcine dissolution
2. Pelletization of calcine
3. Metal matrix formation
4. Sintered glass-ceramic production
5. Actinide removal

The estimated costs for these processes range from $35 to 500 million. The benefits (in terms of reduced risk to the public) from each processing and storage alternate will be compared with the costs to calculate a cost-risk ratio. An example cost-risk methodology section has been completed and will be used as a guide for calculating cost-risk ratios.

Dose to the public at the INEL boundary location was calculated for various quantities of calcine which could be released during postulated accidents. Total population doses are presently being calculated.

Plans to model the dispersion of activity from the accidental release of activity to the aquifer below the INEL were discontinued. Activity reaching the aquifer will be considered as an incredible event in the DWD.

The document will be sent to ERDA-ID by April 30, 1977.

II. ICPP PLANT PROCESS IMPROVEMENT

1. Zirconium Fuel Recovery Process

(M. L. Gates)

The principal task of the process Improvement Group this quarter was development and design verification studies in support of the Fluorinel Project. Significant accomplishments this quarter include: 1) cadmium depletion studies, 2) installation of pilot-plant equipment, 3) dissolver mockup installation and operation, and 4) dissolution studies of unirradiated PWR Core-2 Seed-1 and -2 material.

Two unirradiated subassemblies of the PWR were obtained. These will be used to generate pilot-plant information for processing the irradiated Shippingport reactor fuel.

The present Fluorinel pilot-plant dissolver has reached the end of its useful life. A new pilot-plant dissolver has been designed and will be built by Brighton Corporation.

The transfer of all the unirradiated Fluorinel scrap fuel pieces to the Unirradiated Fuel Storage Facility from other INEL areas is 95% complete.

1.1 Cadmium Depletion Studies (S. Wildman)

A study of the depletion of cadmium, to be used as a nuclear poison in the Fluorinel process solutions, has shown that the probability of soluble cadmium depletion by plate-out, precipitation, and/or co-precipitation is negligible. Tests to determine cadmium plating on metallic dissolver components such as Hastelloy C-4, 304L stainless steel, and undissolved fuel surfaces indicated cadmium plating on Hastelloy to the extent of 1.9 g/m^2 (0.0012 g Cd/sq in.) during a 264 hour period. The decrease of soluble cadmium in the contact solution was negligible (0.2 g Cd/l) compared to 24 g/d cadmium in the makeup solution. No significant amount of cadmium plate-out could be detected on either the 304L stainless steel or the fuel surfaces. The analysis of precipitates caused by dissolvent evaporation and complexing procedures showed only trace amounts of cadmium in the presence of large amounts of insoluble Zr compounds.

1.2 Flourinel Pilot Plant

1.21 Filter System (K. F. Childs)

During the dissolution of fuel in the Fluorinel Process, miscellaneous insoluble solids are produced. The majority of these solids must be removed before the solution reaches the ICPP extraction system to prevent column upsets. Two methods for removing these solids are being investigated: filtration and centrifugation.

For filtration, two filters appeared to be suitable during scoping studies. They were the Mott cross-flow sintered-metal filter and the Vacco etched-disk filter. An evaluation/comparison of these two potential filter systems for the Fluorinel process, based on vendor information and other literature, was performed and submitted to Fluorinel Project personnel. The evaluation showed the Vacco etched-disk filter better suited for the Fluorinel process due to superior corrosion resistance and operating characteristics. A system to allow the testing of both filters is presently being installed in the pilot-plant.

The centrifuge has been installed in the pilot-plant and is ready for testing.

1.22 Dissolver Mockup (K. F. Childs)

The R. M. Parsons Company (architect/engineer for the Fluorinel Project) has proposed a design for the bottom of the Fluorinel Process dissolver, the type of which has never been used at the ICPP. Before this design is accepted, the operating characteristics of the design must be investigated. The largest practical size for testing in the CPP-637 Low-Bay Engineering laboratory is approximately one-half full scale. Design of this semi-scale Fluorinel dissolver bottom mockup was completed.

A bench-scale test apparatus was set up to run erosion tests on Hastelloy C-4 coupons under sparge conditions likely to be encountered in the Flourinel dissolver.

1.3 PWR Core-2 Dissolution (S. Wildman)

Unirradiated Shippingport PWR Core-2 Seed-1 and 2 fuels have been dissolved in the laboratory. Ninety-eight percent of the uranium was recovered using 8 M HF - 1 M HNO_3 as the dissolvent. The high percentage of uranium recovered from the batch dissolution of these PWR fuels showed that packing density does not affect uranium extraction from the fuel. Vigorous sparging was found to be required during dissolution to prevent the formation of a hard cement-like mass that could result from the packed, undissolved residue of graphite and CaO.

Plans for Next Quarter

The effort of the ICPP Process Development Group will be directed principally at design verification studies for the Fluorinel process. These studies will involve both pilot-plant and laboratory work. The pilot-plant work includes completing the Fluorinel pilot-plant safety analysis report, operating the pilot-plant filter and centrifuge systems, and operating the dissolver mockup. Studies on peroxide stability in hydrofluoric acid (HF), methods of decomposing peroxide, and the effect of trace peroxide in HF solutions on the corrosion rate of Hastelloy C-4 will be included in the laboratory work.

2. Corrosion of Nickel Alloys

(B. E. Paige, T. F. Rich)

High nickel alloys have been tested previously[a,b] for use in the severely corrosive solutions which are required for the processing of the Shippingport, Core-2, fuels. To process this fuel, the Zircaloy cladding will be dissolved in 6.8M hydrofluoric acid to form zirconium dissolver product containing 1.3 to 1.4M zirconium, and then, nitric acid will be added to the dissolver product at a concentration of 0.5M to dissolve the oxide fuel wafers.[c] In the previous work, Inconel 625 and Hastelloy C-4 were the best candidate alloys, particularly in the hydrofluoric acid-nitric acid mixture. Varying degrees of weld decay occurred in welded coupons of Hastelloy C-276, G, Inconel 690, and Incaloy 825. Preferential weld attack occurred in all alloys tested in dissolver product containing zirconium and hydrofluoric acid with or without the addition of nitric acid.

The results of previous tests showed that the following process conditions would help to reduce the corrosion rates: (1) maintain hydrofluoric acid concentrations below 10M, (2) maintain fluoride-to-zirconium molar ratios at less than 12 in zirconium dissolver product solutions and less than 5 when 0.5M HNO_3 is present, and (3) complex the excess fluoride in zirconium dissolver product with aluminum nitrate as quickly and completely as possible.

The present work was performed to compare weld behavior of coupons prepared locally to those prepared by the alloy manufacturers and to determine the effect of the solution annealing of Hastelloy C-276 and C-4. All coupons used in the current tests were fabricated and, in

---

[a] B. E. Paige and N. A. DePue, Corrosion of High Nickel Alloys in Combined Fluoride Solutions for Nuclear Fuel Reprocessing, ICP-1053, (July 1975).

[b] B. E. Paige, "Corrosion of Nickel Alloys in Nuclear Fuel Reprocessing", Materials Performance, Vol. 15, No. 12, pp 22-28, (December 1976).

[c] B. E. Paige, Dissolution Process for ZrO_2-UO_2-CaO Fuels, U. S. Patent 3,965,237 (June 1976).

some cases, heat treated by the manufacturer of the alloy being tested. Only welded coupons which passed X-ray examination were used. Coupons were exposed for 168 hours to test solutions at the boiling point (630 mm mercury).

2.1 Testing of Inconel and Incoloy Coupons Welded by Manufacturer

The welds in coupons of Inconel 690, Incoloy 825, and Inconel 625 which were prepared by the Huntington Alloys Division of International Nickel Company performed similarly or more poorly than coupons welded at ICPP which had been previously tested in similar Fluorinel solutions. The heat number and chemical composition of the particular heats tested in these studies are presented in Table 5. Solutions tested were: (1) 8M hydrofluoric acid, (2) zirconium dissolver product (6.8M fluoride, 1.35M zirconium), and (3) zirconium dissolver product containing 0.5M HNO_3.

The welded coupons, shown in Figure 2, have been exposed for two weeks to the Fluorinel test solutions indicated. Of the three alloys tested, Inconel 625, which performed the best in previous ICPP coupon tests, was free of weld decay. However, the preferential weld attack was particularly severe in the present tests in the hydrofluoric-nitric acid mixture [Solution (3)]. Inconel 690 suffered weld decay in dissolver product both with and without nitric acid present; this alloy has been suggested for use in solutions with higher nitric acid and lower fluoride concentrations by other authors.[a] Pits developed in the Incoloy Filler Metal 65 used for the Inconel 690 coupons; porosities had not been detected by X-ray examinations made prior to exposure. Incoloy 825 suffered severe weld decay in the high temperature heat affected zone similarly to previous tests. The Inconel Filler Metal 625 was severely attacked in both Incoloy 825 and Inconel 625 coupons when both hydrofluoric acid and nitric acid were present.

Table 6 presents the average corrosion rates for the two weeks exposure of the coupons shown in Figure 2 together with the rates for the first and second weeks of exposure. The rate for Inconel 625 was nearly three times the rate obtained in previous tests, presumably because of the excessive preferential weld metal attack observed in the present test. The weld metal was checked by X-ray and confirmed to be Inconel Filler Metal 625. The Inconel 690 had a ten-fold higher rate than Inconel 625 in dissolver product which did not contain 0.5M nitric acid; this resulted from severe attack of the parent metal. The 8M hydrofluoric acid attacked Inconel 625 severely, and again, exhibited exfoliation making it less desirable for a Fluorinel dissolver. Incoloy 825 had a low initial rate in 8M HF, but the rate accelerated with exposure. Overall, the alloy behavior determined by coupons prepared at ICPP was confirmed.

---

[a] R. Mah, et al., "Corrosion of Distillation Equipment by HNO_3 HF Solutions During HNO_3 Recovery", Materials Performance, Vol. 14, No. 11, pp 28-31, (November 1975).

TABLE 5

CHEMICAL COMPOSITION OF INCONEL AND INCOLOY HEATS INVESTIGATED

Alloy and Filler Rod	Heat Number	Chemical Analysis of Alloy Heat Tested, Percent												
		C	Mn	Fe	S	Si	Cu	Ni	Cr	Al	Ti	Mo	Nb & Ta	Other
Inconel 625 plate	NX72B3AK	0.04	00.05	03.51	0.004	00.24	--	60.74	22.36	0.17	0.32	08.92	3.62	P 00.000
Inconel 690 Plate	NX10C1H	0.03	00.17	09.38	0.007	00.15	--	60.42	29.82	--	--	--	--	--
Inconel 825 Plate	HH3432F	0.03	0.63	29.74	0.007	0.27	1.94	41.90	21.61	0.01	0.75	3.09	--	--

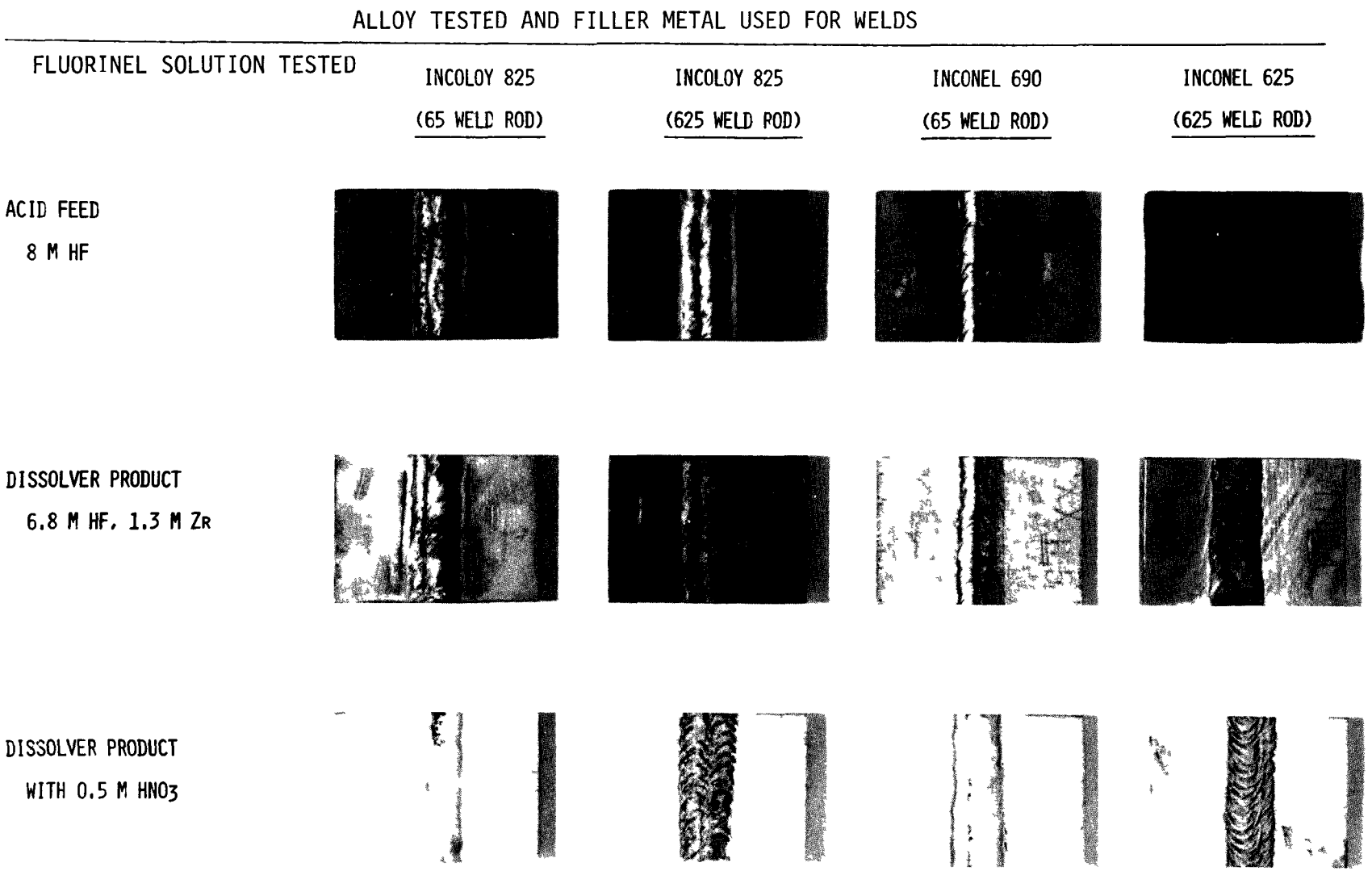

Figure 2. Weld Behavior of Factory Welded Coupons After 2 Weeks

TABLE 6

CORROSION RATES ON ALLOYS AND WELD ROD AT THE BOILING POINT OF PROCESS SOLUTIONS (Rate in mils per month)

INCOLOY 825 with INDICATED FILLER ROD

	Process-Type Solutions Tested					
	8M HF		Dissolver Product, 6.8M HF, 1.3M Zr		Dissolver Product +0.5M HNO_3	
	Filler Metal		Filler Metal		Filler Metal	
	65	625	65	625	65	625
1st Week	4.2	3.8	2.7	2.1	31	36
2nd Week	29	28	1.7	1.6	37	45
Average	17	16	2.2	1.8	34	40

INCONEL 690 with 65 FILLER ROD

1st Week	15	20	14
2nd Week	16	22	14
Average	15	21	14

INCONEL 625 with 625 FILLER ROD

1st Week	92	2.0	28
2nd Week	70[a]	1.0	32
Average	81	1.5	30

[a]Coupon was replaced after the first weeks' exposure due to extremely severe parent metal attack.

2.2 Hastelloy Heat Treatment Tests

The purpose of these tests was to determine if the weld performance of Hastelloy C-276 and Hastelloy C-4 could be improved with solution heat treatment followed by either a rapid air quench or a water quench. The coupons, which were welded and heat treated by the Stellite Division of Cabot Corporation, were subjected to two Fluorinel process solutions at the boiling point (630 mm Hg) for 1 week. Solutions tested were dissolver product solution (6.8M fluoride, 1.35M zirconium) and dissolver product solution containing 0.5M nitric acid. The order in which the coupons were tested was randomized to minimize the effect of variables in the testing procedure. The chemical analysis of the heats tested are shown in Table 7.

The results of the heat treatment on weld performance is summarized in Table 8. The solution heat treatment of Hastelloy C-276 coupons alleviated weld decay in the hydrofluoric-nitric acid mixture when the treatment was followed by either quench method. The Hastelloy C-4 did not exhibit any weld decay in the untreated coupons and remained the same after heat treatment. The preferential weld attack, which occurs in both solutions was not improved in either alloy by solution heat treatment and rapid quenching. Since most of the process equipment at ICPP must be welded into place in the field, the Hastelloy C-4, which does not require solution heat treatment to avoid weld decay, is preferred. It should be noted that the Hastelloy C-276 with the lower carbon (0.003%) content had slightly less weld decay, while the higher carbon heat (0.007%) appeared to have slightly less weld metal attack.

During the tests which were made to determine the effect of solution heat treatment upon weld performance, corrosion rates were obtained for all coupons. Table 9 presents the rates obtained for duplicate coupons of both Hastelloy C-4 and C-276 after one week exposure to dissolver product solution. In Table 10 are rates for coupons exposed to dissolver product containing 0.5M HNO_3. The difference observed between the two alloys is not as great as the effect of relatively small changes in the composition of dissolver product solution; therefore, selection of the alloy must be based on weld performance. The Fluorinel solutions can only be prepared by dissolving Zircaloy metal in hydrofluoric acid. Within the precision of the analysis for fluoride and zirconium in this type of solution, the solutions appear to be the same. However, data indicates that Solution 2 may have had a slightly lower zirconium content (less than $\pm$ 0.05M difference), and therefore, a slightly higher fluoride-to-zirconium molar ratio.

Plans for Next Quarter

The materials of construction test program for the Fluorinel Project will include further corrosion testing and weld procedure development of Hastelloy C-4. The corrosion testing will include long-term vessel tests, cyclic testing of welded coupons, and other tests to verify corrosion allowances on auxiliary equipment. The weld procedure development will be directed to qualifying a procedure for the Gas Metal Arc Welding (GMAW) process.

TABLE 7

COMPOSITION OF HASTELLOY ALLOYS TESTED

Heat Alloy Number	Chemical Analysis of Alloy Heats, Percent											
	C	Mr	Fe	S	Si	Ni	Cr	Co	Mo	V	W	P
2455-3-7142	0.001	0.04	0.46	0.003	0.03	Bal.	15.32	0.07	14.48			0.007
2455-3-7137	0.006	0.10	0.26	<0.0	0.04	Bal.	16.10	0.17	15.55			0.007
2760-3-125	0.003	0.59	5.65	<0.005	0.04	Bal.	15.79	2.09	15.21	0.019	3.43	0.019
2760-3-3065	0.007	0.47	5.55	0.009	< .01	54.76	15.35	1.66	15.70	0.24	3.40	0.012

TABLE 8

EFFECT OF HEAT TREATMENT

Factory Specimens Exposed 1 wk at Boil in Zirconium Dissolver Product + HNO_3

HASTELLOY C-4	HASTELLOY C-276
As-Welded Condition	
Weld Metal Attack	Severe Weld Attack
No Weld Decay	Severe Weld Decay
Solution Heat Treated and Rapid Air Quenched	
Weld Metal Attack	Severe Weld Attack
No Weld Decay	No Weld Decay
Solution Heat Treated and Water Quenched	
Weld Metal Attack	Severe Weld Attack
No Weld Decay	No Weld Decay

TABLE 9

CORROSION RATES FOR HASTELLOY WELDED COUPONS IN DISSOLVER PRODUCT
(Exposed 1 week at boil in 6.8M HF, 1.3M Zr - Rate in mils per month)

Heat Number	Solution Number[a]	Post Weld Heat Treatment: None	Rapid Quenched	Water Quenched
Hastelloy C-4				
2455-3-7142	1	1.2	1.0	1.5
2455-3-7142	2	.9	.7	.7
2455-2-7137	1	3.0	3.5	3.9
2455-2-7137	2	.6	.7	.8
Hastelloy C-276				
276-3-3125	1	.9	1.2	1.2
276-3-3125	2	.4	.5	.4
276-3-3149	1	3.2	3.3	4.3
276-3-3149	2	1.1	.7	.6

TABLE 10

CORROSION RATES FOR HASTELLOY WELDED COUPONS IN DISSOLVER SOLUTION plus 0.5M HNO_3
(Exposed 1 week at boil in 6.8M HF, 1.3M Zr, 0.5M HNO_3 - Rate in mils per month)

Hastelloy C-4				
2455-3-7142	1	45	25	27
2455-3-7142	2	38	30	31
2455-2-7137	1	35	28	19
2455-2-7137		25	26	21
Hastelloy C-276				
2760-3-3125	1	22	34	22
2760-3-3125	2	30	31	27
2760-3-3149	1	28	23	42
2760-3-3149	2	33	29	28

[a]Solutions 1 and 2 represent two separate dissolutions of Zircaloy metal in 6.8M hydrofluoric acid which were made to prepare a synthetic dissolver product and do not necessarily have exactly the same zirconium-to-fluoride ratio.

3. TORY IIA Dissolution Process

(B. E. Paige, M. E. Jacobsen)

A process flowsheet to recover TORY IIA fuel has been developed on the basis of laboratory dissolution, stability, and corrosion tests. TORY IIA fuel consists of $BeO-UO_2$ ceramic which contains fully enriched uranium with a low burnup. The hexagonal fuel tubes have been crushed to a size of less than 40 mesh, placed in aluminum cans, and shipped to ICPP where the fuel is currently stored in the Fuel Storage Basin (FSB). Previous work with $BeO-UO_2$ fuel[a] indicated the best reagent for dissolution of the oxide is a sulfuric acid-nitric acid mixture, and therefore, the present work was limited to combinations of these reagents.

Dissolutions were made using actual irradiated TORY IIA fuel. The crushed fuel was removed remotely from the sealed aluminum storage cans and weighed into batches in the Multicurie Cell (MCC). Radiation levels of these batches were sufficiently low (< 20 mr/hr) to permit dissolutions and dilutions to be made in a hood using glass equipment.

3.1 Fuel Dissolution

Irradiated fuel pieces and fines of TORY IIA fuel were dissolved in 12M H_2SO_4-1M HNO_3 at 145°C and in 6M H_2SO_4-1M HNO_3 at 120°C using 1 liter of reagent per 66 grams of oxide fuel; the volume of reagent was selected to produce a maximum of 22 grams of berylium per liter to prevent precipitation of $BeSO_4$ in the hot dissolver product.

Data presented in Figure 3 shows that 12M H_2SO_4 - 1M HNO_3 entirely dissolved the fuel in 12 hours. In 6M H_2SO_4 - 1M HNO_3, 26 hours were required to entirely dissolve the uranium; however, about 95% of the uranium was dissolved in 18 hours. Approximately 20% of the uranium was leached in the first 30 minutes, probably from the fuel fines, but dissolution of the uranium was not complete until the berylium was completely dissolved. These slow dissolution rates for the ceramic fuel show that TORY IIC fuel must be crushed similarly to TORY IIA fuel if it is to be dissolved and processed. TORY IIC fuel is not currently available for dissolution studies.

The decomposition of nitric acid during fuel dissolution was determined by nitrate analysis. A decrease of less than 0.2M nitrate occurred in 13 hours of dissolution in 6M H_2SO_4 - 1M HNO_3 showing that no additional nitric acid is required. During dissolution in 12M H_2SO_4 - 1M HNO_3, the nitric acid concentration decreased to 0.7M nitrate in 30 minutes and leveled off at 0.5M nitrate in 8 to 10 hours. Additional nitrate, as either 1.2M aluminum nitrate or 2M nitric acid, did not increase the dissolution rate.

3.2 Can Dissolution

Aluminum bar stock was dissolved in 6M HNO_3 with 0.007M mercury as catalyst in the presence of crushed oxide fuel to simulate dissolution of the aluminum fuel cans. About 20% of the uranium was leached from the fuel into the cladding solution in 30 minutes; this was similar to the

[a] L. A. Decker, USAEC Report "IDO-14585", June 1, 1962.

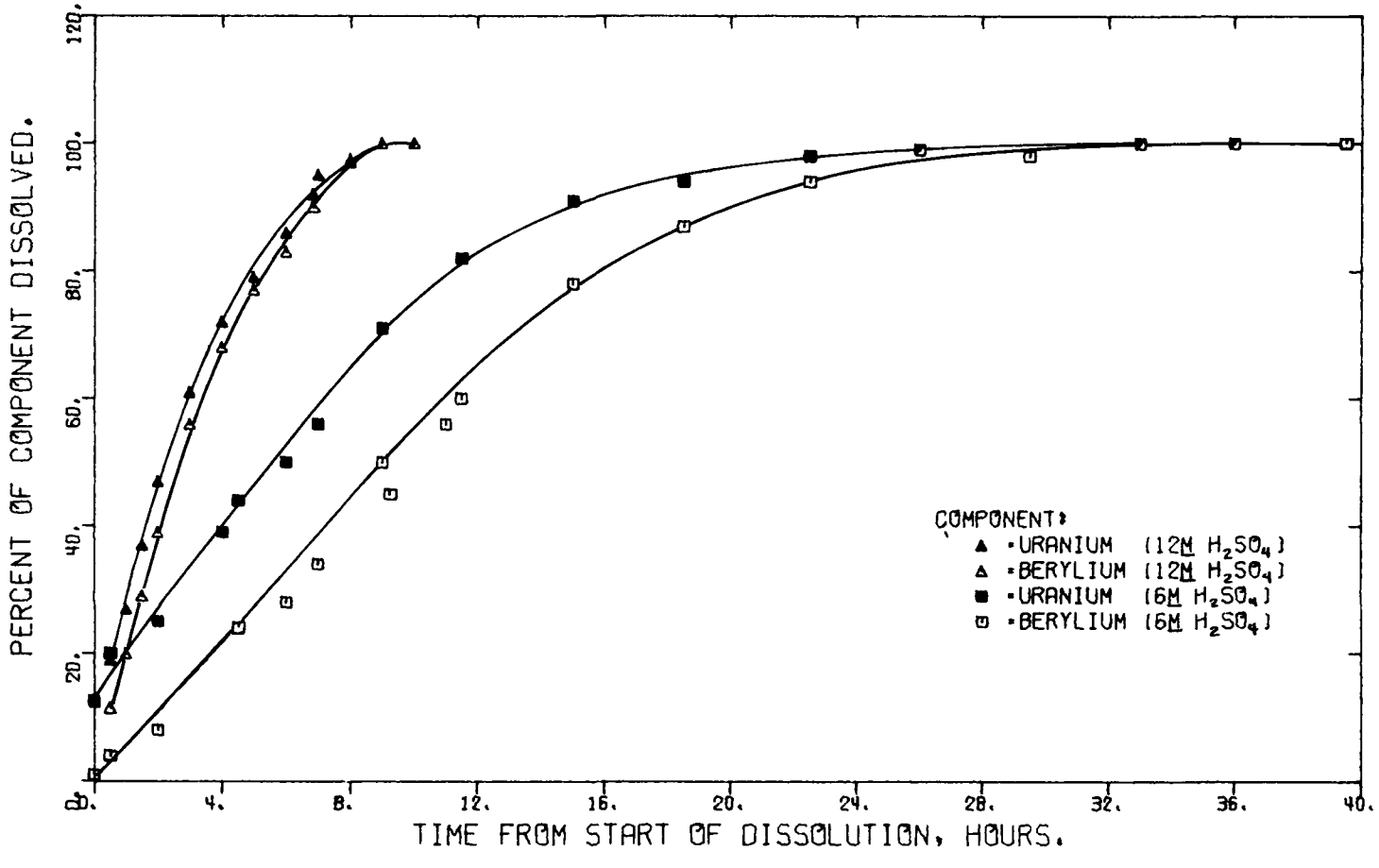

Figure 3. Dissolution Rate for TORY IIA Oxide Fuel

amount of uranium leached by the H_2SO_4-1M HNO_3 reagents during dissolution of the ceramic. Additional leaching for 6 hours did not significantly increase the uranium concentration. Essentially no beryllium was dissolved until sulfuric acid was added. The dissolution rate of fuel was considerably lower in 6M H_2SO_4-1M HNO_3 with the aluminum nitrate present; therefore, the decladding solution should be removed prior to addition of the oxide fuel dissolvent.

3.3 Adjustment and Extraction

Dilution studies showed that the BeO-UO_2 dissolver product requires only a 1:1 dilution with water to prevent precipitation of beryllium sulfate after the solution is transferred from the dissolver. However, a five-fold dilution will be required to prevent precipitation when aluminum nitrate from the decladding step and the nitric acid for extraction are added to the beryllium dissolver product. Based on extraction experience for the Vallecitos Boiling Water Reactor (VBWR) stainless steel fuel in 1965 at ICPP, the five-fold dilution of the sulfate ion is adequate for extraction of uranium with tributyl phosphate when adequate nitrate is present.

3.4 Corrosion in Dissolver Alloys

Corrosion data were obtained for Inconel 625, Incoloy 825, Hastelloy C-276, and Hastelloy C-4 because these alloys were being considered for a dissolver which could also be used for fluoride and/or nitric acid for other fuels requiring processing at ICPP. An existing dissolver of Carpenter-20 has previously been used for sulfuric acid dissolution of stainless steel fuels at ICPP. Table 11 presents corrosion rates for sulfuric acid-nitric acid mixtures and temperatures considered for dissolution of the fuel. In 12M H_2SO_4-1M HNO_3 at the boiling point, the weld attack was extremely severe in Incoloy 825, Hastelloy C-276, and Carpenter-20. Weld performance was only fair in the other two alloys. The high rate in Hastelloy C-4 resulted from pitting and uneven surface attack which resulted partly from solids adhering to portions of the surface. Reducing the temperature to 100°C reduced the rate of general corrosion proportionately for all alloys, but weld attack remained severe. Weld performance in 6M H_2SO_4-1M HNO_3 was good for Inconel 625 and Hastelloy C-4, but poor weld performance was observed for the other three alloys. All alloys and welds performed well in 3M H_2SO_4-1M HNO_3.

3.5 Recommended Flowsheet

From these studies, it was concluded that 6M H_2SO_4-1M HNO_3 was the best choice as dissolvent and that Inconel 625 was the best of the alloys investigated for resistance to weld attack and general corrosion. Although 12M H_2SO_4-1M HNO_3 dissolves the oxide fuel much more rapidly, the 6M H_2SO_4-1M HNO_3 mixture should be used to prevent catastrophic attack of the dissolvers at ICPP. The severe weld attack of alloys in 12M H_2SO_4- 1M HNO_3 at 100°C does not warrant consideration of using the lower dissolution temperature.

On the basis of the dissolution and stability data, the flowsheet shown in Figure 4 has been prepared for TORY IIA fuel using 6M H_2SO_4-1M HNO_3 to dissolve the ceramic fuel. The flowsheet assumes that a new fuel

TABLE 11

CORROSION DATA FOR TORY IIA DISSOLVENTS
Welded Coupons Exposed 168 Hours

	Corrosion Rate, mm/yr			
ALLOY	12M H_2SO_4 - 1M HNO_3 Boil, 145°	12M H_2SO_4 - 1M HNO_3 Boil, 100°	6 M H_2SO_4 - 1M HNO_3 Boil, 120°	3M H_2SO_4 - 1M HNO_3 Boil, 110°
Inconel-625	14.3	.33	0.29	0.06
Incolloy-825	9.8	0.30	0.51	0.07
Hastelloy-276	20.4	2.3	7.2	0.84
Hastelloy C-4	33.65[a]	0.89	2.8	0.58
Carpenter-20	12.8	0.61	3.9	.030

[a]Solids, deposited on surface, and excessive pitting and crevice attack occurred.

charge can be made when 95% of the uranium is dissolved and that the heel will remain constant since residual fuel will be dissolved during the next cycle. The ceramic dissolution will require approximately 20 hours for each batch. Sufficient dilution has been provided after dissolution to prevent precipitation of the beryllium. The aluminum can is dissolved in nitric acid and utilized as part of the salting agent for the uranium extraction.

Plans for Next Quarter

The project has been completed.

STREAM		1	2	3	4	5	6	7	8	9	10	11
DESCRIPTION	FUEL CHARGE	Aluminum Fuel Can Dissolvent	Aluminum Dissolver Solution	Fuel Dissolvent	Beryllium Dissolver Product	Acid and Dilution	Adjusted Extraction Feed				VBWR IAF 1965	
Volume, Liter/batch		338	338	424	424	1358	2120					
Be, g/ℓ					21.9		4.4	(≈0.5m)			25g ss/f	
U, g/ℓ					4.69		.94				1.56	
Al, M			1.7				0.27					
H^+, M		6.4	1.5	13	10.6	2.8	4.15				4.17	
SO_4, M				6	6		1.2				1.22	
NO_3, M		6.4	6.4	1	1	2.8	3.0				3.0	
Hg, M		0.007	0.007				0.001					
6 cans per batch												
BeO, Kg	25.88											
UO_2, Kg	2.25											
Al (can), Kg	15.5											
U^{235} Kg	1.85											

Figure 4. Headend Flowsheet for TORY IIA Fuel

III. ADVANCED GRAPHITE FUELS REPROCESSING

(L. W. McClure)

The Rover processing equipment, currently being installed at ICPP, will serve as the headend process for recovering uranium from the Rover Nuclear Rocket graphite fuels. In this process, the bulk of the graphite fuel matrix is converted to CO_2 in a primary burner. The residual graphite is then combusted in a secondary burner to produce an ash consisting of U_3O_8, Nb_3UO_{10}, and Nb_2O_5. This ash is then dissolved, leaving 60% of the Nb_2O_5 as a solid residue. These undissolved solids are removed by a continuous solid bowl centrifuge, and the clarified solution is fed to the existing ICPP solvent extraction system. Current pilot-plant work consists mainly of verification of process designs which have been specified for the Rover facility and recommendations for rectifying design deficiencies.

1. Sintered Metal Filter Design Verification

(H. S. Meyer)

The blowback systems for cleaning sintered metal filters in the Rover plant were mocked up and tested for effectiveness. The systems as designed were found to be inadequate. Various modifications were tested and a solution recommended.

Table 12 is a summary of the filter systems as designed for the Rover plant.

The purpose of the sintered metal filters is to trap carbon fines and return them to the secondary burner bed for burning, or to return them to the collection vessels for transport to another vessel.

The filter tests consisted of loading the filters with a graphite cake, allowing the pressure to increase, and blowing back the filters at a predetermined pressure differential across the filters. A successful blowback is one in which the pressure across the filters returns to the same value after each blowback. Design criteria requires the blowback system to successfully maintain the filters at a maximum of 2 psi (55 in. H_2O) pressure differential during operation.

A series of tests were conducted to determine the best combination of the following factors: (1) jet size, (2) pulse duration, and (3) solenoid valve orifice size for blowing back the secondary burner cylindrical filters and the collection vessel cluster filters. The data from these tests are summarized in Tables 13 and 14.

The conclusions reached as a result of the tests on the secondary burner cylindrical filters are:

(1) A single solenoid valve will not blowback five filters as designed for the secondary burner.

TABLE 12

SUMMARY OF IN-VESSEL FILTERS AS DESIGNED FOR THE ROVER PLANT

	VESSEL NAME					
	Bed Storage Vessel	Primary Collection Pot	Secondary Burner Weigh Pot	Secondary Collection Pot	Dissolver Weigh Pot	Secondary Burner
No. of Filters	4	10	4	4	4	10
Type of Filters[a]	C	C	C	C	C	S
Type of Blowback Jet[b]	C	C	C	C	C	A
No. of Blowback Supply Lines	2	2	2	3	2	2
Approx. Distance from Filter to Solenoid[c], ft	16	23	15	24	27	15
Pipe Size, in. Schedule 40	1/4	1/4	1/4	1/4	1/4	1/4
Air Flow Rates ACFM/ft^2	10	7	10	7	10	7
Filter Length, in.	14	20-3/4	16-1/4	20-1/8	12	17
Porosity, μ[d]	5	5	5	5	5	10

[a]Type of Filter is designated as follows:

C = Cluster filter containing six, 3/4-inch-diameter filter tubes hanging from a common fitting. The outside diameter of the cluster is 2-3/4 in.

S = Cylindrical filter with a 2-3/4-inch-diameter.

[b]Type of Jet is designated as follows:

A = 28 in. long, 1/4 in. OD x 0.065 wall thickness tubing.

C = 1/2 in. OD x 0.065 wall thickness tubing with 13/64 in. orifice at end.

[c]Solenoid valves - 2-way valves, 1/4 in. pipe, 7/32 in. orifice, normally closed.

[d]Porosity - size of holes in filters in micrometers.

TABLE 13

RESULTS OF SELECTED TESTS OF SECONDARY BURNER FILTERS [a]

Number of Filters/ Solenoid	Jet Type [b]	Pulse Duration (Sec.)	Tubing Length (Ft.)	Throughput Rate (cfm/ft^2)	Solenoid Valve Orifice (In.)	ΔP Before Blowback [c] (In. H_2O)	ΔP After Blowback [d] (In. H_2O)
1	A	0.4	20	7	7/32	20	13
1	A	0.4	20	7	7/32	20	[NS]
1	A	0.4	12	7	7/32	20	[NS]
1	A	0.4	20	7	5/8	20	[NS]
1	A	0.4	12	7	5/8	20	13
1	B	0.4	12	7	7/32	40	13
1	B	0.4	12	7	7/32	46	[NS]
1	B	0.4	12	7	5/8	35	13
1	B	0.4	12	7	5/8	55	[NS]
1	B	0.4	20	7	7/32	40	20
1	C	0.4	20	7	7/32	55	13
2	B	0.4	20	7	7/32	20	13
2	B	0.4	20	7	7/32	30	[NS]
2	B	0.9	20	7	7/32	26	[NS]
2	C	0.1	20	7	7/32	35	16
2	C	0.4	20	7	7/32	55	15
2	C	0.9	20	7	7/32	55	16
3	C	0.4	20	7	7/32	35	13
3	C	0.4	20	7	7/32	45	[NS]

---

a Secondary Burner Filters
5 μ, 1/16 in. thick, 2 3/4 in. OD x 18 in. cylinders

b Jet type
A = 28 in. long, 1/4 in. OD tubing with wall thickness of 0.065 in.
B = 20 in. long, 1/4 in. OD tubing with wall thickness of 0.065 in.
C = 1/2 in. OD tubing with 0.065 wall thickness with 13/64 in. orifice at end

c Pressure Drop Before Blowback
The pressure differential across the filters when the solenoid valve is opened.

d Pressure Drop After Blowback
The pressure differential across the filters immediately after the blowback. ([NS] if not successful.)

TABLE 14

RESULTS OF SELECTED TESTS OF COLLECTION VESSEL FILTERS[a]

Number of Filters/ Solenoid	Jet Type[b]	Pulse Duration (Sec.)	Tubing Length (Ft.)	Throughput Rate (cfm/ft^2)	Solenoid Valve Orifice (In.)	Filter ΔP Before Blowback[c] (In. H_2O)	Filter ΔP After Blowback[d] (In. H_2O)
1	B	0.4	12	7	7/32	20	[NS]
1	C	0.9	27	10	7/32	55	18
1	C	0.4	27	10	7/32	55	18
1	C	0.1	27	10	7/32	20	18
1	C	0.1	27	10	7/32	30	[NS]
1	C	0.4	27	10	7/32	95	18
1	C	0.9	20	10	7/32	55	19
1	C	0.4	20	10	7/32	55	18
1	C	0.1	20	10	7/32	30	18
1	C	0.1	20	10	9/32	30	18
1	C	0.1	20	10	5/8	70	18
1	C	0.1	27	7	7/32	20	13
1	C	0.1	20	7	7/32	35	15
1	C	0.1	12	7	7/32	45	13
1	C	0.1	20	7	9/32	35	13
2	C	0.4	20	7	7/32	20	[NS]
2	C	0.4	12	7	7/32	20	13
2	C	0.1	12	7	7/32	20	[NS]
2	C	0.4	12	7	5/8	65	13
2	C	0.4	27	10	5/8	60	18
3	C	0.4	27	7	5/8	30	12

a Collect Vessel Filters
6-5 μ, 1/16 in. thick, 3/4 in. OD manifolded together to 2.75 in. OD, 20 in. long

b Jet Type
B = 20 in. long, 1/4 in. OD tubing with wall thickness of 0.065 in.
C = 1/2 in. OD tubing with wall thickness of 0.065 in., 13/64 in. orifice at end.

c Pressure Drop Before Blowback
The pressure differential across the filters when the solenoid valve is opened.

d Pressure Drop After Blowback
The pressure differential across the filter immediately after the blowback or [NS] if not successful.

(2) The design of the present jets in the secondary burner is inadequate to allow one filter to be blown back using one solenoid valve at all distances, pulse durations and frequencies tested.

(3) Replacing the 7/32-inch orifice solenoid valve with a 5/8-inch orifice solenoid valve will not significantly affect the number of filters that can be blown back, but the larger orifice will improve the blowback of one filter per solenoid valve.

(4) Replacement of the 1/4-inch tubing jets with a 1/2-inch tubing jet with a 13/64-inch orifice will produce a successful blowback at 27 feet using one of the present solenoid valves at a 0.4-second pulse duration.

(5) In general, a solenoid valve with a 5/8-inch orifice was found to have better blowback characteristics than the solenoid valve with a 7/32-inch orifice.

The conclusions reached as a result of the tests on the collection vessel's cluster filters were:

(1) A single solenoid valve with a 7/32-inch orifice will not blowback two or more cluster filters as designed.

(2) A solenoid valve with a 5/8-inch orifice will give a successful blowback for two filters (only one filter per solenoid valve is recommended) and allows utilization of a 0.1-second pulse for blowing back one filter.

(3) A 7/32-inch orifice in the solenoid valve (as in the plant design) will produce a successful blowback for one filter at 27 feet from the filter using a 0.4-second pulse and a 13/64-inch orifice in a 1/2-inch jet.

2. Long-Term Testing of Rover Sintered Metal Filter

(H. S. Meyer)

The long-term effects of loading and successfully blowing back sintered metal filters are being investigated. The long-term filter tests consisted of loading cluster filters with graphite cake, allowing the pressure to increase, and blowing back the filters at a given time interval. The pressure differential across the filters after each blowback cycle was recorded. The filters must be kept at a pressure differential less than the design value of 55 inches H_2O. For these tests, 17 feet of tubing were used to connect the 1/2-inch OD tubing jets with 13/64-inch orifices to the solenoid valves with 7/32-inch orifices.

The long-term test at 7 acfm /ft^2 was conducted using three cluster filters and a fluidizing velocity of 0.86 ft/sec. The results of the 310-hr test (approximately 5000 blowback cycles) showed that the pressure differential following the blowback cycle leveled off at 25 $\pm$ 2 inches H_2O in about 8 hours (120 cycles for the remainder of the test).

Long-term tests at 10 acfm/ft^2 were conducted using two cluster filters at a fluidizing velocity of 0.81 ft/sec. After 110 hours (approximately 3500 blowback cycles) the pressure differential, after the blowback cycle, increased steadily from 22 inches H_2O to 31 inches H_2O. Tests were conducted to determine a method to eliminate this steady increase in the pressure drop. The best method was to replace the 7/32-inch orifice air supply solenoid valves in the blowback system with 5/8-inch orifice valves. The test was repeated, and the pressure differential increased to 41 $\pm$ 2 inches H_2O in 3 hours (approximately 50 cycles) where it remained constant for an additional 160 hours (approximately 2300 cycles).

3. Rover Solid Samples Funnel Testing

(H. S. Meyer)

The slide-valve funnel, designed for the Rover plant solid sampler, was tested for possible plugging by Rover burner material. The ease of handling and compatibility with the remote sample bottles was also investigated. In Figure 5 is shown the Rover solids sampling system; the funnel tested is circled.

The tests were conducted using a full-size funnel fabricated from aluminum. The sample bottle was a wide-mouth, 5 ml glass bottle with an "X" split rubber diaphragm cap similar to that used for ICPP calciner solid samples. The experimental procedures were to: (1) slip the sample bottle on the funnel, (2) fill a 0.53-inch-diameter glass tube with the test material, (3) slide the tube along a horizontal platform at various speeds, and (4) stop directly above the top of the funnel.

The flow characteristics of each material were also tested after packing the material in the glass tube by light tapping of the tube. The materials tested were: (1) 60-mesh Al_2O_3, (2) Rover graphite, (3) 90 wt% Al_2O_3-10 wt% graphite mixture, (4) 80 wt% Al_2O_3-20 wt% graphite mixture, and (5) reduced iron powder (simulating UO_2). The results showed that Al_2O_3 and 90% Al_2O_3-10% graphite mixture did not plug the funnel at any of the various tube speeds or under vibrational packing. The graphite, the 80 wt% Al_2O_3-20 wt% graphite mixture, and the iron powder did not plug the funnel at the various horizontal tube speeds, but the three materials would pack if the tube was lightly tapped. After packing, the materials would fall into the funnel, form a stable arch, and plug the funnel. However, the material would flow out of the funnel under vibration. Allowing the graphite to settle in the tube by gravity without tapping for up to one hour did not cause plugging. Testing of the glass sample bottle showed that the bottle performed satisfactorily by slipping on and off the funnel easily and remaining in position during filling.

The experimental work showed that the sample funnel will not plug with Al_2O_3 bed material; however, it could plug if over 10 wt% graphite were present and the material were packed by vibration. Tapping the funnel with the sampler tongs may be sufficient to empty the funnel. In general, material flowed easier if the tube was moved slowly over the funnel.

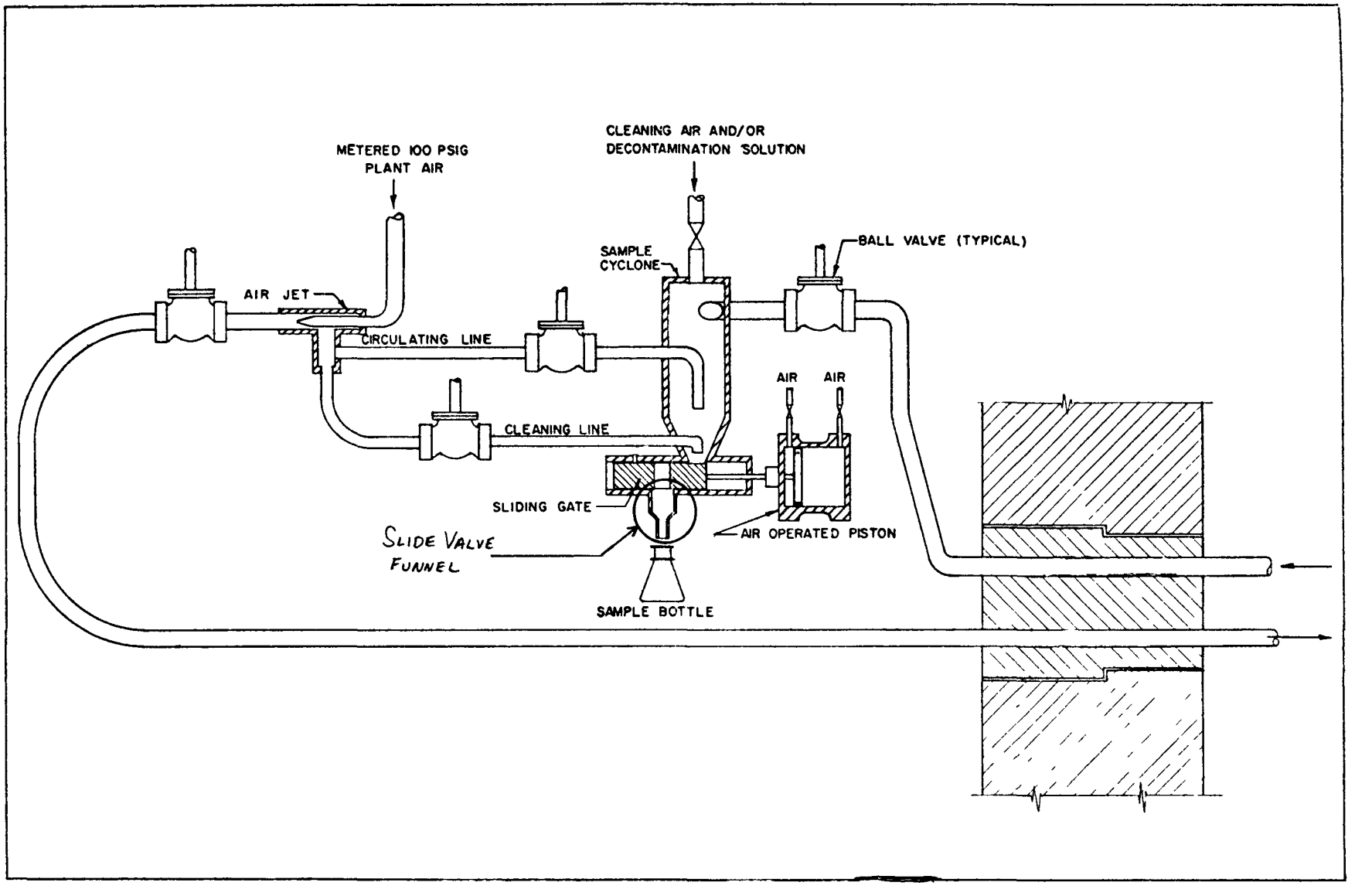

Figure 5. Rover Solids Sampling System.

4. Rover Solids Transport Testing

(H. S. Meyer)

The operability of the solids transport system - as designed in the Rover process - was tested. The venturi, or ejector, jet-type transport systems performed satisfactorily under all conditions tested.

The effect of pressure in the receiving vessel on the transport of solids was determined. Material was transported into a filter vessel from a conical bottom feed vessel. The pressure in the vessel was allowed to increase by not blowing back the filters. The solids transport rate at various vessel pressures was determined. The effect of vibration on the transfer rate at various vessel pressures was also determined.

The results using a Penberthy Jet 63A with simulated Rover primary burner ash are summarized in Table 15. The solids flow rate decreased with increased pressure in the receiving vessel and decreased when vibration was applied to the vessel.

TABLE 15

Solids Transfer Rate Test with Jet 63A - Simulated Primary Burner

	Test 1	Test 2	Test 3
Motive air pressure (psi)	20	40	60
Solids transfer rate at 55 in. H_2O ΔP across filters (g/m)	400	1200	1800
Solids transfer rate at 55 in. H_2O while vibrating transfer vessel (g/m)	375	800	1400
ΔP across filters at zero solids flow rate (in. H_2O)	70	138	206
ΔP across filters at zero solids flow rate while vibrating transfer vessel (in. H_2O)	80	143	230

During the tests, simulated ash would not flow out of a 1-1/2-inch outlet from the 60° cone by gravity. It did flow when the vessel was vibrated or pressurized above 40 inches H_2O. Under vibration or pressure, solids also flowed out of a 3/4-inch outlet. No plugging of the jet or lines was observed in any of the tests.

Preliminary tests have been run with simulated primary burner ash with Jet LL1 and secondary burner ash with Jets 62A and LL 3/4. No experimental difficulties occurred during testing and the jets behaved similarly to Jet 63A.

5. Rover Secondary Burner Tests

(A. G. Westra)

Rover secondary burner tests were completed to establish the maximum ash-to-bed ratio in the 4-inch pilot-plant burner, and six operator training runs were made. The maximum amount of ash that could be added to the alumina bed before sintering occurred was found to be 37% of the weight of the alumina.

Elutriation tests have shown that all ash cannot be removed by the fluidizing gas. The composition of the burner bed after elutriation averaged 14% U_3O_8 and 85% alumina. However, the pilot-plant burner has no jet grinders. Elutriation with a fluidizing velocity of 1.3 ft/sec was 90% complete after 3 hours. Two to three more hours were needed to complete the elutriation. Further time provided no additional elutriation of ash.

Blowback of the sintered metal filters in the burner at 15- to 60-second intervals during the burn never lowered the bed temperature more than 5°C. Intervals between filter blowbacks of 2 to 5 minutes caused 10-15°C drops in the bed temperature.

If the oxygen concentration in the burner off-gas exceeded 30%, above-bed burning was likely to occur.

6. Rover Pilot Plant Centrifuge

(A. G. Westra)

Previous pilot-plant tests showed erosion on the chrome-oxide ceramic coating on the Rover centrifuge auger. A more erosion-resistant material is being installed for testing.

The auger of the 6-inch Bird centrifuge used in Rover pilot-plant experiments was weld overlaid with Tribaloy 700 hardfacing material in preparation for erosion tests. Thickness and height measurements were made on the auger blades. The centrifuge auger and bowl were balanced and the centrifuge was reassembled for further erosion tests. Erosion tests will be made with a slurry of Nb_2O_5 and Al_2O_3 in water.

7. Neutron Interrogator

(A. G. Westra)

Further tests were conducted using the neutron interrogation unit which will determine the ^{235}U concentration in the solids from the Rover centrifuge. One-gram samples of uranium were dispersed in matrices of Nb_2O_5 and sand to determine if sand could be used as a substitute for an Nb_2O_5 matrix in making calibration standards. With the same amount of uranium in each matrix, the Nb_2O_5 matrix showed higher neutron count rate than the sand matrix for the same amount of uranium. Further tests are needed to conclusively decide if sand can be used.

Parts of the neutron interrogator which need to be modified before the neutron interrogator is installed in the cell were identified. The proposed modifications are:

(1) The entire neutron detector should be shielded from gamma radiation with 1 inch of lead.

(2) A switch should be installed so the direction of the scanning mechanism can be manually reversed at any time.

(3) The scanning mechanism should be modified to allow scanning of the upper portion of the solids collection vessel (VES-110).

(4) The double chain drive system for raising and lowering the scanning mechanism should be replaced with a single chain drive system.

(5) The relays that reverse the drive motor to raise and lower the scanning mechanism should be placed outside the cell to facilitate maintenance.

(6) Carbon steel and aluminum parts of the neutron interrogator should be replaced with stainless steel parts or covered with a protective paint to minimize corrosion.

8. Support Burner for Rover

(A. G. Westra)

Design and fabrication of a 1/4 scale, 4-inch-diameter pilot-plant primary burner was completed. This burner will be used for technical support of the Rover plant primary burner.

9. Rover Dissolver Sample Jet

(R. L. Ring)

Two Kynar jet ejectors were evaluated for use in the Rover plant to circulate the dissolver solution through a sample bottle. The plant jets will be required to lift the dissolver solution a vertical height of 11 feet through 35 feet of pipe.

The sampling loop was mocked up and both jets were tested by circulating a sodium nitrate solution with a specific gravity of 1.35 at 70°C to simulate the dissolver solution.

Both jets provided the required flow of 100 ml/min. One of the jets tested achieved a higher maximum rate than the other; therefore, it was recommended as the jet to install where the highest lift is needed.

Plans for Next Quarter

The erosion on elbows and deflector plates in the solids transport system by alumina (Al_2O_3) and burner ash will be determined. Erosion testing of the Tribaloy 700 surface on the centrifuge auger will be completed. Standards for initial and periodic recalibration of the neutron interrogator will be made. The cost estimate, expenditure authorization, and procurement of parts for a plant support dissolver will be completed. Preparation of a contingency plan for plant operating failures will be initiated.

IV. WASTE TRANSFER SYSTEMS

(B. E. Paige, D. W. Siddoway)

This program is directed toward the development of guidelines for standards pertaining to the design and construction for safe means of intraplant transfer of radioactive wastes. Included in this program are laboratory evaluations of pipeline coatings and determination of relative corrosion resistances of pipeline materials, field testing of pipeline coatings and bare metals, evaluation of the use of cathodic protection on stainless steel pipes, and studies of general encasement and piping design.

1. Coating of Stainless Steel Pipe

1.1 Sample Preparation (R. E. W. Birch)

Test specimens of one-inch nominal Type 304L stainless steel pipe have been coated with various commercial external coating materials. Test specimens will be evaluated in both the laboratory and field programs. Laboratory specimens are 9 inches long and have 37 $in.^2$ external surface area while field test specimens are 18 inches long and have 74 $in.^2$ external surface area.

Samples were prepared by cutting the pipe into sections, machining the ends to remove burrs, smoothing with Al_2O_3 grinding paper, ultrasonic cleaning in a low chloride detergent solution, and finally, degreasing in an acetone bath. Samples were rinsed in hot water between steps. Half of all test sections were commercially sandblasted with flint abrasive (100% silica sand) to a 2-4 mil profile depth while the other half of the specimens remained intact. The specimens were sent to various coating vendors where different types of coatings were applied to both sandblasted and unsandblasted sections. Laboratory testing should determine the necessity of sandblasting stainless steel before coating.

1.2 Laboratory Testing (R. E. W. Birch)

A test apparatus, shown in Figure 6, has been developed for analyzing the resistance of coatings to cathodic disbonding. The cell consists of a nonconductive linear-polyethylene container, DC power source (rectifier), and a platinum plate electrode with a surface area of 72 $in.^2$. The pipe samples are electrically connected to the power source, and a copper/copper sulfate reference electrode is included so that potential readings may be taken. The test, which will be run on the coated pipe sections, is a modified version of published ASTM methods.[a] Information obtained from preliminary lab testing and testing performed by individuals from other companies for coatings on carbon steel were incorporated into the test.[b] Cathodic disbonding will be initiated with impressed DC voltages of 1.5 VDC, 5.0 VDC, and 10.0 VDC and evaluated periodically by visual inspection. The test medium will consist of moist soil or soil leachate.

2. Field Testing

(R. E. W. Birch, D. W. Siddoway)

Two large fiberglass reinforced polyethylene tanks have been buried at ICPP and will be utilized as part of the isolated field testing of various types of stainless steel piping. The tanks are buried two feet below surface grade to achieve a constant year-round temperature. A constant moisture content, near saturation, will be artifically maintained and monitored in the tanks for the duration of the study. Test sections are pulled at intervals of 1, 2, 4, 8, and 20 years and their corrosion resistance assessed. Tank monitoring and environmental control systems are presently nearing completion.

3. Encasement Evaluations

(D. W. Siddoway)

A program has been drafted and submitted to Applied Mechanics of EG&G to initiate seismic evaluation of various secondary pipeline encasements. The program includes a study of stainless steel pipe encasements, fiberglass reinforced polyester pipe encasements, stainless steel-lined concrete trough encasements, and walk-in manways constructed of reinforced concrete. Encasements are to be evaluated via theoretical computer techniques to determine their resistance to earthquake stresses common to Zone I, Zone II, and Zone III seismic areas.

---

[a] Standard Test Methods for Cathodic Disbonding of Pipeline Coatings, ASTM G8-72.

[b] G. R. Silkworth, CH_2M-Hill, Pipeline Coatings and Wrappers . . . A 3-Point Study, Private Communications (January 1977).

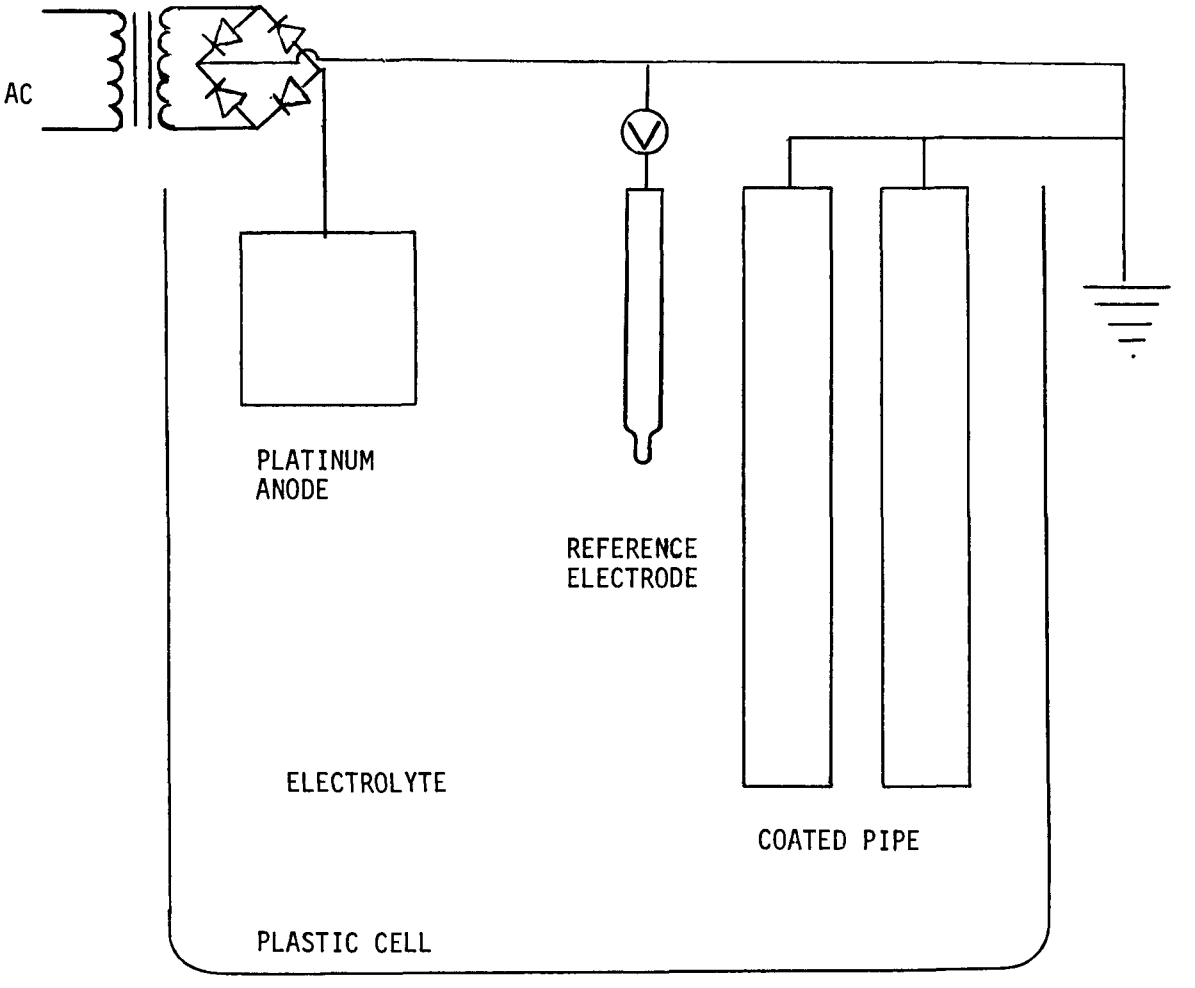

Figure 6. Test Cell for Disbonding

Plans for Next Quarter

Laboratory testing of coated pipe specimens for resistance to cathodic disbonding will be performed. Field testing of coated pipe will also begin.

The field corrosion laboratory and instrumentation will be completed and test specimens of Type 304L, 316L, and 347 stainless steels will be placed for long-term study.

Initial data from seismic evaluation of secondary encasement will be reported and continuing work will be outlined.

V. ICPP WASTE MANAGEMENT DEVELOPMENT

1. Tank WM-183 Flowsheet Development

(A. P. Hoskins, B. J. Newby)

ICPP storage tank WM-183 is filled with a combination of aluminum waste, electrolytic waste, evaporator bottoms, and other non-fluoride wastes. The combined waste contains about 15 g/ℓ sodium nitrate and 250 ppm chloride. Calcination of wastes containing sodium nitrate can cause

fluidized-bed particle agglomeration; calcination of wastes with chloride can cause excessive corrosion of off-gas piping and equipment if the chloride is volatilized.

Differential thermal analyses (DTA) showed that the addition of powdered iron to WM-183 waste might eliminate agglomeration during calcination of the waste. Laboratory studies showed that the gas evolved when powdered iron is added to WM-183 waste does not contain enough hydrogen to constitute an explosion hazard. Laboratory studies also showed that the addition of silver nitrate to WM-183 waste to which iron had been added has potential for retaining chloride in the calciner bed during calcination. Five scoping runs were completed using a 4-inch-diameter, fluidized-bed, in-bed combustion calciner to determine the calcinability of WM-183 waste to which powdered iron has been added. The first run using 0.25 mole of iron per mole of sodium was terminated after 6.5 hours, due to plugging of the distributor plate holes and particle agglomeration. Four other runs of 12-14 hours duration, using from 0.5 to 1.0 moles of iron per mole of sodium, were made without significant operating problems. The product and final bed material in these runs contained some agglomerates.

DTA indicated that the blending of first-cycle zirconium waste with WM-183 waste might eliminate agglomeration during calcination. WM-183 can be boiled down to 60% of its original volume while still maintaining solution stability. Short-term solution stability studies showed that the blends of zirconium waste with WM-183 boiled down by 40% most likely to be used (blends ranged from 1 vol zirconium waste: 2 vol boiled down WM-183 waste to 1 vol boiled down WM-183 waste: 3 vol zirconium waste) contain only a trace of solids after one month of storage with or without magnesium nitrate. These blends, with calcium nitrate added, contained no more solids than the blend of zirconium and ICPP sodium-bearing waste[a] containing calcium nitrate as recommended for calcining sodium-bearing waste.

Plans for Next Quarter

Short-duration runs will be made in a 4-inch-diameter calciner using an alumina rather than a zirconia starting bed and adding powdered iron plus other additives simultaneously to WM-183 waste to suppress particle agglomeration. A 100-hour run will be made using a 4-inch-diameter calciner and the flowsheet utilizing powdered iron that proves most successful during the short-term tests. Chloride volatility will also be monitored. If successful, the flowsheet will be demonstrated by a 100-hour run using a 12-inch-diameter calciner. As a backup flowsheet, additional short duration runs will be made using the 4-inch calciner to test the effectiveness of blending zirconium waste with WM-183 waste to prevent agglomeration.

[a]Previously called ICPP second-cycle waste.

2. Feed Valve Testing

(S. A. Birrer)

Major problems experienced with the Waste Calcining Facility (WCF) feed control valves are: (1) plugging, and (2) bellows failure due to valve cycling. A market survey was made to secure a valve for testing that would eliminate the problems. The valve selected for testing was a 3/8-inch, full-port, ball valve (Model #AS5966SW) with Kynar ball seats and body seals and Grafoil stem packing made by Worcester Valve Company, Inc.

The first test was a 30-hour pressure-leak test. The fully closed valve was subjected to water at 16 psig; no leakage occurred. During the second test, simulated first-cycle zirconium waste was circulated through the 45° open valve for 5 weeks; no leakage occurred during this test. The pressure-leak test was repeated and again no leakage was found.

Plans for Next Quarter

Two additional tests will be made. A pneumatic actuator will be connected to the valve and the valve cycled between fully open and fully closed (0.25 cpm) while circulating simulated zirconium waste through it. This test will be followed by another pressure leak test.

3. Rover Flowsheet

(S. A. Birrer)

Runs were made using 4- and 12-inch-diameter, fluidized-bed calciners heated by in-bed combustion to develop flowsheets for calcination of Rover waste in the WCF. Two runs were made using the 4-inch-diameter calciner and a blend of 1 vol first-cycle zirconium waste-1 vol first-cycle Rover waste as calciner feed. The first run was terminated after 62 hours, due to agglomerate formation; the second run was successfully completed. A 66-hour run was made using the 4-inch-diameter calciner and a 1 vol Rover-2 vol zirconium waste blend as feed without significant operation problems. A 100-hour run was made using the 12-inch-diameter calciner and a 1 vol Rover-1 vol zirconium waste blend as feed without operating problems; some small bed agglomerates appeared after 8 hours of run time, but did not increase in size or quantity during the remainder of the run.

Plans for Next Quarter

A 100-hour run will be made using the 12-inch-diameter calciner and a blend of 1 vol Rover-2 vol zirconium wastes as calciner feed.

*

OTHER PROJECTS SUPPORTING ENERGY DEVELOPMENT

I. NUCLEAR MATERIALS SECURITY

1. Measurement Equipment for Chemical Plants

1.1 In-Plant Process Surveillance System (W. J. Harris, H. R. Deveraux)

An initial version of the plant process system was installed in the ICPP. This version was provided with sensors to monitor operations in the input tank area of the ICPP and will be used for a demonstration in April. The purpose of the system is to aid in the development of sensors and system for a computer based safeguards system for chemical processing plants for spent nuclear fuels.

In the present version, driven by a Hewlett-Packard programmable calculator, the system was used to test the following sensors located in the CPP-601 process building: (1) precision pressure transducers for level, density, solution weight and volume in tanks G-105, G-155, and G-106; (2) pressure switches monitoring transfers in and out of these tanks; (3) usage switches on the tank samplers; and (4) a pressure transducer used for liquid level measurements on tank S-115, the third cycle evaporator.

Future work will include the integration of a gamma absorptimeter and a bubble transit time flowmeter (see below) into the system to provide loadout area monitoring capability.

1.2 Bubble Transit Time Flowmeter (H. R. Deveraux, W. J. Harris)

The transit time flowmeter will provide accurate flowrate measurement for certain plant lines with low flows. No suitable flowmeter has been available. The flowmeter determines the time needed for injected bubble to travel a known distance. A new, sealed ultrasonic bubble sensor was developed. Three sensors are under construction. The electronic package of the flowmeter was changed to make remote readings possible.

II. GEOTHERMAL ENERGY DEVELOPMENT

Liquid Fluidized-Bed Heat Exchanger for Geothermal Applications[a] (C. A. Allen, O. Fukuda, R. E. McAtee)

1. Introduction

Liquid-fluidized-bed heat exchangers are being developed to control scale and improve the rate of heat transfer in geothermal binary systems. A horizontal unit was tested at the Raft River site and the heat transfer

[a]Subcontract to EG&G-Idaho, Inc.

results are included in this report. The unit was transferred to the geothermal site at East Mesa in the Imperial Valley of California for scale control tests.

Successful application of liquid fluidized beds depends on the development of a flow distribution system which insures even flow throughout the vessel. Three particular situations must be avoided: (1) dead spots in the bed where scale can rapidly build up, (2) high velocity streams which will elutriate the bed or cause serious erosion, and (3) high pressure drop to avoid unnecessary pumping costs. A model of a 3-ft-diameter heat exchanger was constructed to study flow distribution. Construction and installation are covered in this report.

2. Horizontal Vessel

The 8-inch-diameter by 16-inch-long horizontal, carbon steel, heat exchanger was operated with three different sizes of bed particles. Closely screened silica sand of 0.7, 1.0 and 2.1 mm diameters were used. Figure 1 shows heat transfer as a function of particle size and average velocity. Maxima occur near 6 ft/min for 0.7 mm particles, 10 ft/min for 1.0 mm particles, and 14 ft/min for 2.1 mm particles. Particle size is one of the parameters which can be varied in the design of a heat exchanger to maximize efficiency.

The dashed line in Figure 1 represents the heat transfer curve of this heat exchanger operated with no bed. The greatest percentage heat transfer increase occurs with the smallest particles. For 2.1 mm particles the increase is only about 10% at the maximum. This probably relates to the relative frequency of collisions between particles and heat transfer surface. The higher frequency occurs with smaller particles and provides more continuous erosion of the thin film heat transfer barrier.

The curve falling between the 1.0 and 2.1 mm curves in Figure 1 represent data from the 6-inch-vertical vessel with a coil exchanger. This exchanger was operated with 1.0 mm sand and the same heat source as the horizontal vessel. The velocity does not vary significantly up the cylinder and is approximately the same as the superficial velocity. Since the heat transfer curves for 1.0 mm particles for both vessels should be similar, it appears that average velocity is not the best way to characterize horizontal heat exchangers. When the same data are plotted as a function of superficial velocity, the two diverge further as shown in Figure 2. The vertical and horizontal heat transfer coefficient curves converge when the horizontal data are plotted vs. the cross section velocity as shown in Figure 3. The cross section velocity (Vc) is defined as the velocity between the tubes at the widest part of the cylinder.

$$V_C = \frac{M}{P_g \ell (d_V - nd_Z}$$

where

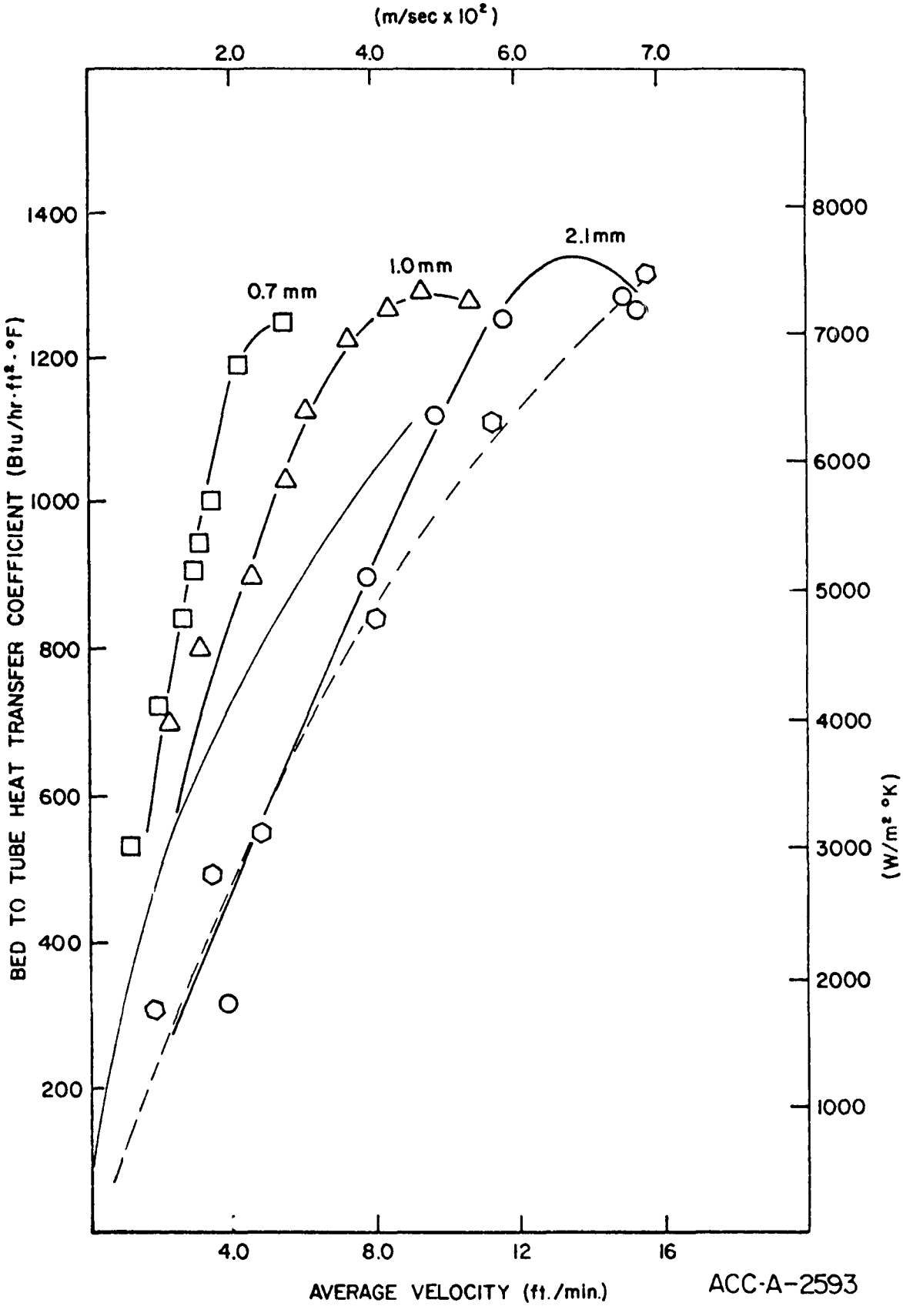

Figure 1. Heat Transfer Coefficients for Three Bed Particle Sizes

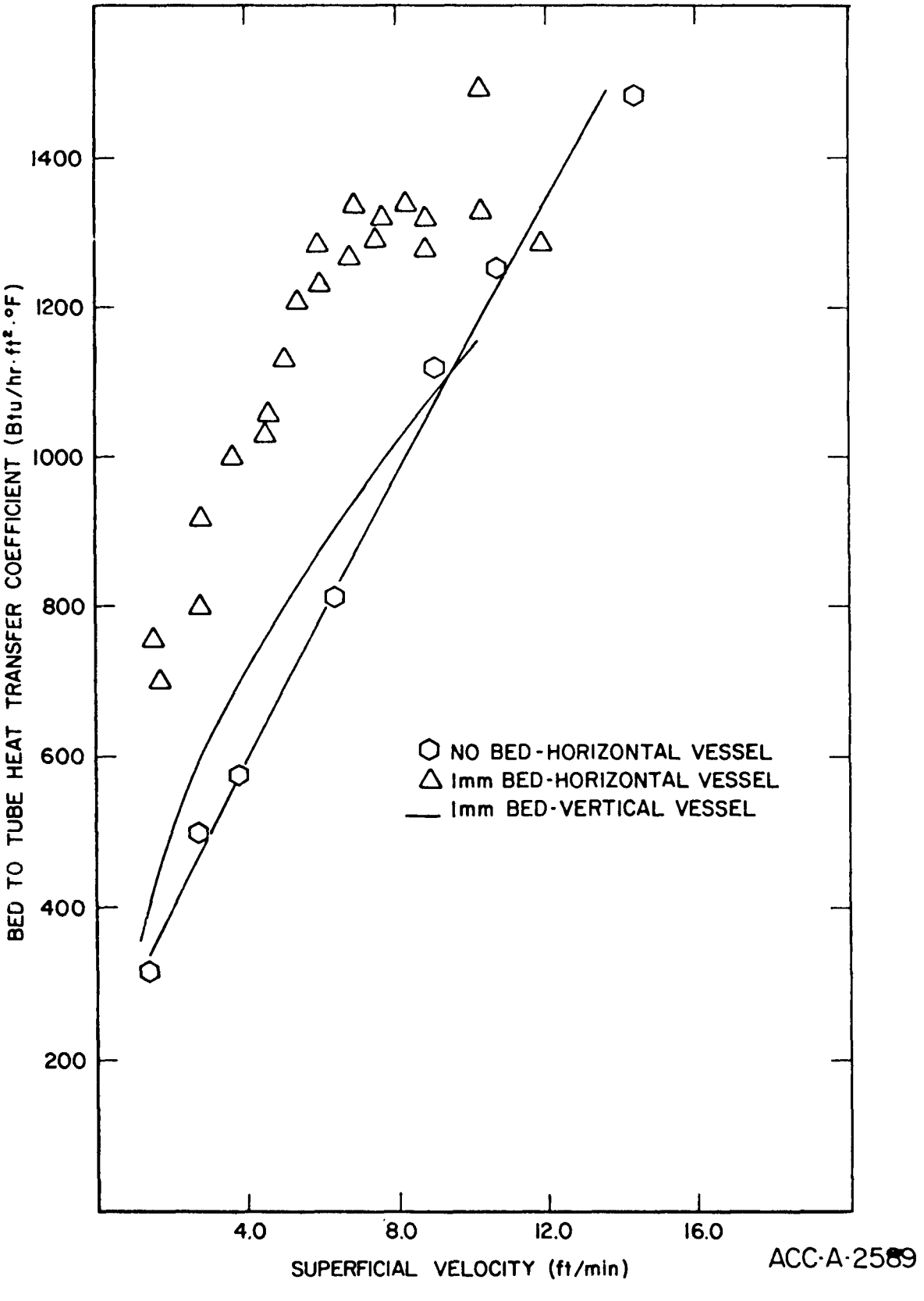

Figure 2. Heat Transfer Coefficients for Horizontal and Vertical Heat Exchangers Plotted Against Superficial Velocity.

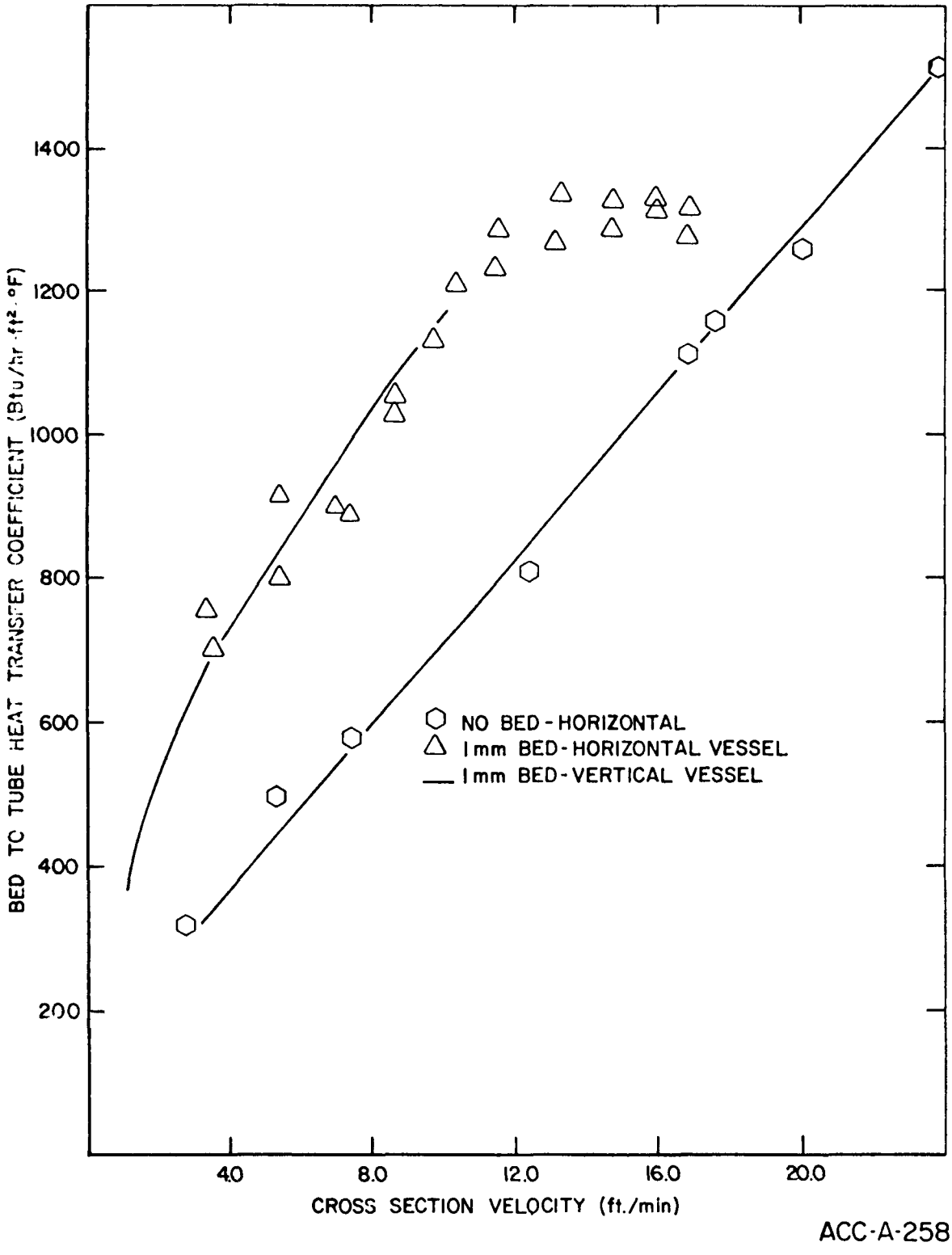

Figure 3. Heat Transfer Coefficients for Horizontal and Vertical Heat Exchangers Plotted Against Cross Section Velocity.

where

M = mass flow rate

P_g = density of geothermal water

ℓ = length of the tube bundle

n = number of tubes in the middle row

d_V = inside diameter of the vessel

d_Z = outside diameter of the tubes

3. Flow Distribution Vessel

The vessel designed to study flow represents a 1-ft-section sliced out of a 3-ft-diameter heat exchanger. The simulated tube bundle is composed of 0.75-inch-diameter lucite rods on a 1.125-inch triangular pitch. The tube sheets and cover plates on the ends of the vessel are lucite to permit viewing of bed circulation. The distributor plates are removable so that a variety of combinations can be evaluated. Instrumentation consists of differential pressure transducer probes located throughout the bed so as to relate pressure drop to flow quality. Specially constructed heat reansfer tubes will allow heat transfer coefficients to be determined at different points in the bed. This vessel is installed at Raft River, but it will be operated with cold water rather than geothermal water.

4. Program Plan

The 8-inch-horizontal vessel was installed on the Geothermal Component Test Facility at East Mesa for a 90-day scale-control test. Geothermal water at East Mesa has a much higher scaling potential than Raft River water. Preliminary tests are underway and the extended test is scheduled to go until July 30.

The first tests in the flow distribution experiment are intended to relate pressure drop across the distributor and across the bed to flow distribution. Preliminary experiments in the 8-inch-diameter vessel indicate better flow distribution is maintained at higher distributor plate pressure drop. We plan to determine if a maximum efficiency exists for liquid fluidized beds as it does for gas fluidized beds.

A pilot-scale liquid fluidized-bed preheater is scheduled to be constructed and tested in FY 1978. This is scheduled to be the second generation heat exchanger for the 60KW(e) binary system being installed at Raft River this summer. Design for the preheaters will begin this quarter.

III. INPLANT SOURCE TERM MEASUREMENTS

(J. H. Keller, B. G. Motes, D. W. Akers, T. E. Cox, S. W. Duce, J. W. Tkachyk)

The measurement program for determining sources of radionuclides at the Fort Calhoun Nuclear Power Station was concluded during this period. The measurements were made during three phases of the reactor cycle.

The initial studies were made prior to a major refueling outage so that the core would be in a "dirty" condition. The study continued throughout the outage and into full power operation with a "clean" core. It should be remembered that only a fraction of the total core is replaced during the refueling, and the "dirty" and "clean" representations are only relative. The three phases of the core cycle should be representative of the load placed on the radwaste system, both liquid and gaseous.

The first report on the measurements at Fort Calhoun has been reviewed by both the plant operation, Omaha Public Power District, and Nuclear Regulatory Commission (NRC) personnel directing the program. The report will be issued as an EG&G-TREE document as soon as possible. A second report covering the remaining data is in preparation and will be ready for NRC review by May 1.

Measurements have continued at the Zion Nuclear Power Station. A preliminary report covering the measurements from the beginning of the program in July 1976 until mid December 1976 is being prepared. This report will also be published, after NRC review, as a TREE document.

Plans for Next Quarter

The measurement program at Zion should be completed during the next quarter.

Personnel from the Effluent Treatment Systems Branch of the NRC are in the process of selecting the next reactor for study, and it is hoped that the measurements can begin at that facility very shortly. An additional report covering the procedures used by both Allied Chemical and EG&G-Idaho personnel in this program has been prepared and is in the review process.

IV. BURNUP METHODS FOR FAST BREEDER REACTOR FUELS (RRD FUNDED)

(W. J. Maeck, R. L. Tromp, J. E. Delmore, A. L. Erikson, W. A. Emel)

The purpose of this program is to measure absolute fast reactor fission yields and to develop methods for the determination of burnup for Fast Breeder Reactor (FBR) fuels.

In the reporting period, two irradiated capsules of ^{241}Am were dissolved and prepared for analysis. Separation procedures to remove the bulk of the ^{241}Am from the samples are being developed. The majority of the analytical work will be done during the 3rd and 4th quarters of FY 1977.

Recent major improvements in the ability to measure very small peaks in the mass spectrometer have resulted in remeasurement of fission products La and Ce in several of the dissolved irradiated capsules. Previously, the errors associated with the La and Ce measurements were larger than desired, because adequate corrections for natural contamination could not be made. Reliable corrections for natural contamination for these two elements require the accurate measurement of low abundance peaks at the 0.01 to 0.10% level. The ability to more accurately measure these small peaks also should improve the quality of the Ce and La yield data. Remeasurements are in progress for the capsules of ^{237}Np, ^{240}Pu, ^{241}Pu and ^{242}Pu.

Preliminary ^{242}Pu fast fission yields for isotopes on the light mass peak are given in Table 1.

TABLE 1

PRELIMINARY ^{242}Pu FAST FISSION YIELDS

Isotope	Capsule 9	Capsule 22	$\bar{X}$
^{83}Kr	0.188	0.187	0.188
^{84}Kr	0.356	0.356	0.356
$^{85}Kr+Rb$	0.348	0.346	0.347
^{86}Kr	0.562	0.557	0.560
^{88}Sr	0.903	0.906	0.904
$^{90}Zr+Sr$	1.47	1.47	1.47
^{91}Zr	1.87	1.84	1.86
^{92}Zr	2.27	2.20	2.24
^{93}Zr	2.90	2.88	2.89
^{94}Zr	3.28	3.15	3.22
^{95}Mo	3.72	3.70	3.71
^{96}Zr	4.38	4.35	4.36
^{97}Mo	4.53	4.53	4.53
^{98}Mo	4.96	4.90	4.93
^{100}Mo	6.15	6.23	6.19

V. ABSOLUTE THERMAL FISSION YIELD MEASUREMENTS (DPR FUNDED)

(J. E. Delmore, F. A. Duce, R. L. Tromp, W. J. Maeck, W. A. Emel)

As an outgrowth of another nuclear measurement program which required the measurement of relative fission product concentrations, ^{239}Pu thermal fission yields were found to significantly differ from previous measurements. Because of the importance of ^{239}Pu thermal fission yields, funding was requested to complete measurements for thermal fission yields for ^{235}U and ^{239}Pu.

VI. LIGHT WATER BREEDER REACTOR (LWBR) - ANALYTICAL SUPPORT

(D. E. Adams, D. H. Meikrantz, G. W. Webb, W. A. Emel)

An agreement has been made between Bettis Atomic Power Laboratory and the Radiochemistry Branch at ICPP to analyze forty-two irradiated LWBR fuel rod sections for uranium depletion. This quarter, twenty of these fuel sections have been received.

The current dissolution technique involves nitric-hydrofluoric acid dissolution of the ThO_2-UO_2 pellets in a pressurized autoclave. This technique has proven successful for samples weighing up to 15 grams. Five of the first nine pellets received weighed 25 to 40 grams each. Tests are in progress to determine what changes in techniques are required to dissolve these samples. Analysis of the first fifteen high priority samples is scheduled to begin in early April.

VII. RESEARCH ON ANALYTICAL METHODS

1. Spectrochemical Analysis of Simulated AGNS Waste Materials

(T. R. Lyon)

Complete analyses of simulated AGNS feed and scrub solutions and calcined solids were requested by the Waste Solidification Group. In order to lower the analysis cost and shorten the turnaround time, spectrochemical methods were studied and compared. The complex composition of the solutions and problems of solubility required that the filtrates and undissolved solids be analyzed separately. Atomic absorption spectrophotometry was chosen for the determination of cadmium and iron in all samples. Cesium, potassium, and sodium were best determined by flame atomic emission methods. Both X-ray fluorescence and emission spectrography were studied for the determination of gadolinium. Emission spectrographic methods were developed for all other elements requested.

Filtrates were analyzed directly by making appropriate dilutions and employing matrix matching of synthetic standards where necessary. The analysis of Gd by X-ray fluorescence was complicated by matrix effects or sampling problems that resulted in poor precision. Results of emission spectrography showed better precision and good agreement with the average X-ray results and could be obtained with little additional effort during the determination of the other elements. Emission results for Fe also compared well with atomic absorption results, and Fe will be determined by emission methods in all later solid sample analyses. The emission spectrographic method used the modified vacuum cup electrode system with $NaNO_3$ as a spectroscopic buffer and vanadium, added to give a concentration of 5 μg/ml, as the internal standard.

Solid samples were initially treated with nitric and sulfuric acids, and the solution was evaporated to initial SO_3 fumes. This treatment was repeated until all CeO_2 had dissolved. A barium sulfate precipitate, accompanied by some zirconium salts, was filtered from the solutions,

and this precipitate was fused in a mixture of 80% $Li_2B_4O_7$ and 20% LiF. This fusion melt was dissolved in dilute HNO_3, and the solution obtained was separately determined by an emission spectrographic methods. The filtrate portions of the solid sample after acid dissolution were analyzed by the methods used for the original sample filtrate.

Analysis time, including all time required for development and calibration, was only 25 minutes per determination for all elements determined by the emission spectrographic procedures. This time will be shortened considerably for subsequent samples submitted for analysis.

2. Computerization of Spectrographic Calculations

(D. A. Pavlica, R. W. Stone, R. A. Smith)

Photographic methods are used for most of the emission spectrochemical measurements in the Spectrochemical Laboratory. Quantitative data from photographic plates for standards and samples are obtained with a microphotometer as percent transmittance. To date, all computations have been performed by hand calculations. To increase the speed of spectrographic analyses and minimize human error, a programmable calculator is being used for computations and transcribing of data. Currently, three programs have been written in HPL language for use with a Hewlett-Packard 9825 calculator to calculate the results of spectrochemical measurements of elements in samples.

Program No. 1 calculates data specifically for standards. To use this program, the wavelength of the internal standard line for the desired wavelength region is addressed on the calculator keyboard. Measured transmittances of the internal standard line are entered as they are read by the user from the digital readout of the micorphotometer. Input transmittances are converted to intensity values by addressing a reference table of intensity values included in the program. Once the internal standard data are entered, relative intensities of a number of element lines can be calculated in succession. When a given element line transmittance is entered and then converted to the corresponding intensity value, the internal standard line of the respective wavelength region is addressed to calculate the intensity ratio of the element line to internal standard line. The intensity ration data along with the corresponding standard concentration data (entered prior to measuring the respective lines) are then stored on a data tape to be used by program No. 2.

Program No. 2 first loads the above intensity ratio and concentration data into the calculator memory and uses these data to generate standard curves relating the logarithm of intensity ratios to the logarithm of the concentrations. The desired element wavelength is addressed by the user and the calculator then plots the logarithm of the intensity ratios vs. the logarithm of the standard concentrations on a Hewlett-Packard 9871A impact printer. The user determines which points on the plot are acceptable and the calculator then performs a second-degree least squares fit for the expression:

$$\log I = A + B \log C + D (\log C)^2$$

where C is the concentration, I is the intensity ratio, and A, B, and D are constants. The curve is then plotted and, at the option of the user, 95% confidence limit on I may also be plotted. The calculator prints the standard curve coefficients and R^2 showing the fit of the standard curve to the data. If data for more than one element line were computed by program No. 1, the above procedure is repeated for the remaining element lines to obtain the respective standard curves. The program then codes and files each standard curve on a data tape.

The third calculator program converts intensity ratios of samples into element concentrations. The procedure used in program No. 1 to convert percent transmittance values to intensity values for a standard element line and the intensity ratios is also employed in this program for sample element lines. When the intensity ratio for a given sample element line is computed, the respective element line standard equation determined in program No. 2 is used to calculate the sample element concentration. Proper coding of the input data permits the direct printout of the concentration of the elements in samples.

Each point in these programs requiring input from the user explains at the calculator display what type of input is expected while halting and waiting for the user's response. Each program has an interactive feature which permits correction, deletion, or insertion of data as part of the program run. The use of these programs is convenient and time saving. The hand-plotting and transcribing of data is very time-consuming and also tends to increase the number of errors. The primary advantage offered by these programs is least square curve-smoothing, elimination of hand-calculations, and the direct calculation of element concentrations from intensity ratios.

The present programs were written specifically for filtrates and residues of low impurity water samples that are analyzed on a routine basis. Such samples require the generation of standard curves only once for a given batch of photographic plates. Therefore, once standard curves are calculated and stored for various element lines, only program No. 3 is needed to retrieve and use a standard curve for any chosen element until a new batch of photographic plates is used at which time programs No. 1 and 2 are reused to generate new standard curves.

Additional programs will be written to calculate the results of emission spectrochemical measurements of elements for a variety of both routine and nonroutine samples. Furthermore, the microphotometer will be interfaced to the HP 9825 calculator via an HP 3437A system voltmeter. This will eliminate entering percent transmittance values by the user via the calculator keyboard and permit automatic calculations of net intensity (background corrected) values if desired.

3. Spark Source Mass Spectrometer

(A. M. Delmastro, P. C. Marushia, W. A. Ryder)

A JEOL Instruments, Inc. Spark Source Mass Spectrometer has been installed. The instrument presently is capable of performing the multi-element trace analysis of a wide variety of materials using photographic detection. The electrical detection components and a computer system are currently on order and will be received shortly. Work is progressing on the calibration of the instrument for quantitative analysis.

VIII. ENVIRONMENTAL IODINE SPECIES BEHAVIOR

(J. H. Keller, B. G. Motes, S. W. Duce, F. A. Hohorst, J. W. Tkachyk)

One of the objectives of the Environmental Iodine Species Behavior program is to obtain a better understanding of the behavior of iodine species, in particular, HOI. In the past, it has been difficult to generate HOI reproducibly and in high purity. In the previous quarter, a method which yields high purity HOI in reasonable yields had been developed. The method involves the generation of gaseous bromine, the introduction of the bromine into a caustic solution of iodide tagged with ^{131}I, and the sparging of this solution to evolve gaseous HOI. Using this method, HOI of 95% purity in approximately 10% yield has been produced.

The behavior of the generated HOI in water-saturated atmospheres is being investigated in a 22-liter glass vessel. The HOI is sparged from the generator and passed into the vessel from which samples are withdrawn as a function of time over several days. As samples are withdrawn, saturated air is allowed to enter the vessel to maintain the humidity and pressure. The concentration of the airborne species is corrected for this dilution. The results of the early tests indicate that the airborne half-time of HOI in this system is long, at least several hundreds of minutes.

Previous field studies have shown that wet deposition is an important factor in the transfer of iodine from air to grass. In many cases, detectable amounts of iodine activity have been measured only after a rainfall. An unexplained phenomenon observed in a study in the environment around a nuclear power station showed, on several occasions, that

elevated levels of iodine activity were measured in milk from cows pastured near the reactor when the iodine levels on the grass and in the air were low. Because of the disparity in these data from that predicted by the accepted models, a new mechanism for the transfer of iodine activity from air to grass was postulated. The mechanism involves the scavenging by fog of iodine activity in chemical forms, such as organic iodides, which are not usually depositing. The grass becomes wetted by the activity-containing fog with the iodine remaining in the water film. The cows ingest the wet grass with the activity. Later in the day, after the fog has dissipated, the moisture evaporates along with the iodine activity. Grass collected after this drying action contains little or no iodine activity. The crucial steps in this mechanism are the iodine scavenging by the fog and the vaporization of the iodine from the wet grass as it dries.

To test this hypothesis, an environmental chamber has been obtained. Initial testing of the chamber has been completed including velocity measurements and methods of producing a fog and condensation on grass. Testing with organic iodine will begin as soon as safety considerations have been satisfied.

*

DISTRIBUTION RECORD FOR ICP-1117

Internal Distribution

1 - Chicago Patent Group - ERDA
9800 South Cass Avenue
Argonne, Illinois 60439

3 - A. T. Morphew
Classification and Technical Information Officer
Idaho Operations Office - ERDA
Idaho Falls, ID 83401

1 - H. P. Pearson, Supervisor
Technical Information

10 - INEL Technical Library

20 - Authors

79 - Special Internal

External Distribution

230 - UC-02 - General, Miscellaneous, & Progress Reports (Nuclear)
UC-10 - Chemical Separations Processes for Pu and U, TID-4500, R65

55 - Special External

Total Copies Printed - 399